Alma Mater Studiorum - Università di Bologna

DOTTORATO DI RICERCA IN

SALUTE, SICUREZZA E SISTEMI DEL VERDE

Ciclo 34

Settore Concorsuale: 07/C1 - INGEGNERIA AGRARIA, FORESTALE E DEI BIOSISTEMI

Settore Scientifico Disciplinare: AGR/10 - COSTRUZIONI RURALI E TERRITORIO AGROFORESTALE

ANALYZING URBAN GREEN ADAPTATION OPPORTUNITIES: CONCEPTS, APPROACHES, & STRATEGIES FOR EXISTING NEIGHBORHOODS

Presentata da: Mansoureh Gholami

Coordinatore Dottorato

Patrizia Tassinari

Supervisore

Alberto Barbaresi

Co-supervisore

Stefano Benni

Davide Gori

Esame finale anno 2022

ABSTRACT

Over the last decades, the growing evidence of human-caused climate change has raised awareness toward the consequences of exceeding global temperature by 2˚C. This awareness has led to a contemporary approach to the conceptualization and management of green adaptation policies in spatial planning. Green adaptation has developed rapidly in Europe due to the opportunities it can provide which are responsive to the challenges in spatial planning. The expansion of green adaptation planning is supported in several comprehensive principles on various scales to gain a multidimensional perception.

This thesis aims to develop a comprehensive methodology for assessing the adaptability of existing neighborhoods to green strategies. The reliability of the proposed method is examined in the cities of Bologna and Imola and it is proved to be applicable in other geoghraphical locations. This thesis integrates three key themes of conceptual and implementation principles for urban green adaptation. Initially, by exploring the roles of integrated energy planning, this thesis defines methods for narrowing uncertainties in urban planning energy forecasting modeling. The second is by exploring green retrofitting strategies in building, this thesis examines the effects of various energy-saving factors in roofing scenarios including a green roof, rooftop greenhouse, and insolated roof. Lastly, this thesis analyzes green strategies in urban spaces to enhance pedestrian thermal comfort through facing urban heat exposure related to urban heat island effects.

Each of these themes proposes specific outcome. First theme, presents an archetype-based coding framework for the city of Bologna and imola and an automated calibration that can calculate the importance of uncertain parameters concerning building energy consumption. The second theme, present an accurate methodology for analyzing roofing scenarios through two-dimensional hygrothermal in WUFI simulation. The proposed method can accurately simulate water content and humidity in green roofs and rooftop greenhouses and offer realistic results. The third theme, proposes a digital twin prototype including a real-time climate model in complex 3-dimensional models of cities. The hierarchical structure of the proposed digital twin not only enables it to overcome the issues of previous models regarding modeling thermally comfortable urban environments, but also makes it faster, more accurate, and higher in quality by combining various, highly efficient engines into an integrated set of 3D visualization and mapping methods.

The contribution of the thesis is empirical, methodological, and conceptual. The roles of integrated energy policies and green strategic thinking are discussed to highlight various aspects of green adaptation on the neighborhood scale. Based on these discussions, the thesis develops approaches by which cities can face the challenges of current green urban planning and connect the conceptual and practical aspects of green spatial planning. Another point that this thesis highlightes is that due to the interdependency of individuals and places, it is hardly possible to assure whether all the adaptation policies on large scale are enhancing the resiliency of the neighborhood or they are simply shuffling the vulnerability through the individuals and places. Besides, it asserts that neglecting to reflect on these reallocations of the effects can generate serious complications, and will result in long-term unforeseeable and dysfunctional consequences.

Keywords: Urban Green Adaptation, Energy Modelling and Forecasting, Green Roofing Scenarios, Microclimate Digital Twin, Green Spaces, Urban heat island mitigation.

ACKNOWLEDGMENT

I would like to thank a number of people for their valued assistance and support during the production of this thesis. I would firstly like to thank my supervision team comprising professors Barbaresi and Toreggiani for their invaluable support and advice throughout my study in Bologna. Without the help and assistance of this team, I am not sure what state this thesis would have ended up in and their friendly guidance has created a flourishing environment beyond measure, professor Barbaresi, for being a patient supervisor and an open-minded problem solver with all his advice and guidance which stuck in my mind, professor Torregiani, for becoming an inspiring person for what I want to be in my future profession with his humble and hardworking personality. I could not imagine myself continuing my research activities without him offering his time and support unconditionally and believing in me more than I expected.

Importantly, my sense of respect goes to the coordinator of my Ph.D. program, professor Tassinari for her constant support of my research and for offering advice and encouragement with her perfect insight. She has been an inspiring Italian woman to me for being understanding and keeping a careful eye on international students to afford them equal opportunities at the University of Bologna.

Many thanks to Ariane Middel, My advisor at Arizona State University during my sabbatical in her lab who endured this long journey with me, always offering unconditional love and support since day one. My sincere thanks to Bjoern Hagen, senior scientist in the School of Geographical Sciences and Urban Planning for all the road trips and exciting experiences he provided me with. Without these people, my stay at ASU could not be this productive and enjoyable.

Financially, I would like to thank the ISA Institute of Advanced Studies for offering me a full-time scholarship and multicultural international coworking activities on cross-cutting themes. I would also like to thank professor Braga, for all the support and care he provides international students with.

Special thanks go to all the people who gave their time, knowledge, and ideas for this thesis. Without all of you and your discussions and information, I would not have been able to develop this research.

Sincerest thanks go to all my family and friends for challenging and supporting me during this research. You’ve all helped me through the good and bad times, as there have been a few of each.

Mansoureh Gholami, Bologna, January 2022

Table of Contents

Chapter 1. Introduction

1.1 Statement of the Problem

The Mediterranean countries are mostly vulnerable regions to climate change, extreme weather events such as heat waves, cold snaps, heavy rainfall or snowfall, ice or hail storms, droughts, extratropical or tropical cyclones, storm surges, and tornadoes.

Cities are notably vulnerable to these climate change and must have a key role in making adaptation policies that require action at the local level. The main aim of these adaptation plans must be to prevent further deterioration of the climate crisis and to slow down the increase in global temperature as it is considered in Paris agreement to reach net-zero greenhouse gas (GHG) by 2050. To accomplish this, it is necessary to keep up-to-date knowledge of the deteriorative impacts of climate change. Because climate change is already expanded to some level, responding to climate change involves a two-pronged approach:

- Mitigation: Reducing emissions of and stabilizing the levels of heat-trapping greenhouse gases in the atmosphere;
- Adaptation: Adapting to the climate change already in the pipeline. The mechanism for climate adaptation which is defined adjusting to actual or possible expected scenarios to future climate (NASA, 2022).

These mechanisms are not limited to the urban public environment but also building complexes and individual buildings.

Global energy demand is set to increase 4.6% in 2021, more than offsetting the 4% contraction in 2020 that occurred due to the covid-19 pandemic(Energy Agency, 2021). From this, building energy consumption are responsible for over one-third of global final energy consumption and 38% of total global energy-related GHG emissions.

The EU climate and energy policy sets the following targets for 2030 (EU 2021):

- At least 40% cuts in greenhouse gas emissions (from 1990 levels)
- At least 32% share for renewable energy
- At least 32.5% improvement in energy efficiency

Europe, However, has made itself committed to raising the 2030 GHG emission reduction target to at least 55% in comparison to 1990. Thus, important measures are needed to reduce energy consumption and also GHG emissions in urban areas. Without consistently pursuing reduction policies in urban areas Europe will miss these targets.

1.2 Theoretical or Conceptual Framework

Italy is in a region that is specifically vulnerable to global climate change. Climate data in Italy shows an increase in extreme temperatures. Italy is at risk of natural hazards and global climate change is expected to even increase its vulnerability to climate-related events over subsequent years.

There is thus a clear need for adaptation to future climate changes. Green adaptation planning significantly contributes to the adaptation to heatwaves and heat islands.

Green adaptation means taking actions to prepare for and adjust to both the effects of climate change and predicted impacts in the future. The main adaptation strategies should respond to two questions, “what to adapt to” and “how to adapt to”.

To date, green adaptation strategies are not developed through an integrated approach and could not meet green adaptation goals and even have unintended negative impacts on the other action plans. To reduce the vulnerability and enhance the implacability, comprehensive green adaptation planning is needed for assessing, evaluating, and making urban scale strategies.

Dense cities usually struggle with low levels of green space per capita and consequently leads to intense urban heat island effects and unbalanced urban energy systems. Regeneration of urban green spaces in dense cities requires an understanding of urban buildings, urban spaces, etc..

Green adaptation planning on a neighborhood scale can reintroduce the urban policies in three main subjects: Energy Efficient Buildings, Green Buildings, and Green Urban Spaces (Fig 1.1).

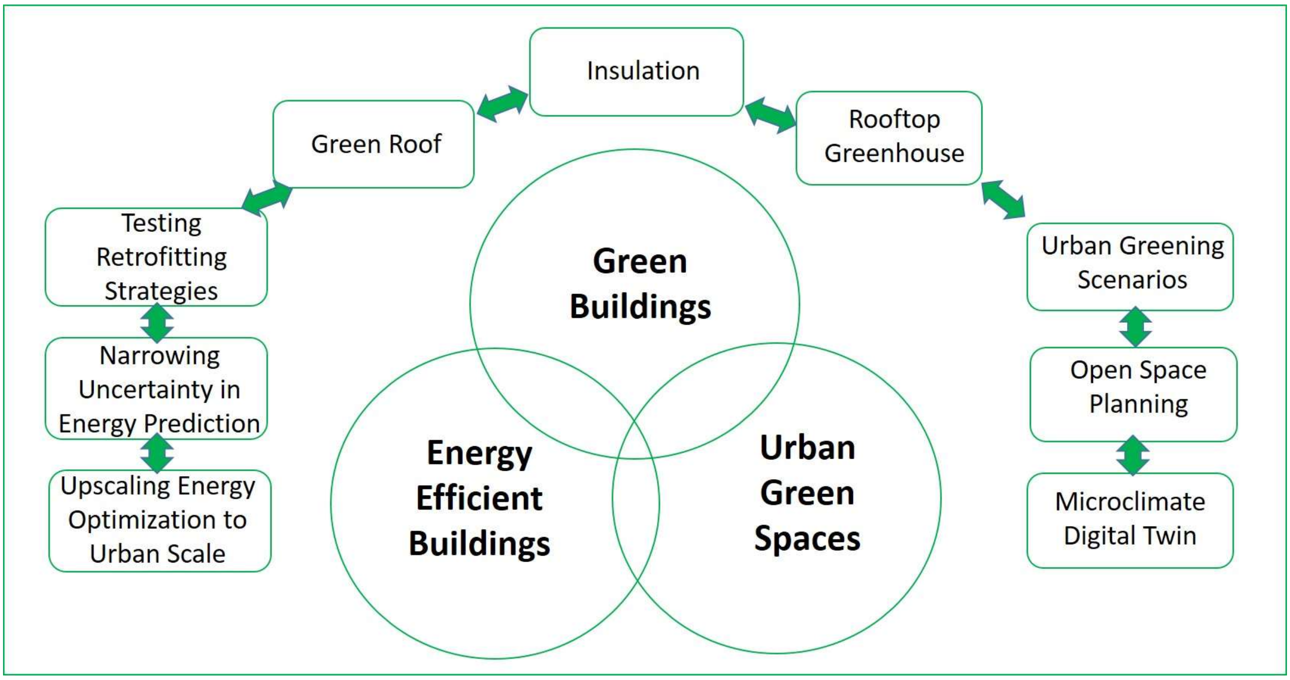

Figure 0.1: The conceptual framework of the thesis

1.3 Statement of the Purpose

This research aims to develop a comprehensive model for assessing the adaptability of existing neighborhoods to green strategies.

There are four main objectives toward this aim:

- **To develop a methodology** to calculate and optimize energy consumption in building on a neighborhood scale for making effective retrofitting strategies on the community scale.

- **To analyze the energy efficiency** of various green roofing scenarios for thermal behavior of buildings

- **To develop a real-time microclimate modeling methodology** to assess climate comfort at the pedestrian level through simulating different green scenarios

Functionality of the proposed model for green adaptivity in the existing neighborhoods has been evaluated through application in the cities of Bologna and Imola, Italy. However, the applicability of the model is not limited to these cities. The model proved to be applicable to a variety of geographical contexts.

1.4 Research Questions

The main question of this study is whether we can move toward a zero impact or even positive environmental impact neighborhood and upscale it to cities. To approach this question, I narrowed it through three more detailed questions:

- How to make the most effective retrofitting policies for buildings on large scale?
- How can we evaluate the thermal behavior of buildings for green roofing scenarios?
- How to develop a real-time model of the urban spaces to monitor pedestrian climate comfort in the neighbourhood through various greening scenarios?

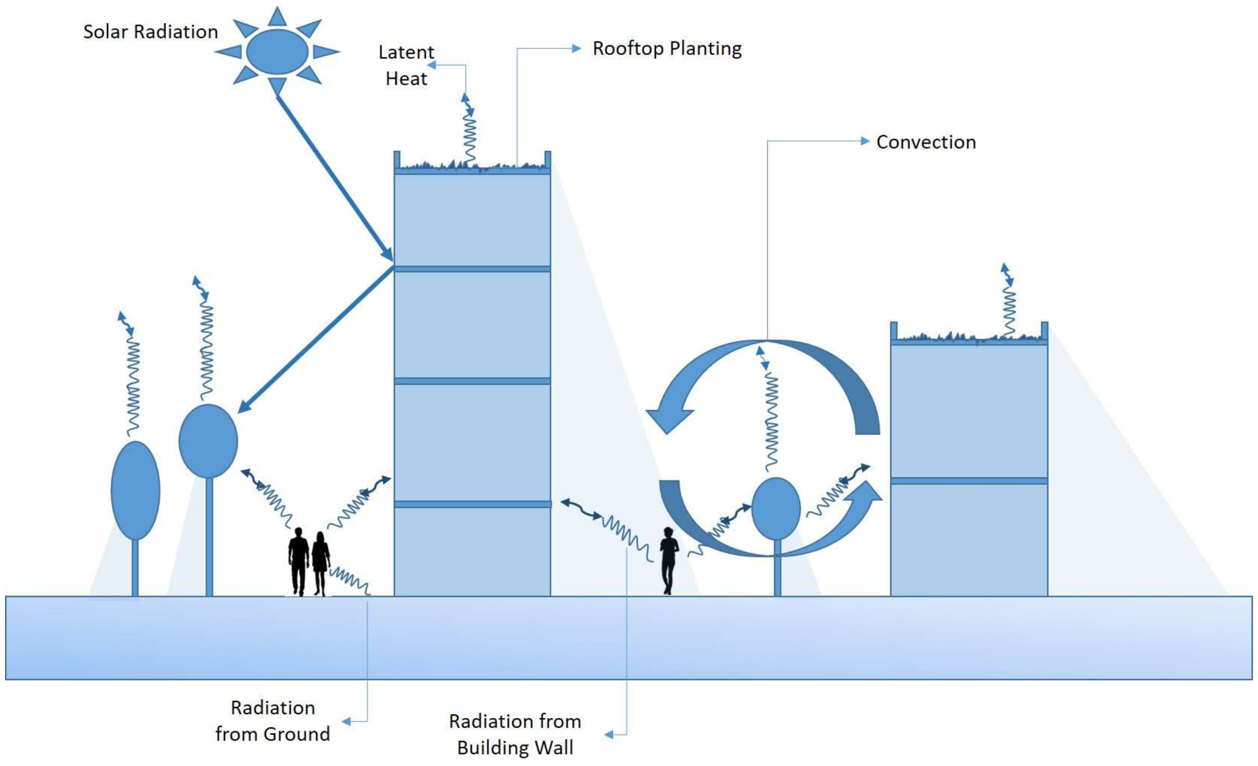

Figure 0.2: Effective factors in green adaptation on the neighborhood scale

1.5 Structure of the Thesis

This dissertation consists of three related studies including energy-efficient buildings, green buildings, urban green spaces. Chapter 1 provides the introduction and conceptual framework for three studies. Chapter 2 reviews the state of the art of the three studies. Chapters 3, 4, 5 describe the three studies in detail with their respective methods, results, and discussion sections. Chapter 6 looks at research questions and future directions. Chapter 3 is focused on the second objective of the thesis and develops the framework for forecasting the energy demand in building stock. This framework can give a broad knowledge of the building stocks and the ideal renovation strategies in every building archetype. In chapter 4, a comparison for energy-saving capacity of green roofing scenarios has been proposed. Chapter 5 proposes a method for the calculation of mean radiant temperature and recognition of the urban heat island at the neighborhood scale. Besides, it practically tests the green scenarios for enhancing the cooling effect in urban spaces.

Chapter 2 . Literature review

2.1 Summary

This chapter will review the state of the art of the three studies. The first section presents the vital role of Integrated Energy Planning (IEP) in the promotion of energy efficiency in the large-scale building stock. IEP can facilitate the evaluation of energy supply and demand in current rural and urban areas for the proper allocation of available resources. This section aims at reviewing large-scale energy planning and a systematic review of the methods employed in urban and regional integrated energy planning (UR-IEP). To this effect, 234 models from 157 published papers have been collected, classified based on their aims and methodologies, and critically subjected to meta-analysis and SWOT table. Thus, this review proposes a framework of the fundamental concepts in energy model design and detailed analysis to support decision making. Further, it provides a clear comparison of the methods and characterizes them based on seven basic criteria of energy models, including purpose, methodology, analytical approach, geographical coverage, mathematical approach, time horizon, and data requirements. This framework provides urban planners with the accurate and helpful basis for the selection of appropriate IEP methods based on the most common-focused methods published between 1960 and 2018. However, achieving reliable models in forecasting energy demand on a large scale has appeared as one of the most challenging issues encountering societies that seek positive-environmental impact districts in highly complicated city structures (Gholami et al., 2020). This complexity has contributed to the recent boost in developing methods for narrowing uncertainties in the forecasting methods. Thus, in section 2.2, these models are classified and reviewed.

In urban areas, a considerable proportion of energy demand is allocated to buildings. Since rooftops constitute one-fourth of all urban surfaces, an increasing amount of attention is paid to achieving the most efficient shapes and component designs compatible with every climate and urban context, for rooftops of varying sizes. Section 2.3 is allocated to the literature review of green roof modeling.

The third section focuses on outdoor climate comfort on the urban scale. Assessing the thermal impact of urban design and landscaping strategies on human thermal exposure and comfort has been progressive in recent years. Long-term solutions for mitigating the urban heat are driving microclimate modeling of cities into smart city planning which requires the adoption of several digital twins. As tree planting has become a priority for many cities around the globe to combat urban heat, the need to optimize tree placement for maximum cooling benefits has increased due to limited resources. A review of the literature on this effect is proposed in section 2.4.

Abbreviations:

IEP: Integrated Energy Planning
UR-IEP: Urban and Regional Integrated Energy Planning
ESS: Energy Storage System
CEP: Community Energy Planning
CRP: Community Regularity Plan
CSP: Community Site Plan
CMP: Community master planning Optimization
CDP: Community Detailed Plan
SH: Space Heating
GA: Genetic Algorithm
GNP: Gross National Production
EI: Energy Intensity
DHW: Domestic Hot Water
GDP: Gross Domestic Production
ACO: Ant Colony

2.2 Upscaling Green Energy Modeling from Building To Community

Integrating energy planning in Master planning

In 2009, the UN-Habitat published a report in which the definition of urban planning was clarified: "*Urban planning is used loosely to refer to intentional interventions in the urban development process, usually by the local government. The term "planning" thus subsumes a variety of mechanisms that are in fact quite distinct: regulation, collective choice, organizational design, market correction, citizen participation, and public sector action*"(Forbes, 2011).
Notably, this report explains urban planning as being a difficult task (or almost impossible). The reason is that there is a wide variety of roles, forms, and perceptions in the scale of time and location. Besides, the combination of the vast topic of energy planning in this definition has made it even more complex. To date, there is no common ground on what energy planning accurately must represent. Thus far, scholars have made several attempts to achieve an integrated definition due to the wide variety of applications, but they have mostly failed. Multi-scale standpoints are employed to address the complicated aspects of this challenge; consequently, the next section will examine the three most important criteria of energy planning on large scales: the allied foresight, integration process, and connection of strategic aspects in large scales and operational levels.

Criteria of large-scale integrated energy planning

- **Allied Foresight:** In master plans, main strategies are formulated based on a specific vision; however, when an energy-oriented future is considered, there, definitely, must be an allied foresight to ensure every aspect of the zero-fossil fuel vision and the vision of the master plan are covered as well. Furthermore, the vision must be adapted to the aims of higher levels, such as national plans, or with parallel programs such as climate-mitigating or environmental programs (Nilsson and Söderström, 1993).

- **Unified energy and planning schemes:** After aligning the perceptions and visions, the next step is to understand where and how the energy aspects must be integrated into the plan. Furthermore, it is crucial to make decisions technically and economically on all sections, including feasibility studies and land use plans or in the energy calculations tools. This process highly requires an easily understandable procedure or process map for any presentation. Notably, the performance of the abovementioned factors is not feasible without involving energy into every step, from the cognitive stages to brainstorming and decision making stages to operational levels in a certain area (Steiner, 2014).

- **Bonded strategic and operational stages:** The energy strategies have to be included in an operational program, to be applicable in the cities. The long-term strategies must go through administrative processes to afford short-term and mid-term strategies. Afterward, instruments at various spatial scales link the main strategies to the short-time ones (Steiner, 2014).

Community Energy Planning (CEP)

The community-scale in energy planning plays a key role since it links buildings to the city context. Community planning is the convergence point in energy planning, in which long-term strategies can be converted into mid-term and short-term tasks and policies. For integrative energy solutions, a community energy plan must focus on 5 tasks (Surhone et al., 2010):

- Identifying the end-user of energy
- Taking advantage of every opportunity to conserve energy
- Seeking renewable energy potentials
- Setting energy aims and objectives for every specific community
- Understanding the community priorities and recognising required resources

To consider a scale in-between the city and buildings, a community will be employed to convey the role of "a group of buildings". In general, a "community" refers to a non-specific-sized social group that occupies a certain locality. In this paper, however, a "community" refers to the small-scale area (approximately 10 km^2), in which mixed-use of lands occurs (Z. Huang et al., 2015).

Seven main steps are applicable to the energy planning process of every community (Steiner, 2014):

1. Recognising a private or governmental operator who is an expert in energy planning to assume responsibilities in the planning process.
2. Publishing the community vision and aims
3. Identifying an energy baseline for the community
4. Recognising all the possibilities of energy efficiency application in the community
5. Considering the economic development feasibilities
6. Identifying the service requirements in all socio-economic aspects
7. Implementing the planned short-term policies.

Community Energy Planning has been examined completely in the three parts of master planning, detailed planning, and architectural design by Huang et al. (Z. Huang et al., 2015). Thus, in this section, only the energy integration process into the master plan and detailed planning will be discussed.

Community master plan

The smallest spatial scale in the planning process is the community master planning in which the main idea for a community usually is shaped, and based on it, planning visions are integrated into the energy visions. Community master plans have a bottom-up statistical approach toward issues; this means it considers the neighborhood as a system and does not enter the details of urban spaces and buildings. This approach helps urban planners to align the aims of the higher-level plans. Subsequently, objectives and main long-term strategies are provided; the last step involves collecting cognition data for the neighborhood for preparing plans in operational levels and mostly place-demand policies.

Community detailed plan

Before developing the architectural energy design, a community detailed plan plays a key role in integrating community master plan and architectural design rules. Therefore, the community detailed plan has both a bottom-up statistical and engineering approaches. The first one is applied as the community regularity plan, and the second one is considered the community site plan(Z. Huang et al., 2015).

Table 2.1: Community Urban Plans Procedures

<table>
<tr><th colspan="2">COMMUNITY ENERGY SUB-PLANS</th><th>Applicable scale</th><th>Methodology</th><th>Strategies and Policies</th><th>Time scales for policies</th><th>Outcome</th></tr>
<tr><td colspan="2">Community master plan</td><td>The whole area</td><td>Bottom-up statistical approach</td><td>Aims, analyzing econometric and technological data, preparing the actions plan and monitoring plans</td><td>Long-Term policies</td><td>Policies and principles</td></tr>
<tr><td rowspan="2">Community detailed plan</td><td>Community regulatory plan</td><td rowspan="2">The whole area and land parcels</td><td>Bottom-up statistical approach</td><td>Linking the goals and strategies to land parcels</td><td rowspan="2">Mid-term Policies and Short-term action plans</td><td>Energy intensity, Renewable energy per cent, investment index</td></tr>
<tr><td>Community site plan</td><td>Bottom-up Engineering approach</td><td>Energy consumption and generation balance Technical models with detailed simulation and accurate data</td><td>Evaluation of the effects of new technologies in energy consumption and decentralization of energy stations</td></tr>
</table>

The transition towards integrated energy planning requires developing methods to provide a clear vision as the prerequisite for making strategies. As has been specified, the focus of this paper is mainly on phase II of the IEP. After reviewing the main features, steps, and requirements of IEP, the next section will describe the different energy methods which were employed extensively in the decades past to address the requirements of the next phases in the IEP process

IEP methods in large scales

Techniques for classification

Thus far, a wide range of energy models has been introduced in various fields and due to the advancements in computer software, the creation of innovative and advanced models has been enhanced in the past years. This trend made it even more complicated to characterize and classify models in a solid and accurate framework. In fact, there are only a few models –if any– that fit into one distinct category. To date, several methods have been adopted to overcome this issue, such as static versus dynamic, univariate versus multivariate, and techniques ranging from time series to hybrid models; however, this paper, instead of classifying models based on one feature, characterizes models based on specific characteristics that are common to all the models. In this section, a parallel system of classification has been adopted to divide the models both in horizontal for spatial scale division and vertical for the level of data input. Thus, the classification commences with splitting the approaches in two, up-down and bottom-up methods; subsequently, the approaches in different spatial scales for every method are examined. Every model in this classification has been examined based on aim and methodology; eventually, a a meta-analysis of the presented models through a SWOT table and the description of the variation of 7 characteristics, including the purpose, methodology, analytical approach, geographical coverage, mathematical approach, time horizon, and data requirements, are presented.

Up-down methods

Up-down methods are referred to methods that consider the historical energy consumption and estimate the energy demand, based on the input variables. The development and employment of these approaches expanded with the energy crisis in the 1970s. In these methods, buildings are not in the center of planning a large area containing a group of buildings is considered as an energy sink. Up-down methods are usually employed when the main aim is taking advantage of aggregated input data, which is usually available and easy to access. Generally, the up-down methods are mostly known in large spatial scaled areas such as national scale or city scale, but it should not be wrongly restricted to this. Even on a community scale, these methods could be employed for better clarification of the energy state of the neighborhood.

The next section includes the definitions from an urban planning point of view of the most well-known models which are employed in various countries. More specific details about their methodology structures are accumulated in Table 16 in section 5.

National scale

Models on a national scale, with the main aim of energy forecasting, exploring possible scenarios, and backcasting from future to current situations, developed specifically to a nation. In this paper, models on the national scale are presented in 11 categories. In decades past, each category has been employed in various countries with a wide variety of functions.

a. Econometric models

Econometric models (Table 2.2) are based on some forecasting, exploring, and backcasting techniques that employ historical data to signify the economic criteria of any change in different fields. In energy modeling, econometric models correlate the energy with economic variables based on historical data through linear programming.

Table 2.2: Summary of econometric Models in Energy Planning

Model developed by	The main aim of the model	Methodology	Country
Samouilidis and itropoulos (Samouilidis and Mitropoulos, 1984)	Examination of energy and economic growth	Developing the econometric models for industrialized countries	India
Arsenault et al. (Arsenault et al., 1995)	Sectorwise prediction of total energy demand	Employing Ordinary Least Square technique (OLS)	Canada, Quebec
Christodoulakiet al. (Christodoulakis et al., 2000)	Prediction of the energy requirement and CO2 emission	Deriving sector wise equations for economic activities and for every sort of energy	Greece

Sharma et al. (Sharma et al., 2002)	Analysis of the requirement of three major forms of commercial energy	Employing sector wise/product wise econometric demand models by regression method	India, state of Kerala
Lu and Ma (Lu and Ma, 2004)	Determination of the energy consumption in industrial, transportation, residential and commercial	Using the consumption of fuel in a sector taking the case of a well off society	China
EDM (Energy Demand Model) by Gori and Takanen (GORI et al., 2007)	Development of the long term electricity consumption patterns	Using cointegration and stationary time series models	Italy
Hunt and Ninomiya(Hunt and Ninomiya, 2005)	Determination of the long-run price elasticity and income elasticity	Exploring the relationship between energy demand, Gross National Product (GNP) and real energy price	Japan
Raghuvanshi et al. (Raghuvanshi et al., 2006)	Determination of the characteristics of the drivers of energy development	Decomposing of primary energy consumption as a product of three variables, population, per capita Gross Domestic Product (GDP) and energy intensity of GDP	India
Saddler et al. (Saddler et al., 2007)	The anticipation of future energy consumption (the year 2040)	Examining the balances between different sector's energy usage	Australia
Fan et al. (Fan et al., 2007)	Analysis of the changes in energy price elasticity and elasticities of substitution	Examining the effect of energy costs on energy and non-energy sectors	China
Steenhof and Fulton (Steenhof and Fulton, 2007)	Analysis of energy supply and demand	Predicting three scenarios for different economic efficiency (high, low and base case) at various national and regional sectors	Asia-Pacific region
H.Sanstad et al. (Sanstad et al., 2014)	A "hybrid" econometric-technology forecasting approach	combining econometric and technological elements in a set of econometric models	Western US
Mirlatifi et al.(Mirlatifi et al., 2015)	Development of an algorithm to estimate the annual peak demand of small utilities and investigate the influence of econometric variables on the power demand of N. Cyprus	Utilizing historical annual databases, analysis of variance (ANOVA), and the statistical methods	N.Cyprus,
Dai et al.(Dai et al., 2016)	An assessment of the economic impacts and environmental co-benefits of large-scale development of renewable energy toward 2050	Using a dynamic Computable General Equilibrium (CGE) model	China
Wang and Li (Wang and Li, 2016)	An estimation of the relationship between the carbon emissions, population, GDP per capita, electricity consumption and energy consumption	employing regression and econometric models and analysing electricity energy development scenarios	China
Tanga et al. (Tang et al., 2018)	Development of EEMD-RVFL model for Energy price forecasting to reduce time and enhance accuracy	using traditional econometric approaches or computational intelligence methods in individual prediction	China

b. Unit root test and cointegration models

Cointegration tests analyze feasible correlations among some time series in the long term. Unit root tests can analyze recognizing stationarity in a time series. Time series have stationarity if a rearrangement in time cannot cause a difference in the structure of the distribution; unit-roots are considered one of the reasons for non-stationarity (Zhao and Wu, 2007). Table 2.3 shows the 14 most creative unit root and cointegration models that have been implemented in the last decades.

Table 2.3: Summary of Unit Root Test and Cointegration Models in Energy Planning

Model developed by	The main aim of the model	Methodology	Studied location
Masih and Masih(Masih and Masih, 1996)	Analysis cointegration between total energy demand and level of income	Using a dynamic vector error-correction model and multivariate cointegration tests	India, Pakistan, Malaysia, Singapore, and the Philippines
Fouquet et al. (Fouquet et al., 1997)	Examination of the disaggregated behavior of the UK energy crisis based on the short and long-run factors of fuel consumption, economic activity, and real prices	Using Cointegration analysis to determine the long-run relationships	UK
Glasure YU. (Glasure, 2002)	Examination of the combined effects of pure money and pure government expenditure on real income and energy demand	Employing five variable vector error correction models (VECMs)	Korea
Hondroyiannis et al. (Hondroyiannis et al., 2002)	Examination of the relationship between energy demand and economic growth	Employing a vector error-correction model	Greece
Galindo LM (Galindo, 2005)	Examination of the relation between different kinds of energy and income levels	Using Johansen procedure and ratio tests	Mexico
Lee and Chang (Chen and Lee, 2007)	Examination of the balance between energy demand and GDP	Employing aggregate and disaggregate data of energy demand in various sorts	Taiwan
Al-Irian (Al-Iriani, 2006)	Analysis of the relationship between gross domestic product (GDP) and energy consumption	Employing panel cointegration and causality techniques	Six countries of the Gulf Cooperation Council (GCC)
Lise and Montfort (Lise and Montfort, 2007)	Analysis of the cointegration between energy demand and GDP	Using the vector error correction model (ECM)	Turkey
Zhao and Wu (Zhao and Wu, 2007)	Prediction energy import demand	Employing cointegration and vector error correction (VEC) model techniques	China
Ang JB. (Ang, 2007)	Examination of the relationships between energy consumption emissions and outputs	Employing cointegration and vector error-correction	France
Yuan et al. (Yuan et al., 2008)	Examination of the effects of energy demand on economic growth	Employing cointegration and VEC approach at both aggregated and disaggregated levels	China
Liu Y. (Liu, 2009)	Analysis of the relation between energy demand and urbanization	Employing autoregressive distributed lag (ARDL) cointegration approach	China
Lin and Moubarak (Lin	Estimation of the energy-saving potential by determining energy intensity under different scenarios	employing Johansen cointegration technique and scenarios analysis	China

and Moubarak, 2014)			
Narayan (Narayan, 2016)	Hypotheses linking energy consumption with economic growth	Employing cointegration and Granger causality type tests	90 countries

a. Time series models

Time series models are the simplest energy models which employ a collection of observations of well-organized data items gained through regulated measurements during a reliable time. Table 2.4 shows the history of this model globally during the last 5 decades. As can be seen, the general function is for energy demand and supply predictions. However, source wise forecasting (GORI et al., 2007) under three different frameworks (Parabolic, linear, and chaotic behaviour), electronic forecasting in different time scales of hours and weeks (Nogales et al., 2002) (Amjady, 2001) (Hagan and Behr, 1987) (Fan and McDonald, 1994), and technology-wise models under four categorisation (Bass, Gompertz, Logistic, and Pearl) have been also developed under the time series models.

Table 2.4: Summary of time series models in energy planning

Model developed by	The main aim of the model	Methodology	Studied location
Bargur and Mandel [49]	Calculation of the energy consumption and economic expansion	Employing trend analysis	Israel
Bodger (Bodger and Tay, 1987)	calculation of the electricity demand	Employing simple logistic functions	New Zealand
Abdel-Aal and Al-Garni (Abdel-Aal and Al-Garni, 1997)	Analysis of monthly electric energy demand	Employing the univariate time-series analysis	Eastern Saudi Arabia
Tripathy(Tripathy, 1997)	Creation of near-optimal models for electricity peak load forecasting	Employing a time-series-based decision support system	India
Ediger and Tathdil (Ediger and Tatlidil, 2002)	Prediction of the initial energy demand	Employing a semi-numerical periodic model	Turkey
Hunt et al. (Hunt et al., 2003)	Development of a sector-wise energy demand model	Employing time series analysis	UK
Aras and Aras (GORI et al., 2007) (ARAS and ARAS, 2004)	The anticipation of the natural gas demand	Employing a regression time-series model	Turkey
Gonzalez-Romera et al. (Gonzalez-Romera et al., 2006)	Prediction of the electricity demand	Using the trend extraction method	Spain
Himanshu and Lester (AMARAWICKRAMA and HUNT, 2008)	Prediction of the electricity demand	Employing time series analysis	Sri Lanka
Mabel MC and Fernandez E. (Mabel and Fernandez, 2008)	Prediction of wind energy production	Employing pearl or logistic function	India
Grey- Markov Grey-Model (singular spectrum analysis) (Kumar and Jain, 2010)	Prediction of the coal, electricity demand	Developing a rolling mechanism for crude-petroleum consumption	India

b. Regression Models

Regression analysis is employed when the model aims at analysing several variables, where the equation has a dependent variable and one or more independent variables. A regression model, basically, identifies the linear or non-linear relation of the dependent variable (Y) to a function, the combination of independent variables (X), and unknown parameters (β)(Lam et al., 2008).

$$Y \approx f(X, \beta). \qquad (1)$$

Specifically, in spatial energy planning (Table 5), regression models have been used to calculate the demand and supply for the coal, oil, gas (Sharma et al., 2002) [62], and electricity load in short-term and long-term forecast, exploration, and even back casting(Moghram and Rahman, 1989) (Papalexopoulos and Hesterberg, 1990) (Haida and Muto, 1994) (Charytoniuk et al., 1998).

Table 2.5: Summary of Regression Models in Energy Planning

Model developed by	The main aim of the model	Methodology	Studied location
Jannuzzi and Schipper (Jannuzzi and Schipper, 1991)	Calculation of the electrical energy consumption for the residential sector	Analyzing the electricity consumption classes and end-uses	Brazil
Harris and Lon-Mu (Harris and Liu, 1993)	Examination of the dynamic links between electricity demand and weather, presented price, and income level	using 30 years data series	South East USA
Egelioglu and Mohamad (Egelioglu et al., 2001)	Examination of the influence of economic variables on the annual electricity consumption	Utilizing historical energy consumption, historical economic databases, and multiple regression analyses	Northern Cyprus
Yumurtaci and Asmaz (YUMURTACI and ASMAZ, 2004)	calculation of the electricity demand based on the population and per capita consumption rates	Using a linear regression model	Turkey
O'Neill and Desai (O'Neill and Desai, 2005)	Examination of the accuracy in the projections of US energy consumption	Using GDP and energy intensity (EI)	US
Tunc et al. (Tunç et al., 2006)	Electric energy demand	Using multiple regression analysis	Turkey
Lee and Chang (Lee and Chang, 2007)	Characterization of the relation between energy demand and economic growth	Examining the linear and nonlinear effect of energy demand on economic growth an inverse U-shape	Taiwan
Al-Ghandoor et al. (Al-Ghandoor et al., 2008)	Identification of the main drivers behind changes in electricity and fuel consumptions in the household sector	Developing two empirical models based on multivariate linear regression analysis	Jordon
Jonsson et al. (Jónsson et al., 2010)	Prediction of wind energy power	Utilization of non-parametric regression model	-
Lam et al. (Lam et al., 2008)	Examination of the electricity consumption pattern in the residential and commercial sector based on principal component analysis of five major climatic variables	Using multiple regression technique.	Hong Kong

Summerfield et al. (Summerfield et al., 2010)	Analysis of consumption data since 1970	Developing two models by employing multiple linear regression	UK
Fumo et al. (Fumo and Biswas, 2015)	Prediction of residential energy consumption	Implementing simple and multiple linear regression and then a quadratic regression analysis	-

c. ARIMA models

Autoregressive integrated moving average (ARIMA) model employs autoregression analysis and moving average methods to a well-behaved time series data. ARIMA assumes that the time series is stationary or fluctuates approximately uniformly around a time-invariant mean (Table 6). Its main application is in the area of short-term predictions and it requires at least 40 historical data points. ARIMA models have been extensively used in energy demand forecasting (Ediger and Tatl\idil, 2002).

Table 2.6: Summary of ARIMA Models in Energy Planning

Model developed by	The main aim of the model	Methodology	Studied location
Gonzales et al. (Chavez et al., 1999)	Analysis of the energy supply and demand	Employing univariate Box-Jenkins time-series analyses (ARIMA models)	Asturias-Northern Spain
Saab et al. (Saab et al., 2001)	Prediction of Lebanon's energy demand	Employing a hybrid model is more reliable in comparison to autoregressive and ARIMA models	Lebanon
Sumer et al. (Sumer et al., 2009)	Calculation of the monthly electric demand	Using three models of ARIMA, seasonal ARIMA and regression models	Balearics Islands, Spain
Ediger and Akar (Ediger and Akar, 2007)	Prediction of fuel production	Employing regression, ARIMA, and SARIMA	Turkey
Erdogdu (Erdogdu, 2010)	Analysis of short and long-run price and income fluidity of sectoral natural gas demand	Using ARIMA transfer function model	Turkey
G.boroojeni et al. (Boroojeni et al., 2017)	Development of a multi-time-scale approach is proposed for electric power demand forecasting	The historical load is modeled as a time-series ARIMA with multiple seasonality levels and Bayesian model for evaluation	-

d. Input-output models

Input-output models can analyse an economic system based on the table of inputs-outputs and based on the monetary matrix. Most of the input-output models have been employed in China since 2006 (Table 7).

Table 2.7: Summary of Input-output Models in Energy Planning

Model developed by	The main aim of the model	Methodology	Studied location

Wei et al. (Wei et al., 2006)	Projection of China's energy requirements	Evaluating the socio-economic factors in energy usage based on six scenarios	China
Liang et al. (Liang et al., 2007)	Examination of the energy demand and emission	Developing a multi-regional input-output model for 8 regions	China
Liu et al. (Liu et al., 2009)	Examination of the indirect energy demand and the effect of energy strategies on economic factors	Developing a multi-regional input-output model with a scenario and sensitivity analysis	China
Arbex and Perobelli (Arbex and Perobelli, 2010)	Analysis of the impacts of economic growth on energy consumption	Employing an integration of growth model with an input-output model	Brazil
Mu et al. (Mu et al., 2010)	Identification of dominant sectors that has a high electricity demand.	Using an input-output table of electricity demand (IOTED)	China
Alcantara et al. (Alcántara et al., 2010)	Examination of the electricity consumption pattern	Developing an input-output table	Spain
Zhang et al. (Zhang and Wang, 2016)	The gain of supply-chain energy and emissions by China's building sector	Developing a hybrid input-output approach	China

e. Decomposition models

The decomposition models break data into its component parts. In energy planning, decompositions consist of two approaches: the first is energy consumption, by which the total production and diversion in sectoral and structural energy intensity are modeled; the second is the energy intensity approach that is able to explain the changes in sectoral and structural energy intensity, but not in total production. These models could be applied in period-wise, source-wise methods (Table 2.8)(Suganthi and Samuel, 2012).

Table 2.8: Summary of Decomposition Models in Energy Planning

Model developed by	The main aim of the model	Methodology	Studied location
Ang BW (Ang, 1995a)	Calculation of the decomposition of industrial energy demand at two levels of sector disaggregation	Using the energy intensity (EI) approach	Singapore
Ang BW (Ang and Lee, 1996) (Ang, 1995b)	Analysis of the impact of structural and sectoral change on energy efficiencies	Decomposing the industrial energy consumption	Singapore and Taiwan
Sun JW (JW, 2002)	Calculation of the future total energy demand and analysis of the sectoral energy intensity, structure change, and GDP	Using a decomposition model to gain separated components	15 European Union countries
Sari and Soytas (Sari and Soytas, 2004)	Examination of the relationship between changes in national income growth and source wise energy demand and employment	Employing a generalized forecast error variance decomposition technique	Turkey
Sadorsky (Sadorsky, 2009)	Examination of the effect of GDP and CO2 on renewable energy demand	Employing panel cointegration	G7 countries
Odhiambo (Odhiambo, 2009)	Analysis of the relationship between energy demand and economic growth in a defined time duration	Employing the panel cointegration	Tanzania
Lean and Smyth (Lean	Analysis of dispersed petroleum demand	Employing univariate and multivariate Lagrange Multiplier (LM) tests for segment integration.	US

and Smyth, 2009)			
Lee and Chien (Lee and Chien, 2010)	Examination of the relationship between energy demand, capital stock, and real income	Employing a Granger causality test, the generalized impulse response approach, and variance decompositions in a multivariate setting	G7 countries
Gil-Alana et al. (Gil-Alana et al., 2010)	Examination of the energy demand by the US electric power	Employing various energy sources employing segmental integration	US
Afshar and Bigdeli (Afshar and Bigdeli, 2011)	Prediction of Iran short-term electricity demand	Employing singular spectral analysis (SSA)	Iran

f. Artificial systems – Expert systems and ANN models

An expert system is an Artificial Intelligence (AI) application, which can employ any fact or rule to facilitate decision-making and problem-solving. The purpose of an artificial neural network is to recognise patterns in the data. Although these models were previously employed in electricity demand, they are currently mostly used to predict energy demand regarding macro-economic variables. Electricity price prediction and short, mid, long term load forecasting are also considered in recent researches (Table2.9) (Xia et al., 2010).

Table 2.9: Summary of Artificial models in energy planning

Model developed by	The main aim of the model	Methodology	Studied location
Aydinalp et al. (Aydinalp et al., 2002)	Calculation of the energy consumption of appliances, lighting, and space-cooling in Canadian residential sector	Employing a neural network	Canada
Hsu and Chen (Hsu and Chen, 2003)	Examination of the peak load planning to predict regional consumption	Using unsupervised and supervised ANN	Taiwan
Sozen et al. (Sözen et al., 2005b)	Presentation of two models for calculation of energy consumption: 1-population, 2-gross generation.	Employing the ANN technique	Turkey
Yalcinoz and Eminoglu (Yalcinoz and Eminoglu, 2005)	Examination of the impact of variable climates for prediction of short-term load consumption	Employing ANN and historical data	Nigde, Turkey
Sozen et al. (Sözen et al., 2005a)	Prediction of the solar potential	Employing four models of SCG, LM, learning algorithms and a logistic sigmoid transfer function	Turkey
Benaoudaa et al. (Benaouda et al., 2006)	Examination of short-term electricity loads	Using ANN (employing wavelet-based non-linear decomposition) [127]	-
Gareta et al. (Gareta et al., 2006)	Examination of the hourly electricity price	employing ANN	-
Pao (PAO, 2006)	Prediction of the electricity requirements based on national income, population, gross of domestic production, consumer price index	Employing regression, ARMA, and ANN	Taiwan
Maia et al. (Maia et al., 2006)	Prediction of electricity loads [131]	Using AR, ARIMA, and ANN	-

Ermis et al. (Ermis et al., 2007)	Examination of the world green energy consumption	through artificial neural networks (ANN)	-
Sozen et al. (Sözen et al., 2007)	calculation of sectoral energy consumption and greenhouse gas mitigation	Employing ANN	Turkey
Hamzacebi (Hamzaçebi, 2007)	Estimation of the net electricity consumption on a sectoral basis	Employing ANN	Turkey
Gonzalez-Romera et al. (González-Romera et al., 2007) (González-Romera et al., 2008)	Prediction of monthly electricity demand and its fluctuation by proposing a hybrid forecasting model	Employing ANN	Spain
Azadeh et al. (Azadeh et al., 2007)	Prediction of Mid-term load	Employing ANN and neural network as a hybrid model	Iran
Pao (Pao, 2009)	Prediction of electricity consumption and petroleum	Examination of 6 linear models to present two hybrid non-linear model	Taiwan
Sözen (Sözen, 2009)	calculation of energy needs as a model of energy dependency (ED), the first is focused on total electricity generation, gross energy consumption and the second model on sectorial energy consumption (Yokoyama et al., 2009)	Employing two models of ANN model	Turkey
Ekonomou (Ekonomou, 2010)	Examination of the long-term energy demand in a residential area	employing ANN, inputs are yearly electricity consumption and total domestic generation and power potential	Greek
García-Ascanio and Maté (Garc'ia-Ascanio and Maté, 2010)	prediction of monthly electricity demand per hour	Employing vector autoregressive (VAR) and internal multi-layer perception model	Spain
Kankal et al. (Kankal et al., 2011)	Prediction of energy consumption based on GDP, demographic data and employment and the number of exports and imports	Employing ANN and regression models with the calibration of RMSE	Turkey
Limanond et al. (Limanond et al., 2011)	Prediction of the gas requirements for transportation	Employing ANN and linear regression and using by historical and demographic data and quantity of vehicles	Thailand

g. Grey prediction models

Grey models (GM) are based on the concepts of "lack of information" and interdisciplinary, cutting across specialized fields to fill the gap between them. Their popularity in energy fields is due to simplicity since in energy forecasting and appraisal modeling, these models can calculate the energy demand by a few data points (Table 2.10).

Table 2.10: Summary of Grey prediction models in energy planning

Model developed by	The main aim of the model	Methodology	Studied location
Mu et al. (Mu et al., 2004)	Examination of the relation of biofuels consumption on rural household	Employing multivariate GM analysis	China

Yao and Chi (Yao and Chi, 2004)	Calculation of electricity demand	Optimizing the inputs through GM	China
Zhou et al. (ZHOU et al., 2006)	Prediction of the Electricity demand	Employing GM and trigonometric residual modification	China
Akay and Atak (Akay and Atak, 2007)	Prediction of the gross energy demand and in the industrial sector	Employing an approach of GM with rolling mechanism (GPRM)	Turkey
Lu et al. (Lu et al., 2008)	Prediction of the transportation vehicles' energy consumption	Employing GM considering the number of vehicles, vehicle kilometres of travel and GDP	Taiwan
Lu et al. (Lu et al., 2009)	Analysis of the relation between the number of vehicles, energy usage, and emission	Employing multivariate GM	Taiwan
Bianco et al. (Bianco et al., 2010)	Prediction of the non-residential electricity usage	Examining GDP and cost analysis	Romani
Lee and Tong (Lee and Tong, 2011)	Prediction energy demand	employing grey prediction model and genetic algorithm	China
Lee and Shih (Lee and Shih, 2011)	Prediction of the cost of renewable energy technologies and the effects of cost on power production	Employing a multivariate GM	China
Pao and Tsai (Pao and Tsai, 2011)	Prediction of the interrelation between pollution energy intensity and emission	Employing GM and calibration by ARIMA	Brazil
Hamzacebi and Avni Es (Hamzacebi and Es, 2014)	Prediction of Electricity demand and supply until 2025	Developing Optimized Grey Modeling technique for both direct and iterative manners	Turkey
Wang et al. (Wang et al., 2014)	Investigation of the relationship between urbanization, energy consumption, and CO2 emissions	Using panel unit root tests, panel cointegration test, and panel Granger causality test	China

h. Metaheuristic models

As heuristic means finding by error, meta-heuristic means high-level discovery. Metaheuristic algorithm employs a certain trade-off of randomization and local search and can operate the optimization even with a few of imperfect input data.

- **Genetic algorithm (GA):** Genetic algorithm is a problem-solving procedure based on Darwinian evolution and natural selection. In mathematics, it starts from random models and finds more optimized solutions according to the minimization or maximization of a fitting function considering a chromosome as a string of genes. In this model, mathematical genetics can calculate the rate of spread of a special gene. This model has been used frequently in Turkey to achieve different forecasting methods (Ozturk et al., 2005).
- **Fuzzy logic:** Fuzzy logic is a method for carrying out calculations based on "degrees of truth" instead of the usual "true or false". Fuzzy models are a group of statements that are manageable based on historical data and weather data and usually, is employed in

short term electric load forecasting (Table 2.11)(Kiartzis et al., n.d.)(Miranda and Monteiro, n.d.)(Song et al., 2005)(Mamlook et al., 2009)(Jain et al., 2009).

- **Particle swarm optimization models (PSO):** The concept of particle swarm optimization originates from a series of evolutionary calculation methods, which are based on flocks of birds or any other similar bio-social behaviors. Specifically, the idea is based on the fact that when birds seek food, the birds that find food emit some signals to other birds, calling them toward the food (Sadaei et al., 2014). In PSO, birds are the particles, the emitted signals are positions and velocities, and the solutions act as food. Therefore, it can be interpreted that positions and velocities correlate with the indicators of solutions and the speed of particles toward the solutions (Rini et al., 2011).
- **Ant Colony Optimisation (ACO):** Ant Colony Optimisation (ACO) is a paradigm for designing metaheuristic algorithms for combinatorial optimization problems (Carbonaro and Maniezzo, 2003).

Table 2.11: Summary of metaheuristic models in energy planning

Metaheuristic models	Model developed by	The main aim of the model	Methodology	Studied location
Genetic algorithm	Padmakumari et al. (Padmakumari et al., 1999)	Prediction of the long-term distribution demand	employing the Neuro-Fuzzy method	-
	Ceylan and Ozturk (Ceylan and Ozturk, 2004)	Examination of the coal, oil and gas demand	Employing economic indicators based on a GA model	Turkey
	Ozturk et al. (Ozturk et al., 2004)	Prediction of future petroleum consumption	Employing the GA specialized in Exergy	Turkey
	Ceylan et al. (Ceylan et al., 2008)	Examination of the transport energy demand	Employing a specialized sort of GA named – HArmony Search Transport Energy Demand Estimation (HASTEDE)	Turkey
	Cinar et al. (Cinar et al., 2010)	Analysis the electricity usage, GNP, primary energy intensity, installed potential, demographic data	Employing ANN and GA	Turkey
	Forouzanfar et al. (Forouzanfar et al., 2010)	Prediction of the sectorial natural gas demand	Employing GA and non-linear programming (NPL)	Iran
Fuzzy logic	Kucukali and Baris (Kucukali and Baris, 2010)	Examination the short-term total annual electricity consumption	Employing GDP as the mere parameter and validating it by comparing the results with regression-based forecasts and MENR projections (MAED)	Turkey
	Zheng et al. (Zheng et al., 2019)	development of a national saving retrofit model through Monte Carlo simulation	Employing fuzzy multiple attribute decision	China
PSO model	Ünler (Ünler, 2008)	Prediction of energy demand	(PSO) based energy demand forecasting (PSOEDF) based on the indicators such as Gross domestic	Turkey

			product (GDP), population, import and export	
	El-Telbany and El-Karmi (El-Telbany and El-Karmi, 2008)	short term forecasting of Jordon's electricity demand	Employing PSO and then using the back-propagation algorithm and autoregressive moving average method to compare the results	Jordon
	AlRashidi EL-Naggar (AlRashidi and EL-Naggar, 2010)	annual peak load forecasting in electrical power systems (Wang et al., 2010) (Hong, 2010)	Employing PSO and then using the least error squares estimation technique for validation	Kuwaiti and Egyptian
ACO models	Toksari (Toksar\i, 2007)	Prediction of the energy demand	based on separated indexes such as GDP, demography data, and import and export amounts	Turkey
	Toksari (Toksar\i, 2009)	Prediction of the electrical energy demand	Employing Ant Colony Optimization	Turkey

i. Integrated models

Integrated energy models have a high level of information consciousness, and this means that they can consider a high level of input data dependency. In integrated energy planning, they are defined as models that are able to calculate the optimisation for a wide range of criteria, such as socioeconomic, biological, and environmental criteria.

- **Bayesian vector autoregression (BVAR) model:** Vector autoregression (VAR) is a kind of linear time-series model that can identify the joint dynamics of multivariate time series (Miranda-Agrippino and Ricco, 2018). Bayesian VARs (BVARs) with macroeconomic variables were first used in forecasting by Litterman (Litterman, 1979) and Doan et al. (Table 2.12) (Doan et al., 1984).
- **Support vector regression:** The support vector regression (SVR) is an efficient tool in real-value function estimation. As a supervised-learning method, SVR considers asymmetrical loss function, which can equally estimate high and low errors (Awad and Khanna, 2015).
- **MARKAL:** The MARKAL (originated from the linkage of two words: MARKet and ALlocation) depicts both the energy supply and demand sides of the energy system. It is an analytical tool that can be adapted to model different energy systems at the national, state, and regional levels (Kannan et al., n.d.).
- **TIMES:** TIMES (The Integrated MARKAL–EFOM System) is a predictive and modular linear programming model based on the partial equilibrium theory; it is also an energy system cost-optimisation model (i.e. aiming to provide cheapest energy services) that minimises the sum of the annual net present value of annual costs minus revenues for the entire model time horizon (Rout et al., 2011).
- **LEAP:** The Stockholm Environment Institute in Boston developed the long-range energy alternatives planning system (LEAP) (Table 6). The tool can be employed both in bottom-up and up-down forecasting methods.

Table2.12: Summary of Integrated models in energy planning

Integrated models	Model developed by	The main aim of the model	Methodology	Studied location
BVAR models	Crompton and Wu (Crompton	Prediction of energy demand for coal, oil, gas, hydro for 5 years	Employing Bayesian Vector Autoregression (BVAR) model	China

	and Wu, 2005)			
	Francis et al. (Francis et al., 2007)	Examination of the growth in energy consumption and relation between it and energy generation in the residential sector	Employing Bayesian Vector Autoregression (BVAR) model and Granger-causality	Caribbean countries
	Heo at al. (Heo et al., 2015)	Formulating a set of energy and carbon efficiency real retrofit decision-making situations and evaluating the role of calibration	Using the BVAR model	US
SVR models	Fan et al. and Hong (Hong, 2009) (Fan et al., 2008)	Prediction of the electricity consumption based on socio-economic indexes	Employing support vector model electricity load	-
	Wang et al. (Wang et al., 2009)	Prediction of the electricity consumption	Considering SVF for each of the input variables to forecast the electricity consumption	Turkey
	E.Kontokosta and Tull (Kontokosta and Tull, 2017)	development of a predictive model of energy use at the building, district, and city scales	Employing linear regression, random forest, and support vector regression (SVR)	US
MARKAL models	Strachan and Kannan	Calculation of residential energy consumption to achieve a reduction in carbon emission (Kannan and Strachan, 2009) [79, 82]	Employing MARKAL	UK
	Changhong et al. (Changhong et al., 2006) (Kan et al., 2004) (Gielen and Changhong, 2001)	Development of scenarios for reduction of air pollutant emission	Employing MARKAL in various decisions	China
	Chen (Chen, 2005)	Generation of the China's reference scenario for energy demand and carbon emission through the year 2050	Developing an integrated energy-environment-economy model	China
	Jiang et al. [88]	Analysis of the reasons for the increase in natural gas consumption	Employing MARKAL with an economic optimizer	China
	Mallah et al. [89, 90]	Presentation of scenarios to predict sectorial energy consumption patterns	Employing MARKAL	India
TIMES models	Rout et al. (Rout et al., 2011)	Calculation of long-term Sourcewise and sectorwise energy consumption and CO_2 emission	Employing TIMES G5	China
	TIMES-Canada	Analysis of possible futures for the Canadian integrated	using the most advanced TIMES optimization modeling framework	Canada

	(Vaillancourt et al., 2014)	energy system on a 2050 horizon		
LEAP models	Kadian et al. (Kadian et al., 2007)	modeling the total energy consumption and associated emissions from the household sector	Employing LEAP system to analyse different policies	Delhi, India
	Kumar and Madlener (Kumar and Madlener, 2016)	evaluation of the impacts of renewable energy consumption in electricity supply systems and calculation of the CO_2 emissions	developing various scenarios under the least cost approach using LEAP energy model	India

Urban and district level

To align the national level to the community scale in energy planning, up-down models must be downscaled. In this scale, the employed methods are the same as those at the national level; however, they are usually aimed at being sector-adapted to make policies more focused and accurate (Table 2.13).

Table 2.13: Summary of models in urban and district energy planning

Model developed by	The main aim of the model	Methodology	Studied location
Hirst et al. (Hirst, 1978)	Development of an econometric model considering both technology and housing stock (SAHA and STEPHENSON, 1980) ("An Energy Use Model of the Residential Sector," 1980)	Using econometric variables and a component for growth/contraction of the housing stock	US
Saha and Stephenson (SAHA and STEPHENSON, 1980)	Analysis of the total energy demand	Developing a model based on space heating, domestic hot water, and cooking	New Zealand
Nesbakken (Nesbakken, 1999)	Analysis of the sensitivity and stability across a range of income and pricing	Two tier econometric models that examine the choice of the system (discrete) and utilization (continuous)	Norway
Bentzen and Engsted (Bentzen and Engsted, 2001)	Examination of the effects of income and price on energy consumption	based on three different regression models in the residential sector	Denmark
Zhang (Zhang, 2004)	Calculation of the unit energy consumption (UEC) for different regions based on energy demand and the demography data, and a comparison between the Chinese UEC with those of other countries	Using aggregate national residential energy values	China
Tornber and Thuvander(Jonas Tornberg, 2012)	Development of an energy model for housing stock according to real datasets	Employing the entire building register of Goteborg (68,200 buildings) and energy data from the largest energy supplier	Goteborg
U.S. Department of Energy (U.S.	Presentation of mid-term forecasting and policy analysis based on 5 components: housing stock forecast,	Employing the national energy modeling system (NEMS) with a current	US

Energy Information Administration, 2020)	technology, appliance stock forecast, building shell integrity, and distributed generation equipment.	econometric energy model of the USA housing stock	
Labandeira et al. (Labandeira et al., 2006)	Analysis of the residential energy demand in a source wise condition	Employing a regression model	Spain
Balaras et al. (Balaras et al., 2007)	Identification of the effective energy factors that are employed for renovations	Developing an assessment for Hellenic housing stock	Greek
Siller et al. (Siller et al., 2007)	Analysis of the effects of renovating and new constructions on energy consumption and carbon emission	Developing modeling matrices which account for the renovation of buildings and new construction of buildings	Swiss
Wu and Xu(Wu and Xu, 2013)	prediction of energy consumption and CO2 emissions at a regional level	Employing a fuzzy multiple objective programming models	China
Fang and Lahdelma (Fang and Lahdelma, 2016)	Prediction of the heat demand	Employing SARIMA combined with linear regression	Finland

Bottom-up methods

Bottom-up models employ small-scale input data and can be classified into subsets of statistical and engineering models. Totally, bottom-up models could refer to every model, provided the model is adapted to consider buildings as an independent cell of a group. The advantage of these methods is the accuracy since they are based on accurate input data of buildings. However, providing these accurate data for buildings are not as easy as providing the required input data of the up-down methods.

Statistical Methods

Statistical methods are based on historical information. This means they utilize end-user data to calculate energy consumption. In this paper, well-documented models that have been employed in recent years are mentioned (Table 2.14). One of the advantages of these methods is consideration of the occupant behavior impact.

- **Regression:** Regression method employs regression analysis to determine the effects of one or a group of parameters; therefore, after regressing the total energy usage into parameters, the variables with a negligible impact will be ignored to ease the calculation process (Fung et al., 1999).
- **Conditional demand analysis:** The conditional demand analysis employs regression to regress the total energy consumption onto end-use appliances. There is an advantage to this method: the required data could be simply gained through energy billings (provided the methodology proceeds some datasets such as appliance ownership), although reliable results could be achieved only when a wide variety of prerequisite data from a huge number of buildings is available (Swan and Ugursal, 2009).
- **Neural network:** A neural network is an interconnected assembly of simple processing elements, units or nodes, whose functionality is loosely based on the animal neuron.

The function is exactly like regression models in terms of minimisation of errors; apparently, the NN models are rarely employed in modeling energy consumption. The reason might be the complexity of calculation, the prerequisite data, or even the lack of physical signs of the coefficients relating the dwelling characteristics to the total energy consumption (Aydinalp et al., 2002).

Table 2.14: Summary of Statistical models in energy planning

Statistical methods	**Model developed by**	**The main aim of the model**	**Methodology**	**Studied location**
Regression	Hirst et al. (Hirst et al., 1986)	Examination of the weather and non-weather sensitive elements of the household energy consumption of dwellings	Employing Princeton scorekeeping model and regressing the energy billing data onto a non-weather dependent constant	USA
	Tonn and White (Tonn and White TN (USA)), 1988)	Analysis of occupant behaviour	Developing a regression model with four simultaneous equations	-
	Douthitt (Douthitt, 1989)	Development of a model of residential space heating fuel use	Employing regressing in consumption as a function of present and historical database	Canada
	Fung et al. (Fung et al., 1999)	Determination of the impact on Canadian residential energy consumption due to energy price, demographics, and weather and equipment characteristics	Employing a regression model	-
	Raffio et al. (Raffio et al., 2007)	Assessment of the potential energy-conserving changes	Identifying energy conservation potential within a regional area	
	Torabi Moghadam et al. (Moghadam et al., 2018)	Estimation of the energy consumption of several residential building stocks for heating space	Employing a wide range of variables and based on a 2D/3D- Geographic Information System (GIS) and Multiple Linear Regression (MLR)	Italy
Conditional demand analysis	Parti and Parti (Parti and Parti, 1980)	Approximation of the occupant behaviour and determination of the use level of individual appliance	Employing CDA and regression methods	US
	Aigner et al. (Aigner et al., 1984)	Estimation of energy use of appliances in each hour of the day	Employing CDA models	US
	Caves et al. (Caves et al., 1987)	Calculation of the electrical energy consumption of Los Angeles customers	Developing a CDA model of the residential	US
	Bartels and Fiebig (Bartels and Fiebig, 1990)	Determination of the estimates of certain end-uses based on occupant behaviour	Proposing an alternative method based on the CDA model	-
	LaFrance and Perron (Lafrance and Perron, 1994)	determination of the changes in annual energy consumption	Employing an extended CDA method by incorporating energy consumption data	Quebec

	Hsiao et al. (Hsiao et al., 1995)	Identification of values which collaborate behavioural aspects better than a single EM estimation	Employing the work [216] and [217] by utilizing sub-metered end-use energy consumption	-
	Bartels and Fiebig (Bartels and Fiebig, 2000)	Enhancement of ‘‘efficiency’’ of submetering of the model by Hsiao et al. [219]	Employing a review of the house appliance survey prior to the sub-metering measurement	Norway
	Aydinalp-Koksal and Ugursal (Aydinalp-Koksal and Ugursal, 2008)	Analysis of the entire energy consumption of the Canadian residential sector	Developing a national residential CDA model	Canada
Neural network	Cetin and Novoselac (Cetin et al., 2014)	Analyzing the use of patterns of residential appliances and HVAC systems in single and multi-family households.	Using HEMS	US
	Issa et al. (Issa et al., n.d.)	Identification of the gap between actual energy consumption and the EPI rating	Developing a NN model that uses energy performance index (EPI) and conditioned floor areas of a group of dwellings with billing data	US, Florida
	Mihalakakou et al. (Mihalakakou et al., 2002)	Development of an energy model of a house	Using the NN methodology based on atmospheric conditions	Greece
	Aydinalp et al. (Aydinalp et al., 2003)	Development of a comprehensive national residential energy consumption model	Employing the NN methodology in three separate models: appliances, lighting, and cooling (ALC)	-
	Aydinalp et al. (Aydinalp et al., 2004)	Analysis of socioeconomic elements	Employing the NN model and using a dataset of alternative energy sources	-

Engineering (physics-based) Methods

Engineering methods calculate energy consumption based on geometry, envelope fabric, equipment and appliances, climate characteristics, and indoor environment criteria. The advantage of this model is as follows: since new technologies do not have any historical data, the occupants’ behaviour must be considered to obtain an accurate model, which differs considerably case by case and is completely unpredictable (Table 2.15).

Distributions: If the engineering models are developed based on appliance ownership and end-use distribution to forecast energy consumption, they are classified under the distribution sublet methods; even if their scales are national or regional, they will be classified under the bottom-up method due to their level of disaggregation.

Sample: Employing actual building samples can show a wide variety of housing stock and could be a good indicator for ensuring that the sample size is large enough. Since these models require huge databases, the applicability is limited.

Archetype: Archetypes, as a subset of engineering models usually employ various details to link a small group of buildings together. Archetypes modeling methodologies are based on a huge amount of details through computer-aided simulations. The advantage of this method is that due to the few number of archetypes, time efficiency can be enhanced through simulation, and the further the advancement in software, the more the applicability of these methods progresses

Table 2.15: Summary of engineering models in energy planning

EM Models	Model developed by	The main aim of the model	Methodology	Studied location
Distributions	Capaso et al. (Capasso et al., 1994)	Calculation of the total electric demand	Developing a model for a residential sector based on population and lifestyle of residents	Italy
	Jaccard and Baille [228]	Calculation of the unit energy consumption	Employing INSTRUM-R simulation based on the costs and behavioural parameters and historical data and technological distribution	Canada
	Kadian et al. (Kadian et al., 2007)	Development of an end-use energy demand model of a residential sector	Using a simplified endues consumption equation to incorporate the penetration and use factors of all households	Delhi, India
	Saidur et al. (Saidur et al., 2007)	Analysis of the exergy by estimating the total appliance's variable and the dividing of the efficiency	Developing a model for non-space heat residential energy demand	Malaysia
	Wu et al. (Wu et al., 2016)	Design of an optimal retrofitting strategy for achieving maximal energy savings and maximal NPV (Net Present Value)	Developing a TBT (time-building technology) framework	
Sample	Farahbakhsh et al CREEM (Farahbakhsh et al., 1998)	Calculation of the energy usage and calibration process	Developing the Canadian Residential Energy End-Use Model (CREEM) based on 16 archetypes and comparing the billing data	Canada
	Larsen and Nesbakken (Larsen and Nesbakken, 2004)	Development of a model for housing stock	Employing ERAD	Norway
	Ramirez et al. (Ramirez et al., 2005)	Computation of the hourly energy usage of buildings	Employing eQuest simulation software for a commercial region	US
	Guler et al. (Guler et al., 2008)	Analysis of the energy efficiency upgrades and GHG emissions	Employing an economic residential energy model to study	
	Swan et al. (Swan et al., 2009)	Development of a residential energy model	Employing a detailed database of nearly 17,000 houses	Canada
	Ascione et al. (Ascione et al., 2016)	Presentation of the energy behaviour of the explored building stock	Developing SLABE model through Latin hypercube sampling to generate Representative Building Samples (RBSs)	Italy
	Hoos et al. (Hoos et al., 2016)	Development a method to design retrofit scenarios	Employing a method of sampling for categorization of the end-energy for heat use of the public building stock	Luxembourg

Archetype	MacGregor et al. (MacGregor et al., 1993)	Development of a residential energy model based on the 27 archetypes	by employing hourly analysis program (HAP)	Nova Scotia
	Kohler et al. (Kohler et al., 1999)	Decomposition of the big databases into details and basic building elements considering materials and operations	Developing energy, and monetary model	Germany
	Huang and Broderick (Huang and Brodrick, 2000)	Development of an engineering model for SH and cooling loads	Employing prototypes in multifamily and single-family 16 various regions	US
	Snakin (Snäkin, 2000)	Development a model to find the factors of conservation and alternatives for fuel	Employing history databases and population and buildings features	Finland
	Tornberg and Thuvander. (Jonas Tornberg, 2012)	Prediction of many details such as building fabric, glazing, ventilation, water heating, space heating, and fuel costs	Developing energy and environmental model to base on archetypes and employing GIS	UK
	Shipley et al. (Shipley et al., 2002)	analysis of the impacts of building envelope improvements	Developing a monetary and energy emission model based on archetypes and ASHRAE	US
	Carlo et al. (Carlo et al., 2003)	Development of a model based on archetypes for commercial-buildings	Employing some initial parameters such as building energy regression equation to be roof area ratio, facade area ratio, and internal load density	Brazil
	Shimoda et al. (Shimoda et al., 2004)	Identification of the insulation levels for the city scale	Developing a residential end-use energy consumption model based on archetypes	Osaka, Japan
	Wan and Yik (Wan and Yik, 2004)	define different window areas facing the sun	Developing archetypes based on floor plans	Hong Kong
	Palmer et al. (Palmer et al., 2006)	Development of a model to calculate SH and DHW	Employing BREDEM-8 (Building Research Establishment Tool)	UK
	Nishio and Asano (Nishio and Asano, 2006)	Identification of the distribution and housing variables	Developing a tool to generate archetypes to employing Monte-Carlo methodology	Japan
	Petersdorff et al. (Petersdorff et al., 2006)	Developing a European building stock by considering 5 standards and 8 insulation standards	Employing Ecofys's BEAM for modeling heating demand in three different climate zones	EU
	Clarke et al. (Clarke et al., 2009)	Development of a model to calculate the thermal energy demand	Employing ESP-r in the Scottish building stock	UK
	Ballarini et al. (Ballarini et al., 2014)	Implementation of a cost-optimal analyses	Developing a national building Typology for European building stock	Italy

Cerezo et al. (Cerezo et al., 2014)	Development of the visions for a model	Employing a standard input format	US
Yang et al. (Yang et al., 2017)	Estimation of the energy performance	Employing a clustering method to select representative buildings and normative model to calculate energy parameters	China

2.2.1Summarizing and discussion

So far in this chapter, methods in phase II of IEP with related samples in different geographical locations have been provided; however, to clarify the basis on which these methods are employed in different occasions, characterisations of these methods are required. Table 2.16 presents the comprehensive framework of 7 basic features of methods which are employed in IEP.
SWOT analysis is an effective way that energy modelers can find out the weaknesses and strengths of the models and how the threads and opportunities can affect the requirements and outcomes of the calculation. Also, urban planners can understand compatible models that can be employed together. Thus, this SWOT table (Table 2.17) can be a guideline for energy modelers and urban actors to have smarter choices between potential models. Furthermore, SWOT analysis with meta-analysis together is an enhanced helpful approach for decision making because of its ability of presenting an extensive and critical comparison among models.

Table 2.16: characterization of the methods based on 6 criteria

	Purposes							
	General	**Specific**	**Methodology**	**The analytical approach**	**Geographical coverage**	**Mathematical Approach**	**Time Horizon**	**Data Requirements**
Econometric	Fo/Ex/Bc	De/Su/Im	ME/EEQ	UD	Na	L	Sh/Lo	Quant/Ag
Unit root test and cointegration	Fo/Ex	De/Su/Im	ME/MC	UD	Na	L	Sh/Lo	Quant/Qualit/Ag
Time series	Fo/Ex	De/Su/Ap/Im	Opt	UD	Na	L	Sh/Lo	Ag/Quant
Regression	Fo/Ex/Bc	De/Su/Ap/Im	ME/Opt	UD/BU	Na/Reg/Lo	L/NL	Sh/Lo	Ag/Disag
ARIMA	Fo/Ex	De/Su/Ap	ME/Opt	UD	Gl/Na	L	Sh/Lo	Ag/Quant/Qualit
Input-output	Fo/Ex	De/Su	ME/MC	UD	Na/Reg	L	Sh	Ag/Disag/Quant
Decomposition	Fo	De/Su/Ap	ME/Opt	UD	Na	L/NL/MI	Sh/Lo	Ag/Disag/Quant/Qualit
Grey predictions	Fo	De/Su/Ap	ME/Opt	UD	Gl/Na	L/NL	Sh/Med/Lo	Quant/Ag/Disag

ANN	Fo	De/Su/Im/Ap	ME/Opt	UD	Na/Reg/Lo	NL	Sh/Lo	Disag/Quant/Qualit
Genetic algorithm	Fo	De/Su/Ap	Opt	UD	Gl/Na/Reg/Lo	L/NL	Sh/Lo	Ag/Disag/Quant
Fuzzy logic	Fo/Ex	De/Su/Ap	Opt	UD/BU	Gl/Na	NL	Sh/Lo	Quant/Disag
PSO	Fo/Ex	De/Su/Ap	ME/Opt	UD	Na/Reg	NL/MI	Lo	Disag/Qualit
BVAR	Fo/Ex	De/Su/Ap	ME/Opt/MC	UD	Gl/Na/Reg/Lo	L/NL	Sh/Lo	Disag/Qualit
SVR	Fo/Ex	De/Su/Ap	Opt	UD	Na/Reg	L/NL	Sh/Lo	Disag/Qualit
ACO	Fo/Ex	De/Su/Ap	ME/Opt	UD	Na/Reg	NL	Lo	Disag/Qualit
MARKAL	Fo/Ex	De/Su/Im/Ap	ME/Opt/Sp	UD/BU	Na/Reg	L/D	Lo	Quant/Disag
TIMES	Fo/Ex	De/Su/Im/Ap	ME/Opt/Sp	UD/BU	Na/Reg	L/D	Sh/Lo	Quant/Disag
LEAP	Fo/Ex	De/Su/Im	De:ME Su:Simu	UD/BD	Gl/Na/Reg/Lo	L	Med/Lo	Ag/ Quant
Conditional demand analysis	Fo/Ex	De/Im	ME/Opt	BU	Reg/Lo	L/NL	Sh	Ag/Disag
Neural network	Fo	De/Su/Im/Ap	ME/Opt	BU	Na/Reg/Lo	NL	Sh/Lo	Disag
Distributions	Fo/Ex	De/Su	Opt/Simu	BU	Na/Reg/Lo	L/NL	Sh/Lo	Quant/Ag/Disag
Sample	Fo/Ex	De/Su/Im/Ap	Opt/Simu	BU	Reg/Lo	L/NL	Med/Sh	Ag/Disag
Archetype	Fo/Ex	De/Su/Im/Ap	Opt/Simu	BU	Reg/Lo	L/NL	Med/Sh	Ag/Disag/Quant/Qualit

L=linear, Fo=Forecasting, Ex=Exploring possible scenarios, Bc=Backcasting from future to current situation, De=Demand, Su=Supply, Im=Impact evaluating, Ap=Appraisal , ME= Macro Econometric, Opt=Optimization, Sim=Simulation, Sp= Spreadsheet(Toolbox) Models, UD=Up-Down, BU=Bottom-Up, Na=national, Reg=Reginal, Lo=Local, L=Linear model, NL=Non-linear model, MI=Mix Integer Model, D=Dynamic model, Sh=Short-term, Lo=Long-term, Med=Medium-term, Quant=Quantitative model, Qualit=Qualitative model, Ag=Aggregated, Disag=Disaggregated

2.2.2 A meta-analysis of the spatial energy models

Several energy planning models (234) related to phase II of the UR-IEP applications from 157 published paper were examined. These models have been classified based on the employed method in 23 classes. In the next step, after characterisation of the methods based on the 7 distinct variables (Table 2.16), RevMan (version 5.3) is employed to perform a meta-analysis to discuss the approaches that were accomplished during the last decades. The general purpose of the model in phase II could be exploring, forecasting, and backcasting. Table 2.18 shows that from the 234 models, 164 are focused both on exploring future scenarios and forecasting, and specifically, 159 are focused on demand and supply with a very low deviation that shows most of the models are concentrated on demand and supply calculations. Moreover, RevMan recognised that 160 papers are focused on short-term planning. In contrast, the number of modeling that is carried out on the local scale is few. Accompanied by only 54 bottom-up models, it is clear that this trend is not common; however, most of these models have been introduced in recent years and their number is increasing considerably.

Table 2.17: Results of Meta-analysis in collected variables

Variables	Description	Mean	St. deviation
Purpose General: Specific:	 1: if it is Forecasting and exploring ; 0: otherwise 1: if it is demand and supply; 0: otherwise	 0.705 0.688	 0.456 0.208
Methodology	1:if it optimization; 0:otherwise	0.511	0.415
The analytical approach	1: if it is bottom-up; 0: otherwise	0.233	0.423
Geographical coverage	1: if it is local; 0: otherwise	0.330	0.499
Mathematical Approach	1: if it is linear programming and not non-linear; 0: otherwise	0.358	0.479
Time Horizon	1: if it is short-term; 0: otherwise	0.682	0.220
Data Requirements	1:if it is quantitative and aggregated; 0:otherwise	0.426	0.461

Table 2.18: SWOT analysis of the three major methods in phase II of IEP

Approach	Scale	Method		
Up-down	National/ Districts		**Strengths**	**Weaknesses**
Up-down	National/ Districts		• Economical and quick implementation • Typically, an acceptable accuracy (approximately ±5% (Vogt, 2003)) • Easy to track changes in energy consumption • Identifying the effects of employed equipment • Flexibility in the prediction of all utilities (electric, gas, water, …) and non-utility cases such as production inputs • Appropriate for prediction of costs and facility performance	• The gross analysis creates unknown aberration causes
Up-down	National/ Districts		**Opportunities**	**Threats**
Up-down	National/ Districts		• In need of long-term data and Needless of collecting detailed data • Capable of handling calculation both linear and nonlinear data in socio-economic and demographic aspects	• In need of historical data to form a model but even extensive historical data cannot consider technology progresses • Incapable of output division in terms of technology, end use, etc.
Bottom-up	Community	statistical	**Strengths**	**Weaknesses**
Bottom-up	Community	statistical	• Consideration of occupant behavior • The inclusion of socio-economic effects down to the level of individual building • Detecting any change in individual facility process • Extreme accuracy in modeling due to the exact data collection in small scales	• Highly dependency on historical data and forecasting future trends without consideration of technology progresses • Unresponded to multicollinearity • Disregarding the variation of end-uses by selecting surveyed samples
Bottom-up	Community	statistical	**Opportunities**	**Threats**
Bottom-up	Community	statistical	• Utilizing billing data and simple survey information	• In need of weather, billing or surveyed data
Bottom-up	Community	Engineering	**Strengths**	**Weaknesses**
Bottom-up	Community	Engineering	• Consideration of variation in end-uses • Flexibility and accuracy in simulation through softwares • Accommodating the effects of each process employing a linear or nonlinear submodel.	• Disregarding the socio-economic aspects • In need of complicated energy modeling • Unable to generalize the model to other models
Bottom-up	Community	Engineering	**Threats**	**Opportunities**
Bottom-up	Community	Engineering	• Needless of historical data	• In need of detailed weather, architectural, and technological data

2.2.3 Uncertainty in Urban Building Energy Modeling

Attainment of reliable urban building energy measurements has appeared as one of the most challenging issues encountering societies that seek positive-environmental impact districts in highly complicated city structures (Gholami et al., 2020). This complexity has contributed to the recent boost in Urban Building Energy Modeling (UBEM) whereas lack of precise urban databases has cast doubts on the reliability of UBEM approaches (Reinhart and Cerezo Davila, 2016). In general, UBEM estimates the energy demand based on geometry, envelope fabric, equipment and appliances, climate characteristics, and indoor environment criteria. A common method to model a large number of buildings based on these parameters is to classify buildings in different archetypes according to their features. Archetyping benefits UBEM by time efficiency and data summarization. It has been employed in a wide range of urban energy forecasting methods (Gholami et al., 2020).

The energy performance of the buildings in an urban context is not exactly as software simulates it. Discrepancies between simulation results and the surveyed performance are unavoidably the consequences of inadequate input data, building users' behavior, and replication of simulation (Tian et al., 2018). Calibration aims at creating a correlation between the quantity of a parameter in a specific methodology and the relative measurement of a declared value. Similarly, in UBEM, calibration is the process of tuning known and unknown parameters to reduce the discrepancies between the modeled and measured values (Tian et al., 2018). Due to the complexity of various uncertainties sources on large scales, uncertainties of inputs in UBEM have raised a meaningful difference between predicted and measured values (Cerezo Davila et al., 2016). Indeed, without filling this gap, the UBEM approaches are not reliable in making retrofitting policies, operational promoting, or energy forecasting on the urban scale (Sokol et al., 2017). In a review in 2018, Tian and colleagues (Tian et al., 2018) have divided the calibration methodologies of building stock into two groups of forward and inverse models that the full description of this classification can be found there. However, in this paper, calibration methodologies are classified according to their approaches as user-driven or automated features. The main focus of the paper is on automated calibration methods.

2.2.3.1 Calibration methodologies for UBEM

Manual calibration is based on trial and error methods, which use the iterative manual tuning of input parameters without any systematic and automated procedure. The input data in manual calibration methods are highly dependent on users' experience and knowledge about the buildings. However, automated calibration methods are not user-driven and employ analytical and statistical methods. Among all automated approaches, calibrations with optimization algorithms and the Bayesian approach are the most employed methods in UBEM (Chen et al., 2019a).

- **Bayesian formulation;** is a method for measuring uncertainties through probability dissemination. No matter if the input data is not accessible (epistemic uncertainty) or does not exist (aleatory uncertainty), bayesian calculates the uncertainty that is caused by inadequate input data and measurement errors (P. Huang et al., 2015; Li et al., 2014; Tian and Choudhary, 2012). Bayesian frameworks are well-adaptable in models with uncertain data inputs. Thus, it updates proposed probability dissemination based on model output data which makes it suitable for future predictions. The basic calibration model in building energy models is proposed by Kennedy and O'Hogan (Kennedy and Hagan, 2001), later a guideline for the application of Bayesian calibration has published by Chong and Menberg (Chong and Menberg, 2018). Fernandez and colleagues in 2018 (Fernández et al., 2018) have shown that the Bayesian method takes ten times more than an optimization method for individual buildings.

- **Optimization under uncertainty calibration;** is a technique that aims at minimization of the existed gap between modeled and real values to identify the best variable sets. It employs optimization algorithms to find the best data set of parameters for calibration. It finds a global minimum gap on a set by using global optimization approaches such as genetic algorithm, Particle Swarm Optimization, etc. Most of these methods are applied on individual building scales (Asadi et al., 2019; Chaudhary et al., 2016; Deb et al., 2002; Li et al., 2018; Taheri et al., 2013; Wetter, 2001; Yang et al., 2016).

Although uncertainty methods on building scale do not differ from urban building energy calibration methods in the main steps, they alter to a certain extent. The reason is that there are some limitations on large scales that affect the efficiency of methodologies and their functionality. When the modeling process extends from one building to hundreds of buildings in a city, time, computation cost, and accessibility of supercomputers are among the limitations (Cerezo et al., 2014). To reduce the costs, meta-models can be integrated into the models, meta modeling is resembling a complicated model to a simpler model through a mathematical model. Coefficients in these meta-models are defined based on bounded sets of input and output combinations (Chen et al., 2019b). It acts as a surrogate for the white box simulations. Thus, a Meta model benefits the original model with decreasing calculation time while it ensures the reliability of the model (Manfren et al., 2013). Among all the meta-models, the Gaussian Process (GP) is the most employed model because of the high level of accuracy and reliability in interpolations. This method is employed in some energy calibrations (Lim and Zhai, 2018; Manfren et al., 2013) A study by Lim and Zhai (Lim and Zhai, 2017) has proved that GP models in building energy calibration are the most precise metamodel among others.

Some specific studies in recent years have led the urban energy building calibration to a more reliable status and sped it up. Booth and colleagues in 2012(Booth et al., 2012) introduced a UBEM based on clustering buildings and calibrated four unknown parameters through Bayesian calibration with 61 days of measured data. Later the model was improved by developing building archetypes based on the form and age of the buildings on city scales (Booth et al., 2013; Booth and Choudhary, 2013; Tian and Choudhary, 2012). Kim and colleagues in 2015 (Kim et al., 2015) employed optimization for the estimation of five unknown parameters. In 2016, Zhao and colleagues (Zhao et al., 2016) developed a method based on Bayesian calibration using a wide variety of variables for clustering buildings, later Evins et al. (Evins et al., 2016) investigated the impact of user behavioral factors and buildings' properties on a large scale. Sokol and colleagues in 2016 (Sokol et al., 2017) continued this subject by classifying archetypes based on uncertain parameters through Bayesian calibration. In 2018, Nagpal and colleagues (Nagpal et al., 2019) modeled 3 buildings with different numbers of unknown parameters and iteration. They found out that when envelope parameters of the buildings are known, the model is more precise and fast. The latest model is trained with 6 years of measured data for heating demand by Wang and colleagues in 2020 (Wang et al., 2020). They have simulated the model in CitySim. Building archetypes are classified based on the construction year and are calibrated by the Bayesian method.

2.3 Green Buildings

The energy consumption of urban buildings constitutes a considerable proportion of the world's energy demands. Thus, examining innovative strategies to create climate-conscious designs and harnessing the potential of urban areas to reduce the energy demand of urban buildings through controlling solar heat gains are increasingly attracting attention (Asadi et al., 2014). Since urban rooftops constitute 20% to 25% of the total urban surfaces (Costanzo et al., 2016), rooftop strategies are counted as some of the most effective methods among all the other solutions and they have been considered since they can provide a wide variety of benefits in various scenarios such as added insulation, the structures of phase change materials, cool roofs, green roofs, rooftop greenhouses, water roofs, etc. Many European local governments are more and more interested in the implementation of these urban building strategies to make a net-zero energy vision achievable by 2020("World Energy Outlook – Topics - IEA," n.d.). Implementing these strategies is highly dependent on the construction and energy-saving systems but in general, the role of these roofs in saving energy varies; some of them just reduce heat transfer while others may impact the energy-saving rate through thermal inertia (Hasan, 1999; Sisman et al., 2007).
Green roofs are increasingly attracting attention due to the wide range of benefits they provide, green roofs decrease urban temperature (Ouldboukhitine et al., 2014) and subsequently relieve the effect of Urban Heat Island in the cities(Bowler et al., 2010). Even on the roofs with photovoltaic installations, green roofs enhance electrical performance (Chemisana and Lamnatou, 2014; Lamnatou and Chemisana, 2015). During last decades, green roofs have been studied in a wide variety of aspects such as water runoff mitigation (Palermo et al., 2019), aesthetic, or social impacts (Jungels et al., 2013).

Several studies have focused on investigating the thermal-energetic performance of roofs, especially green roofs and insulated roofs. Green roofs are most common in Northern European countries as they enhance the effect of insulation and also save energy in hot and dry climates due to their thermal effect on heat transfer. The most significant feature of green roofs is the evapotranspiration effect of plants on the temperature and providing considerable cooling effect (Cascone et al., 2019) especially on the upper floors of buildings (Barrio, 1998). An examination of the thermal behaviour of an extensive green roof of a one-story building in Italy has been done by Gagliano et al.(Nocera et al., 2016) in which comfort level, energy consumption, and temperature reduction of green roof have been compared to a traditional roof. Results showed the maximum temperature drops from 54.5°C to 36°C for green roofs. Sailor (Sailor, 2008) ran a simulation in EnergyPlus Environment for a green roof in two cities with different climate conditions, the results showed green roofs improve electricity balance and increase gas consumption in winter. Following this model Silva et al.(Silva et al., 2016) examined the energy consumption of three types of green roofs and black and white roofs. The results showed the best roof solution is intensive one with 8cm of insulation and the worst solution is extensive without insulation. A four-story building has been examined based on cooling, heating, lighting, occupation, and mechanical ventilation by Ferrante et al.(Ferrante et al., 2015) and founding out that green roof had more stable temperature during the day and also better performance as well in energy saving during the whole year. They also concluded that energy saving in heating period is more than the cooling period (Silva et al., 2016). Zeng et al.(Zeng et al., 2017) developed an experimental simulation for the optimization of green roof features to optimize energy consumption; their results showed that the best thermal behaviour of the roof is achieved with the optimized thickness of the soil of 0.3 and Leaf Area Index (LAI) of 5. They have also proved that in hot arid climates green and cool roofs have the same results(Ávila-Hernández et al., 2020). Huang et al. (Huang et al., 2018) examined the heat gain reduction and temperature fluctuation reduction of four kinds of green roofs in subtropical climates. Collins et al. (Collins et al., 2017) investigated in an experimental set up the heat transfer reduction of bare and vegetated roofs in cold climates and especially when frozen. Another study, conducted by Jaffal and Ouldboukhitine (Jaffal and Ouldboukhitine, 2012) in France, proved that green roofs can be up to 6% effective in reducing energy needs(Congedo et al., 2020; Kalmár, 2016). There are other studies done in various climate conditions that have examined the functionality of green roofs in terms of thermal gain and their economic benefits. Economic feasibility of green roofs in different climates and various rainfalls and irrigation has been examined in a modern office building and the simulation showed that, in hot climates, green roofs reduce cooling demand and in cold climate green roofs lead to less heating demand (Ascione et al., 2013).

The majority of these studies were done using one-dimensional heat transfer simulations. However, recently, new methodologies were used to improve the analysis and calculation. But developing more advanced methods of multi-dimensional modeling is still necessary to yield results closer to the reality of the functionality of various roofing technologies in different climates.

Rooftop greenhouses are not a new subject. However, there are only a few studies on their feasibility and functions in comparison to other methods. Greenhouses can benefit urban areas providing food, energy, healthy environments, etc. There are many examples of this kind of roofs built during the last decade: Gotham Greens, with a 1394 m^2 roof area("Gotham Greens: Brooklyn's New High-Tech Rooftop Farm," n.d.), The Vinegar Factory, built-in 1993("The Vinegar Factory - Eli Zabar EliZabar.com," n.d.), Sky Vegetables, with a 743 m^2 area, built-in 2013 ("Sky Vegetables," n.d.), Public School ("NYC Rooftop Hydroponic Garden Classroom Urban Farm Greenhouse," n.d.), and Arbor House, with a 1000 m^2 rooftop greenhouse ("Developer Raises the Bar in the Bronx | Architect Magazine," n.d.) in New York, and Lufa Farms, built on a 31000 m^2 roof area, in Montreal. Also, there are many cases in Europe, such as inFarming of Fraunhofer, UMSICHT in Berlin, Newcastle University in the UK, The Hague of the UF002 De Schilde in Switzerland, the University of Barcelona in Spain, with a 128 m^2 area, and Ferme Abattoir in Paris. Rooftop greenhouses can be integrated into buildings and take advantage of their heat waste or assist their energy-saving by creating shading and insulation on the roof. Despite the various cases that were built over recent decades, there are just a few scientific studies that analysed their functions concerning the energy efficiency of buildings. In 2007, Caplow(Caplow and Nelkin, 2007) examined the integration of RGs into buildings as a means for cooling. Nadal et al.(Nadal et al., 2017) examined an actual case in the University of Barcelona from energy-need and carbon-emission standpoint, using EnergyPlus, and in a more recent study, he investigated the possibility of implementing RGs in a social housing neighborhood in Latin America (Nadal et al., 2019). The feasibility of using RGs in social houses in Tampines New Town for hydroponic farming has also been studied (Astee and Kishnani, 2010). Benni et al.(Benni et al., 2016) analysed the effects of roof and opening configurations on temperature reduction in a greenhouse in hot climatic conditions.

Although the local climate has a direct impact on the energy loads of a building, few studies have examined roofing scenarios in the context of the building. Most studies have been limited to macroscale climate modeling. However, there are many local parameters, such as the urban heat island effect in every urban area that can impact cooling and heating loads and actual local temperatures. Further attempts are needed to bring energy simulation results closer to reality.

Besides, simulation in one-dimensional models neglects some important parts of energy simulation and simplifies the heat transfer in different layers and shapes to remarkably reduce the simulation time. To overcome these limitations and achieve more realistic results, a two-dimensional hygrothermal simulation has been developed in WUFI by which water surface exposure, absorption, and intrusion are examined to model rainfall and irrigations and moisture in the roof materials. Besides, an accurate localized weather model has been developed to take into consideration the impact of urban context on microclimate conditions.

To accomplish this, the next section will explain the methodology and will review the details of hygrothermal calculation for green roofs and rooftop greenhouses. In Section 3, the results will be analyzed and the details of the simulation will be explained. Section 4 concludes the study with recommendations for future research.

2.4 Real-Time Micro-climate Modeling for Developing Green Scenarios

Rapid urbanization places additional demands on cities that are constrained to combat urban heat and further challenges in human health and well-being by altering the thermal properties of the area (Middel et al., 2021). Furthermore, the attainment of a livable urban environment is one of the measurements for sustainable urban development (Gholami et al., 2020). The growing urbanization raises many environmental challenges including urban heat, rate of air pollution, resource reduction, poor pedestrian level microclimate. These issues have persuaded governments to seek long-term solutions. In this context, a wide variety of methods and models have been developed to evaluate or forecast different aspects in the urban area separately. Various models have been proposed in different aspects such as evaluation of air quality modeling, climate comfort, energy balance on the city scale. However, cities consist of complex interdependent elements on different scales that affect their interactions(Cioara et al., 2021). This complex interconnectivity and dependency in city environments demand a unified approach to analyze urban climate issues comprehensively. However, urban climate models are still relatively oversimplifying in interpreting urban heating elements. As a solution, multilevel modeling is an appropriate approach for this concept, it allows to run of any number of single models as a part of a comprehensive model. A city model is based on a multilevel modeling approach and consists of various interdependent models that are considering different functions in an urban environment (Austin et al., 2020).

Generating a digital twin that is representative of the interdependent individual elements in the urban environments is not easy. The core of every digital twin is information technology that mainly includes data collection and analysis (Qi and Tao, 2018). Every digital twin is a virtual space for the integration of key components of urban infrastructures. digital twins are based on virtual models which propose real-world city environments (Cioara et al., 2021). Since the data is collected in real-time, the ability of the digital twin relies on the power of processing data flows (Zhou et al., 2019). digital twins perform change predictions and scenario modeling for what-if questions (Cioara et al., 2021).

A city digital twin is a series of interconnected digital twins representing certain aspects of the functioning of the urban environments. Every digital twin receives a continuous flow of data collected by sensors in real-time, analyses the data, and presents the outcome in various virtual models (Coelho et al., 2017). A city microclimate model should provide complementary and supportive roles in the collection and processing of micrometeorological data and automated modeling and it cannot be a context-free technology. Thus, a city microclimate digital twin provides complementary and supportive roles in the collection and processing of micrometeorological data, and automated microclimate modeling and represents urban climatic interactions virtually.

In comparison to the traditional simulations, digital twins benefit the decision-making process more effectively. While simulations may help through understanding what may happen when changes are introduced, a digital twin helps with understanding both what is currently happening and what may happen within a process. Besides, in traditional modeling datasets in statistical calculations become outdated, however, big data in DT can be processed in real-time and digital twin enhances the quality and speed up the decision making. So, Through the use of sensors or any kind of Internet of Things (IoT) system, digital twins can help build customized predictive maintenance workflows that guarantee accurate forecasting (Wright and Davidson, 2020)

Chapter 3 . Forecasting Energy demand in buildings on a neighborhood scale

3.1 Summary

This chapter aims at indicating and certifying the implemented framework for forecasting buildings' energy demand of the city of Bologna and Imola in Italy. Two different methods are considered for narrowing uncertainties in forecasting buildings energy demand in these two cities. The methods are developed through automated calibrations and are based on 7 known, physics-based building parameters and 6 unknown, and highly uncertain variables. The proposed methods focus on reducing computing time while keeping the accuracy of the output by narrowing the uncertainties in predicting unknown parameters.

To accomplish this task, in the first method, for the city of Bologna, 11 archetypes are defined which are representatives of the buildings in a specific neighborhood in Bologna, Italy. For calibration bayesian calibration is selected. bayesian inversion is responsive to many parameter estimation issues such as estimating unknown parameters and quantifying uncertainties. For every defined archetype, the most informative unknown variables are recognized and the Gaussian Process (GP) is employed to emulate the variable-to-data map. A wide sampling of the GP outputs is then applied by No-U-Turn Sampler (NUTS). The methodology is validated for 1156 Italian urban buildings based on the city database. The level of evaluation metrics demonstrates no bias in the output of the long-term forecasting while it accelerated the prediction of building energy demand and calibration on the city scale. The method is flexible for application in other contexts and various available urban datasets.

In the second section, since computation time is a serious obstacle for Urban Building Energy Modeling (UBEM) through Bayesian, a method is employed that provides a foundation for systematic Bayesian uncertainty quantification within UBEMs, which relies on the proven power of the Ensemble Kalman Inversion (EKI) method. To accomplish this, the methodology consists of one step for pre-processing of the urban dataset and 3 steps for parameter estimation, namely calibration, emulation, and sampling. calibration has implemented through EKI. Gaussian Process (GP) is employed to emulate the variable-to-data map. A wide sampling of the GP outputs is then applied by No-U-Turn Sampler (NUTS). two samples of the archetypes representing 2-storey and 4-storey buildings in a specific neighborhood in the city of Bologna, Italy.

Abbreviation:

A: Roof Surface [m2]

ε: Thermal emissivity [–]

F: Net heat flux [W·m−2]

Is: Total incoming short wave radiation [W·m−2]

r: Solar reflectance

ε1: View factor

η: Efficiency

p: Density of air [kg·m−3]

σ : Stefan-Boltzmann constant [W·m−2·K−4]

Is: Total incoming longwave radiation [W·m−2]

H: Sensible heat flux [W·m−2]

L: Latent heat flux [W·m−2]

k: Dry soil thermal conductivity [W·m−1·K−1]

T: Temperature [K]

t: Time [h]

P_{sat}: Saturation pressure [Pa]

h: Enthalpy [J·m−3]

FKD: Fest Körper Dränagen(Firm Body Drainage)

LAI: Leaf Area index

HVAC: heating, ventilation, and air conditioning
UBEM: Urban Building Energy Modeling

GP: Gaussian Process

NUTS: No-U-Turn Sampler

Hamiltonian Monte Carlo (HMC)

Latin Hypercube Sampling (LHS)

σ f: Fractional vegetation coverage

δ_p: vapour permeability

∇: gradient of a divergence

λ: Fictitious thermal conductivity

Subscripts

v: Relative to vapour

g: Soil layer

f: Foliage layer

sat: Saturation

3.2 Contribution of this chapter

As mentioned in the state of the art of this study, UBEM approaches have been significantly enhanced during the last decade. Yet, several unsolved issues exist in automated calibration approaches. UBEM calibration is still intensive in computation, the reason is that it is usually non-linear and multi-modal such that calibration methods easily fail to be accurately processed. Unknown parameters differ from building to building depending on the building's properties and human behavior. Common methods in individual building calibration are not enough responsive on urban scales. The reason is that there are several unknown parameters on city-scale such as outdoor air temperature or the last date of interior renovations. The challenge becomes more complicated when the number of unknown parameters in calibration increases. Furthermore, although meta-models are supposed to ease the calibration process, they become heavy in processing since the number of sampling and evaluation of variables combination affects the validity of outcomes.

Hence, to address the above-mentioned issues, a UBEM calibration technique has been proposed in this study that employs a coding method for classifying archetypes to cope with hundreds of buildings on the city scale. This approach is developed to ensure the distinction between informative and uninformative parameters and to reduce the computation time and cost for city governments while maintaining the robustness of calibration in UBEM calibrations. In this paper, the proposed technique will answer the main questions as follows:

- How to develop a long-term urban-scale tool for energy demand prediction considering informative parameters for cost-effective retrofitting strategies?
- How to integrate hundreds of buildings in one UBEM calibration while considering different unknown parameters for every building with computation efficiency and reliability?

- How to strengthen UBEM calibration considering the computational burden in large-scale UBEM calibration?

3.3 Method 1: Bayesian calibration

Materials and methodology:

Hence, to address all the above-mentioned factors, the methodology is proposed in 4 steps as shown in Fig 3.1. The methodology consists of 3 key features; first, coding urban archetypes to enhance the time efficiency of computation, second, sampling the data in an equal probability distribution to ensure the combination coherency in all dimensions, and lastly, the involvement of informative data to optimize the complexity of calibration and minimize the error in the evaluation process. The details of the important improvements in the proposed method will be discussed in the related subsections. The proposed methodology needs various modelings and coding engines. In the pre-process steps QGIS was employed to identify buildings on the map and link the geometrical features to the shapefile. The model was more developed in Rhinoceros 7 (McNeel, 2021) and the energy models for every archetype were run by EnergyPlus (U.S. Department of Energy, 2020) through the Grasshopper interface, automation and result collection were performed using Matlab codes (Mathworks, 2017). R-programming was employed to code the main process of calibration and to export the outcomes and results.

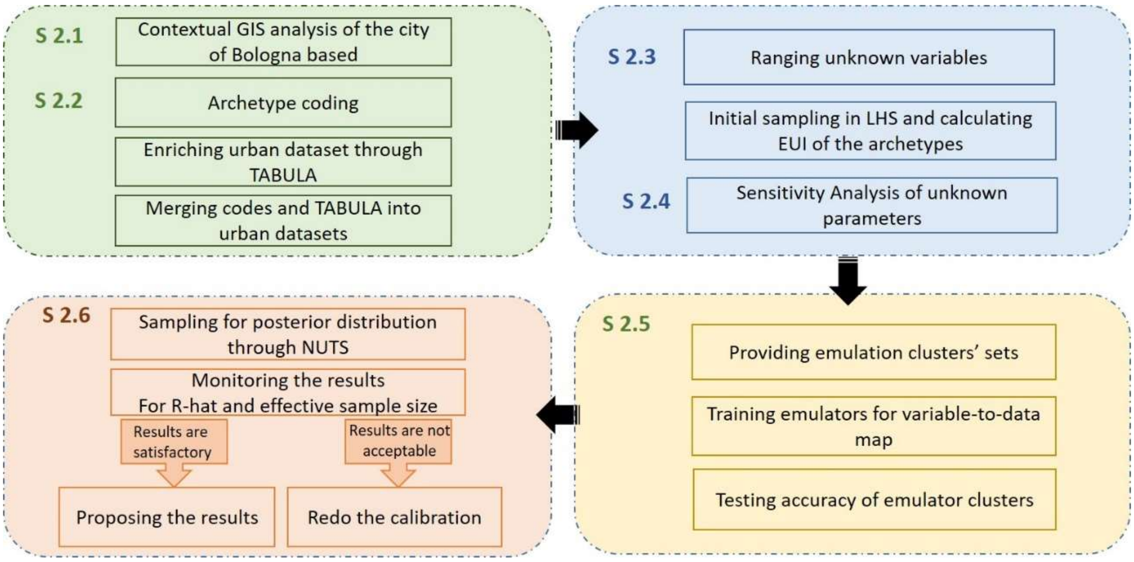

Figure 3.1: The proposed methodology in 4 steps

3.3.1 Developing a GIS database

The input database of the methodology relies upon the accessibility of data, but the contextual analysis of the urban area is based on the GIS database of the existing buildings. In this step, a GIS database is proposed where the buildings are characterized based on definite features consisting of building construction period, building function, number of floors, net floor area, conditioned floor area, ceiling height, building surface area, and perimeter. These building properties are available in municipal urban datasets. The dataset was then enriched through TABULA which is a source for building archetypes available for several European countries. In this methodology, a specific TABULA (Corrado et al., 2012) for the classification of Italian buildings is employed. TABULA classifies urban buildings based on their properties and energy systems. To consider the renovation conditions of the buildings, the official dataset of the municipality has been employed as a reliable and updated source. The GIS shapefile is then merged into this database and every parcel is associated with a building in the district. Fig 3.2 illustrates the 3 steps for developing GIS datasets. Then, six uncertain parameters were selected to be integrated into geo-referenced data. Table 3.1 shows these parameters.

Table 3.1: Uncertain parameters and their range for the initial calibration process

Num	parameter	Short Names	Prior Probability Distribution	Units
1	Infiltration	INF	0-1.5	ACH[1]
2	Occupant density	OCC	15-25	M^2/PP [2]
3	Heat set point	HSP	15-25	°C
4	Cool set point	CSP	23-29	°C
5	Equipment power density	EPD	11-15	W/m^2
6	Domestic hot water flow	DHW	$(1\text{-}20) \times 10^{-8}$	$m^3/s/m^2$

[1] Air Change per Hour
[2] Square Meter Per Person

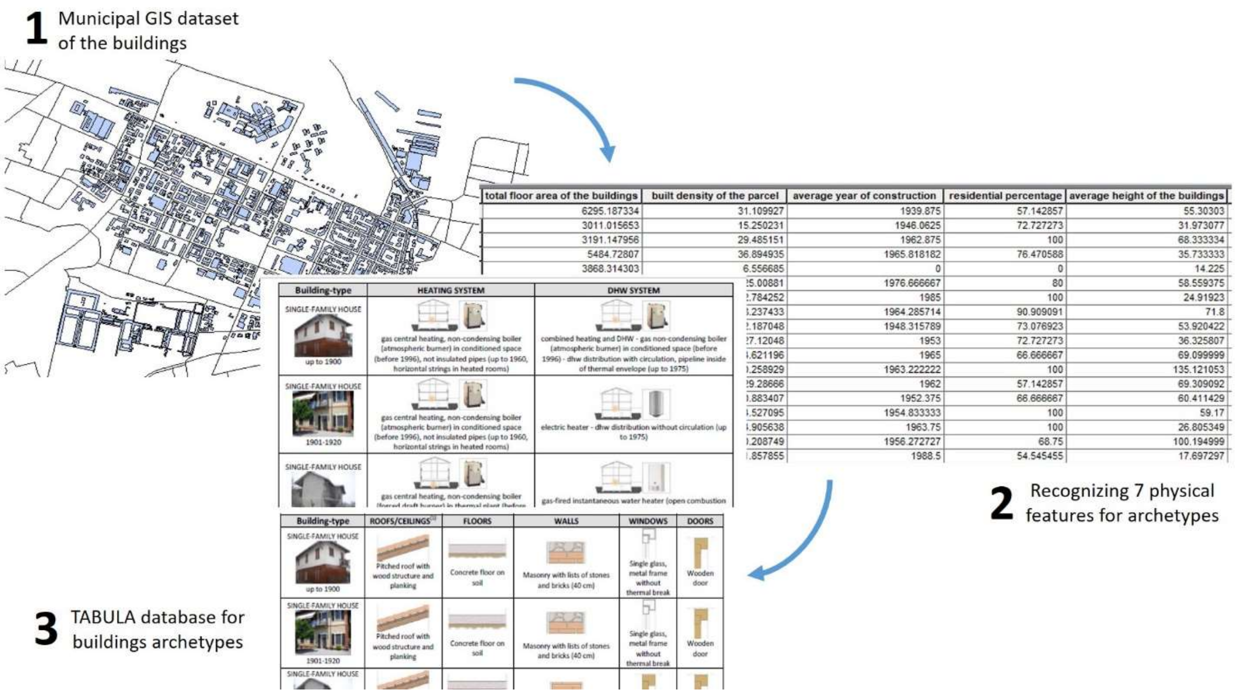

Figure 3.2: Developing GIS database in three steps; step 1: extracting Bologna municipal GIS database, step 2: defining building properties, step 3: enriching urban dataset by TABULA

3.3.2 Archetype coding

To define representative buildings in the neighborhood, a two-steps coding algorithm is designed to generate urban building archetypes. In the first step, each archetype will be classified by seven definite parameters such as function, age, orientation, construction type, window-wall-ratio, and heating and cooling systems of the buildings as it is illustrated in Table 3.2 It should be noted that geometric parameters of the building are not included in the archetype coding since the 3d geometry will be considered in the white box energy modeling in EnergyPlus and their specific context. In the second step, six highly uncertain variables (introduced in Table 3.2) will be defined within specific ranges and the calibration process in the next steps will define the values of the uncertain variables for every archetype. Table 3 shows the coding guideline of the building, for example, code A1234512 shows that this building is a residential, built-in 1901-1920, a multi-family house, with Northeast- Southwest orientation, and 40-50% window-wall-ratio, facilitated with "gas central" heating system and "combined heating and DHW system" as the DHW system.

Table 3.2:Classification of known and physics-based features

Archetype coding	**Function**	**Building age**	**Building type**	**The orientation of facades with openings**	**WWR**	**Heating system**	**DHW system**
1	Residential	Before 1900	Single-family house	East-West	Less than 10%	Gas-central heating	Individual DHW sys per apartment

2	Office	1901-1920	Terraced house	South-North	10-20%	Gas-decentral-heating	Combined heating and DHW
3	Retail	1920-1946	Multi-family house	Southeast-Northwest	20-30%		Gas-fired instantaneous water heater
4	Hospital	1946-1960	Apartment Block	Northeast-Southwest	30-40%		Gas central DHW system
5	School	1961-1975		All orientations	40-50%		
6	Hotel	1976-1990			50-60%		
7		1991-2005			60-70%		
8		After 2006			70-80%		

3.3.3 Initial value setting and sampling of initial calibration

After archetype identification, a set of values should be generated as prior distribution set for training the model. To ensure robust performance, the set of samples must cover the full training range equally. In the proposed methodology, Latin Hypercube Sampling (LHS) has been employed. LHS can generate different realizations of dependent random variables with any probability distribution shape. An N-dimensional LHS ensures that every combination of N conditions is sampled equally, while it is likely that a random sampling pattern misses a few combinations of conditions and samples other combinations more than once per repetition.

3.3.4 Sensitivity analysis

To identify influential parameters on the building energy demand among six uncertain parameters, a sensitivity analysis should be calculated for every archetype separately since parameters' ranks can vary from one archetype to another depending on the known parameters. This study employs standardized regression and random forest importance variables to consider linearity and non-linearity variation of the data for ranking the importance of the parameters based on the annual energy consumption of archetypes. R sensitivity package (Bertrand Iooss et al., 2020) has been used in this study for bootstrapping and calculation of the intervals of sensitivity index.

3.3.5 Emulation

Due to the complexity of building energy modeling in iterative calibration, a surrogate is employed to reduce the computation time. GP model has been selected for this step to combine simulated and observed data. For a GP emulation, a mean (η) and a covariance (δ) functions should be defined for field measured parameters (x) with p number, and the target parameter for calibration (u) with q number. To do so, the equations are:

$$\textstyle\sum_{\eta,mn} = \frac{1}{\lambda_\eta}\, exp\{-\sum_{k=1}^{p} \beta_\kappa^\eta\, |x_{nk} - x_{mk}|^\alpha - \sum_{k'=1}^{q} \beta_{p+k'}^\eta |u_{nk'} - u_{mk'}|^\alpha\} \quad (1)$$

$$\textstyle\sum_{\delta,mn} = \frac{1}{\lambda_\delta}\, exp\{-\sum_{k=1}^{p} \beta_k^\delta\, |x_{nk} - x_{mk}|^\alpha\} \quad (2)$$

Where:

λ_η is the precision hyper-parameter

$\beta_1,\ldots, \beta_{p+q}$ correlation hyper-parameter

The last equation for calculating the relationship between observation parameters (x) and prediction parameters (u) is the vector z with this definition below:

$$\mathcal{L}(z\,|u, \beta^\eta, \lambda_\eta, \beta^\delta, \lambda_\delta, \lambda_\varepsilon) \propto |\Sigma_z|^{-1/2} \exp\left\{-\frac{1}{2}\,(z-\mu)^T \Sigma_Z^{-1}(z-\mu)\right\} \quad (3)$$

$$\Sigma_z = \Sigma_\eta + \begin{bmatrix} \Sigma_\delta + \Sigma_y & 0 \\ 0 & 0 \end{bmatrix} \quad (4)$$

Σ_η matrix of the mean (η) in the GP which is the output of equation 1

Σ_δ matrix of the covariance δ in the GP which is the output of equation 2

Σ_y is the matrix of observation error

So, the joint posterior probability relies on GP correlation hyper-parameters and precision hyper-parameters, and prediction parameters (Chong and Menberg, 2018).

3.3.6 Calibration

Bayesian calibration (Equation5) has been employed to analyze the uncertainty in every archetype, the analysis was carried out through a formulation introduced by Kennedy and O'Hagan (Kennedy and Hagan, 2001). The six unknown parameters will go through the calibration process to demonstrate whether the outputs of the simulation are compatible enough with observed data. The Bayesian inference equation is as follows:

$$P(u|x, M) = \frac{P(x|u, M) .\ P(u|M)}{P(x|M)} \quad (5)$$

Where:

x is the observed data

u is the target uncertain parameter

M is the building energy model

For posterior distribution to ease sampling No-U-Turn Sampler (NUTS), an extension of the Hamiltonian Monte Carlo (HMC) for the MCMC sampling has been selected(Betancourt, 2018).

In this paper, separate GP models have been employed to emulate the simulator and the discrepancy. The trained emulators will be new clusters for the next step of correlation. The iteration number was set to 40,000 and validation has been proceeded by one data set from the test data and has been considered as the target archetype code. The assessment was achieved through the Coefficient of Variation of the Root Mean Squared Error (CVRMSE, Equation 6) and the Mean Absolute Percentage Error (MAPE, equation 7).

$$CVRMSE = \sqrt{\frac{\frac{\sum_{t=1}^{n_t}(y_t - y_t^*)^2}{n_t}}{\bar{y}}} \tag{6}$$

$$MAPE= \frac{\sum_{t=1}^{n_t}\left|\frac{y_t - y_t^*}{y_t}\right|}{n_t} \tag{7}$$

3.4 Step-wise description of the method implementation in the city of Bologna

The case study of this thesis is the building stock in the Saffi area in the Saragozza-Porto quarter of the city of Bologna. 1156 buildings have been classified into 11 representatives. The input data is collected through the municipality of the city of Bologna, ARPAE Emilia-Romagna (ARPAE, 2020), local weather data, and some other public datasets in urban databases.

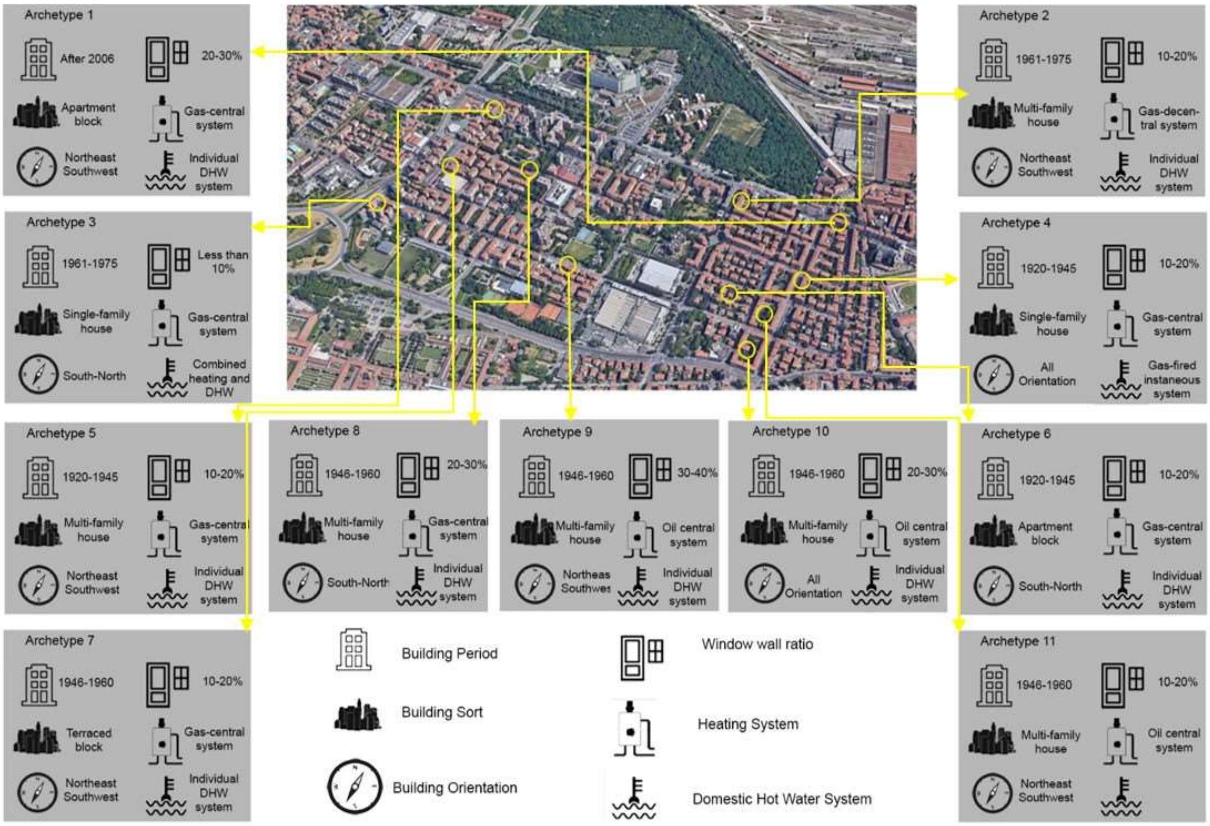

Figure 3.3: Identification of the 11 archetypes and the sampled building for every archetype

3.4.1 Developing a GIS database

For this case study, the municipality of Bologna has provided a dataset for the case studies of this UBEM, which includes (a) Building geometry; consisting of the 3d shape and characteristics of the buildings from the GIS Shapefile. (b) Features of the building; overview of the building's conditioning and heating systems, restoration dates, exterior conditions and openings, type of the fuel used, as well as materials for façades. Fig 2 shows the steps for developing the GIS dataset for the city of Bologna. For energy simulation, an hourly weather file based on the year 2019 dataset from a local weather station near the selected neighborhood was employed. TABULA (Corrado et al., 2012) has been considered as the source of the properties for archetypes' materials and also conditioning systems of the buildings and lastly, the generated dataset has been modified with the latest changes in the neighborhood based on the official GIS file of the municipality.

3.4.2 Archetype coding

The buildings in the neighborhoods have been classified through the archetype coding algorithm. archetypes are defined according to Table 3.2 Table 3.4 shows the properties of every archetype. Based on the generated code and properties, every building will be simulated in EnergyPlus, and Energy Use Intensity (EUI) for every archetype is calculated.

3.4.3 Initial value setting and sampling of initial calibration

A total of 400 sets of unknown parameters are sampled employing the LHS. From this list, 300 samples were used for training the model and 100 for testing it. The samples were then simulated in EnergyPlus to calculate EUI. The annual gas and electricity usage (kWh/m^2) of every archetype is illustrated in Fig 3.4. Gas usage is limited to the heating and DHW systems due to the data availability. As Fig 3.4 shows, the minimum gas usage belongs to archetype 1. The reason is probably the material properties of this archetype, as it is demonstrated in Table 3.3 the materials' R-value of archetype 1 is higher than other ones. On the other hand, archetype 2 has the highest level of gas consumption. Besides, the electricity consumption of all the archetypes is at the same level, except in archetypes 1 and 2 that consume the lowest and highest electricity.

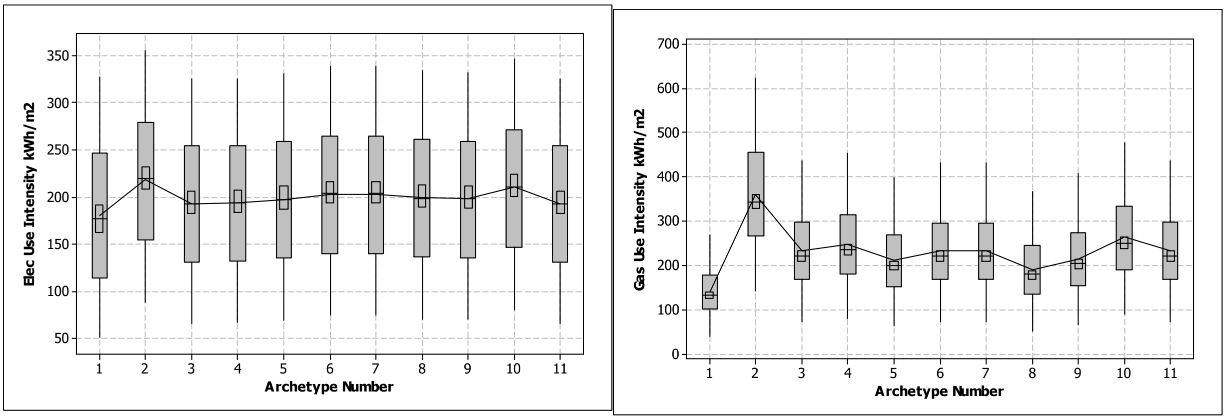

Figure 3.4: Annual Energy Usage Intensity of the archetypes, Electricity Use Intensity in left and Gas Use Intensity in right

3.4.4 Sensitivity analysis

As mentioned in section 2.4, sensitivity analysis in this study is calculated through two different methods: standardized regression coefficient and random forest variable importance. Electricity, gas, and total energy usage data of archetypes are employed to rank every parameter. Fig 3.5 shows the results of sensitivity analysis based on annual datasets. The results show the dominant parameter varies in different archetypes. EPD and CSP are constantly the most dominant parameters in electricity consumption in all the archetypes. On the other hand, the importance ranks for HSP, EPD, and OCC are the highest for gas usage in all the archetypes. The least important parameters in both gas and electricity usage are DHW and INF. However, the ranking figure for annual energy usage shows a stable trend. The four most important parameters in this ranking are EPD, HSP, CSP, and OCC, while DHW and INF have the least impact on annual energy consumption in all the archetypes. This ranking eases the calibration process, for instance, we know in the calibration of gas energy usage, the DHW does not significantly affect the model.

Table 3.3:Identification of the 11 defined archetypes based on the property details

Component	Input Parameters	Arch 1	Arch 2	Arch 3	Arch 4	Arch 5	Arch 6	Arch 7	Arch 8	Arch 9	Arch 10	Arch 11
Envelope	Gross floor area	832	299	594	335	301	678	673	388	254	196	594
	Floor levels	7	4	4	4	4	5	5	4	4	3	5
	Room height	2.8										
	Gross Volume	17871	1646	11076	3750	3160	2818	5120	6197	4337	1975	11076
	Window to wall ratio	20-30%	10-20%	Less than 10%	10-20%	10-20%	10-20%	10-20%	20-30%	30-40%	20-30%	10-20%
	Thermal Zoning	Central zone and perimeter zones										
	R-Value floor	2.88	0.89	0.89	0.11	0.11	0.4	0.4	0.4	0.4	0.4	0.4
	R-Value Roof	2.88	0.89	0.89	0.11	0.11	0.4	0.4	0.4	0.4	0.4	0.4
	R-Value Wall	3.34	0.5	0.5	0.47	0.47	0.57	0.63	0.63	0.63	0.63	0.63
	U-Value Windows	2.87	2.87	5.55	5.05	5.05	5.55	5.05	5.05	5.05	5.05	5.05
	Solar heat gain coefficient SHGC	0.35	0.5	0.5	0.5	0.5	0.5	0.5	0.5	0.5	0.5	0.5
HVAC systems	DHW system	Individual DHW sys per apartment	Individual DHW sys per apartment	Combined heating and DHW	Gas-fired instantaneous water heater	Gas central DHW system	Gas central DHW system	Individual DHW sys per apartment	Individual DHW sys per apartment	Individual DHW sys per apartment	Individual DHW sys per apartment	Individual DHW sys per apartment
	Heating system	Gas-central heating	Gas-decentral-heating	Gas-central heating	Gas-central heating	Gas-central heating	Gas-central heating	Gas-central heating	Gas-decentral-heating	Oil central heating	Gas-central heating	Gas-central heating

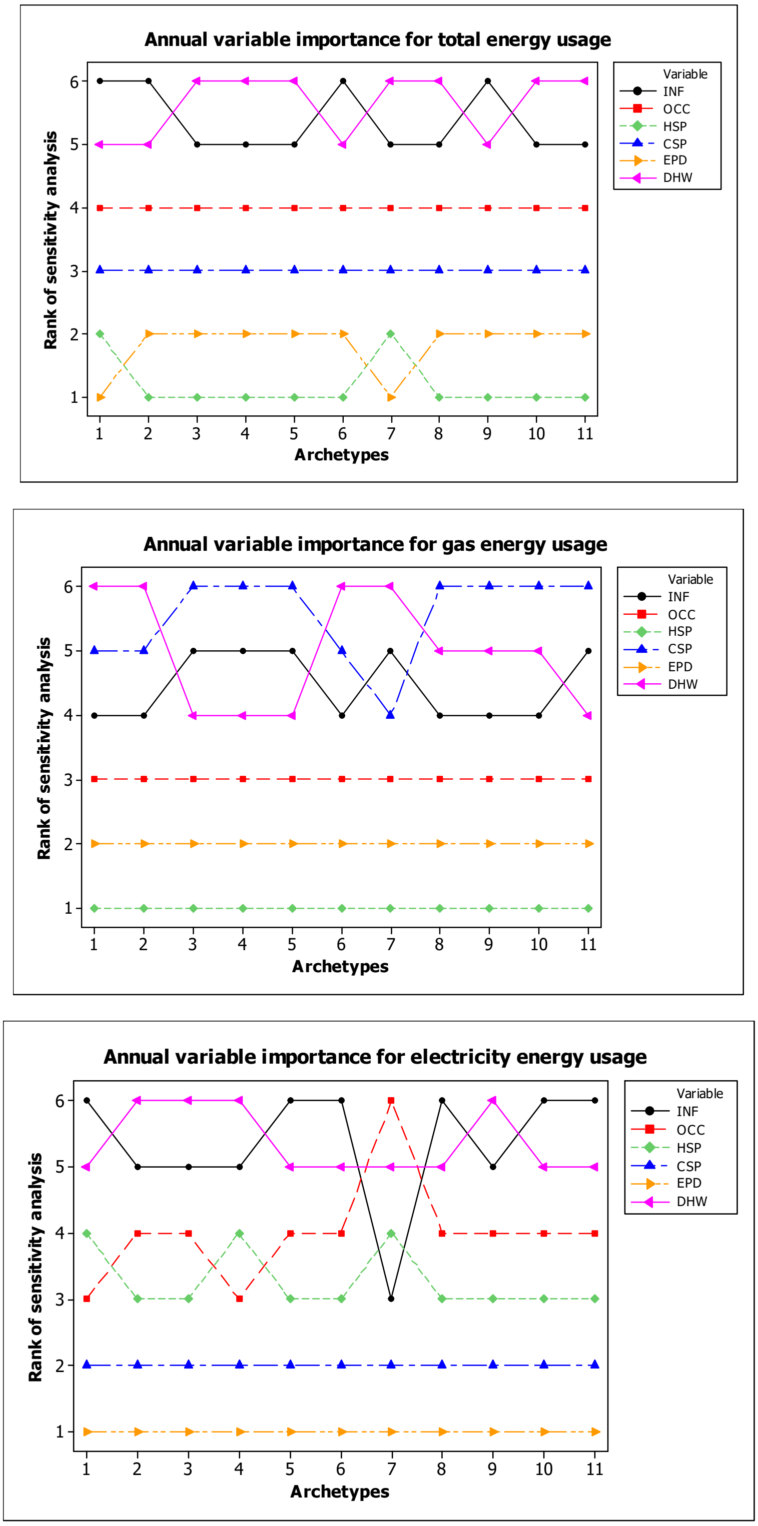

Figure 3.5: The results of the sensitivity analysis for six highly uncertain parameters

3.4.5 Calibration

After listing the uncertain variables and ranking them, the calibration starts with the GP. As it is described in section 2.5, GP trains an emulator to produce a combined set of observations and simulation data. The output of this step will be a group of emulators by which the calibration is assessed later. HMC is applied for drawing samples out of the posterior distribution of parameters. The sampling is being iterated until a desired number of samples is collected.

The prior and posterior distributions of six uncertain variables are shown in Fig 3.6. One archetype from every period of the archetypes is selected to illustrate the density in both prior and posterior distributions. The blue line demonstrates prior distribution and the red line shows the posterior distribution. It is noteworthy that when a parameter is not an informative variable for the calibration, it shows a wider distribution for that archetype. Therefore, in archetype 1, DHW and EPD are the most informative variables, these results are in accordance with the R-value of the construction properties in Table 3.3 that shows the R-value of the materials for this archetype is lower than other archetypes. On the other hand, CSP and HSP are the most informative parameters for archetype 6 which is the oldest building archetype (1920-45). In all the defined archetypes, CSP is the most effective parameter.

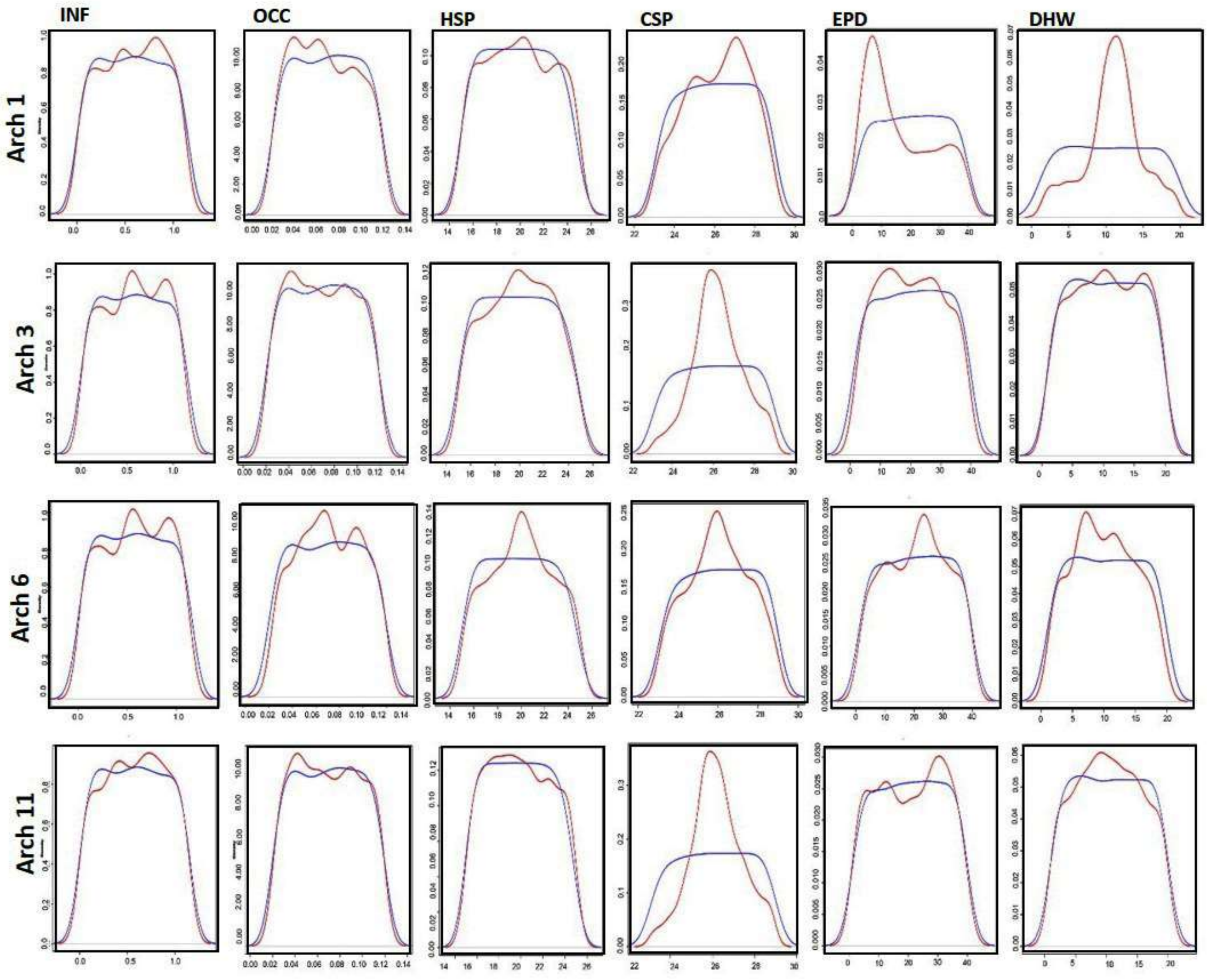

Figure 3.6: prior and posterior distribution of 4 archetypes, every archetype belongs to a specific built period for the sake of comparison. The X-axes show the value of the variable and the Y-axes show the density of the distribution. The blue line belongs to prior distribution and the red line stands for the posterior distribution

The results of the calibration process are shown in Fig 3.7. Each histogram shows the prior and posterior predictive distribution of EUI values. The EUI values of posterior predictive estimations (y_{pred}) in the histograms are based on 1000 draws out of the posterior predictive distribution for every archetype. It is noteworthy that the range of the EUI values of the archetypes has been limited by the illustration frame of the prior distribution. In most of the histograms, the ranges for the prior distributions are compatible with the predictive values of EUI, however, for archetype 2 the predictive range of EUI (y_{pred}) is not quite into the defined axes by the prior distribution. Possibly, the reason is the poorly designed excitation signals in the training that can happen in a data-driven model or simply the prior definition of the training set is not well suited to the actual data.

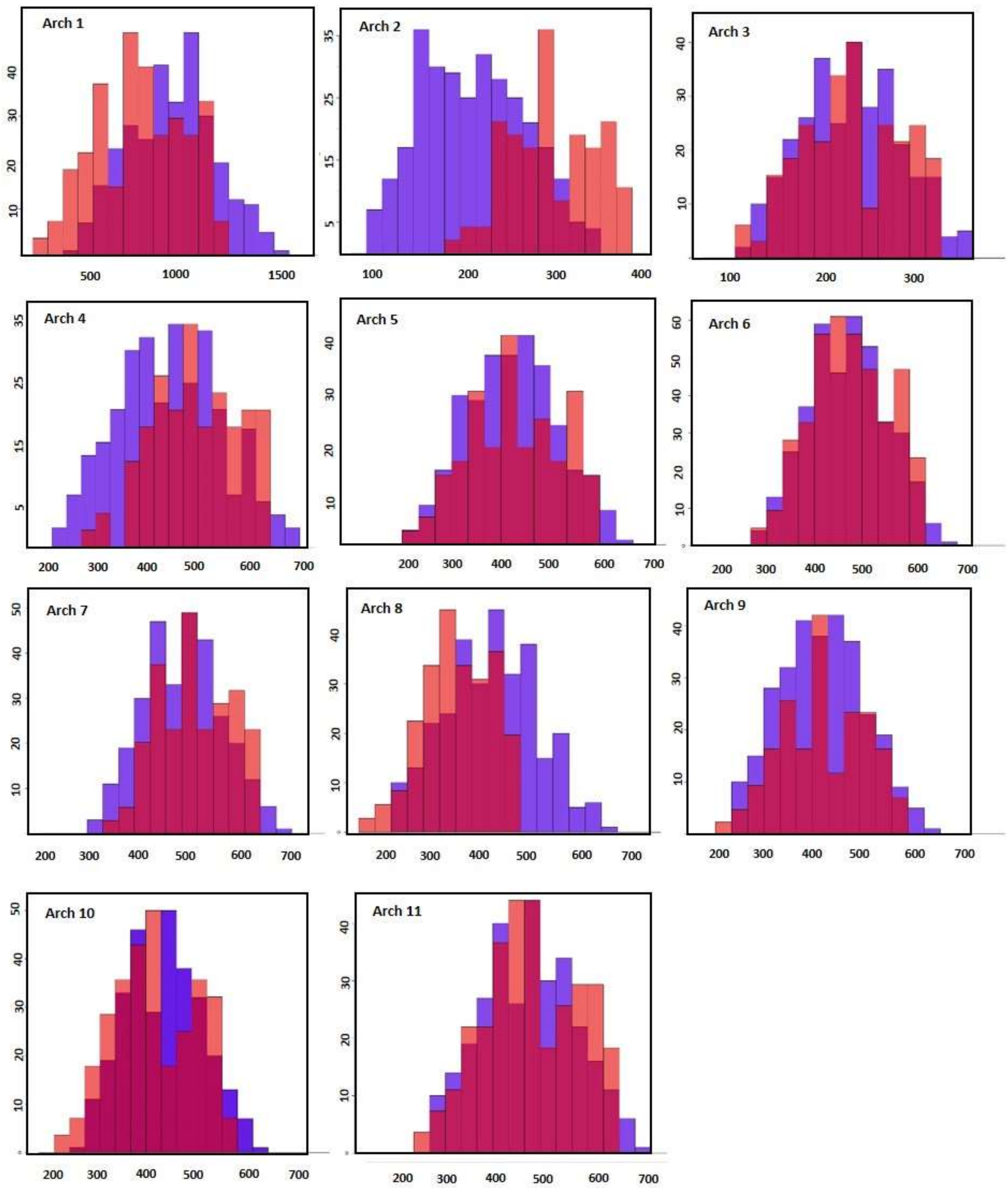

Figure 3.7: prior and posterior predictive distribution of EUI values. Predictive estimations (ypred) are based on 1000 draws out of the posterior predictive EUI. The X-axes show the value of the EUI and the Y-axes show the frequency of the distribution. The blue columns illustrate prior EUI values and the red columns show the predictive values for EUI.

3.5 Evaluation of model performance

The accuracy of the method for forecasting the EUI corresponded to every archetype was tested through random draws out of the y_{pred} from the posterior distribution. The evaluation for each archetype was performed on its building energy model and specific building properties. The archetypes are evaluated through two methods, the Coefficient of Variation of the Root Mean Squared Error (CVRMSE) and the Mean Absolute Percentage Error (MAPE) as illustrated respectively in equations 2 and 3. MAPE is a measure of error, an acceptable range for an excellent forecast in MAPE is less than 10%. However, based on the ASHRAE guideline the acceptable range for CVRMSE for energy prediction is less than 15% (Shailza, 2018).

Fig 3.8 shows the variation of energy prediction from the actual values of EUI based on CVRMSE and MAPE. The CVMRSE of all the archetypes is less than 0.5% except Archetype 1. This archetype is a new-built building model that is simulated based on TABULA (Corrado et al., 2012). The reason for this gap could be simply a difference in the defined structure, R-value of the materials in practice and simulations, or imprecise defined ranges for unknown parameters in input data.

The outputs of MAPE also show the same results for Archetypes 6 and 1. To achieve a better understanding of the evaluation results, probably it is helpful to calculate the level of accuracy for the variables in the archetypes.

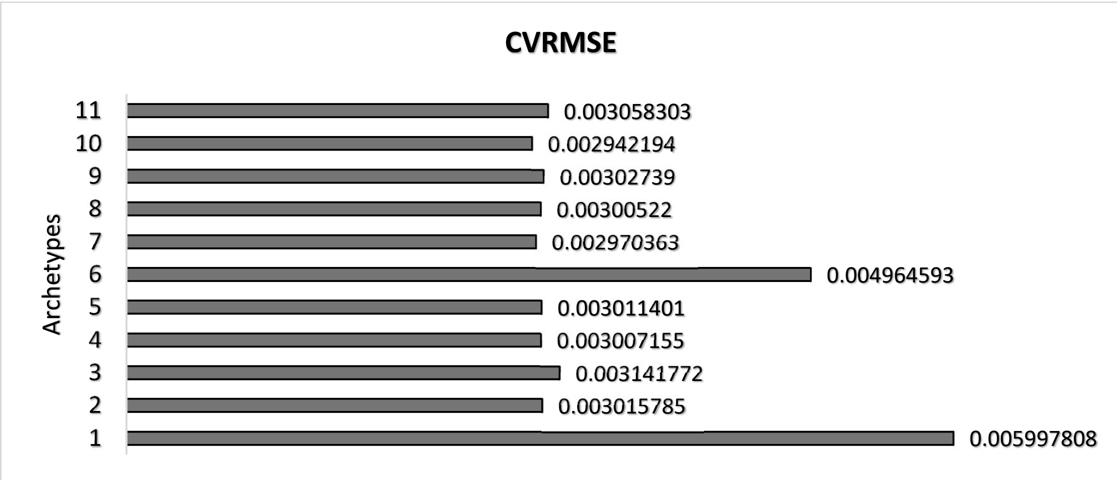

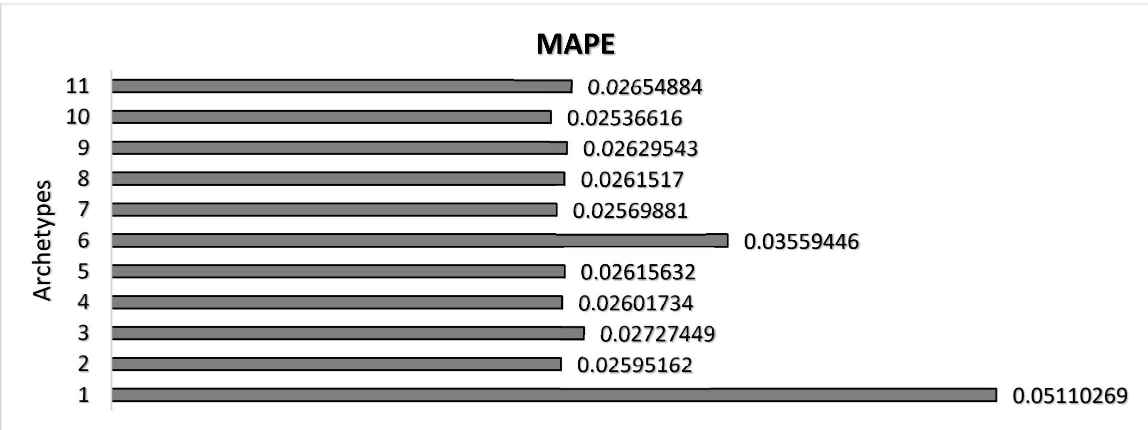

Figure 3.8: Performance metrics of the 11 defined archetypes for energy demand forecasts of the training buildings and testing buildings

Fig 3.9 shows the CVRMSE of the 6 unknown variables for every archetype in 1000 draws of the posterior distribution and the measured values. The results show that HSP and CSP are the most accurate estimated parameters in almost all the archetypes. The CVRMSE for OCC alternates in the different archetypes from 0.0035 in archetype 4 to 0.65 in Archetype 1. This means that the model is not precise in predicting the occupancy density in most of the archetypes. The results show that archetype 1 demonstrates the highest level of error in all the six variables among the archetypes. The reason is probably due to the large floor area in this archetype that has reduced the level of accuracy in modeling zones, heating and conditioning systems, and also the level of insulation.

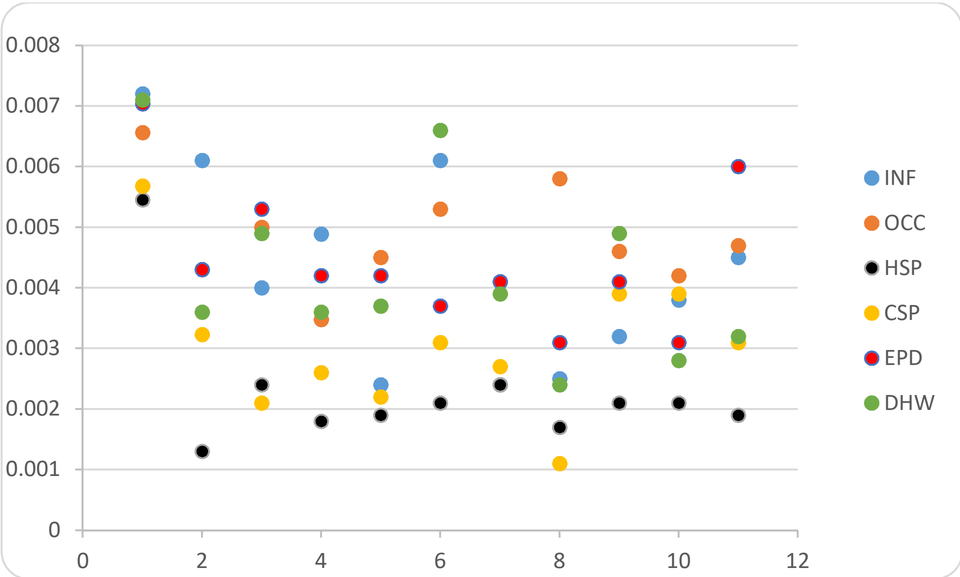

Figure 3.9: Performance metrics of the 6 uncertain variables in the 11 archetypes

3.6 Method 2 : Ensemble Kalman

Materials and methodology:

3.6.1 Developing urban building database

While forming the database for the methodology relies on the accessibility of data, the contextual analysis of the urban area is based on the GIS database of the existing buildings. For this case study, the municipality of Bologna has provided a simple dataset for the case studies of this UBEM, which includes (a) Building geometry; consisting of the 3d shape and characteristics of the buildings from the GIS Shape file. (b) Features of the building; overview of the building's conditioning and heating systems, restoration dates, exterior conditions and openings, type of the fuel used, as well as materials for façades, and (c) Weather data; an hourly weather file based on the year 2019 dataset from a local weather file near the selected communities was used.

TABULA (Corrado et al., 2012) was considered as the source of archetypal material properties and building conditioning systems, and finally, the created dataset was modified with the latest changes in the neighborhoods. In the next step, for finding representative buildings in the neighborhood, a two-step coding algorithm generates urban building archetypes. In the first step, each archetype will be classified by seven definite parameters such as building construction period, building function, number of floors, net floor area, conditioned floor area, ceiling height, building surface area, and perimeter, as it is shown in Table 3.2 It should be noted that geometric parameters of the building were not included in the archetype coding since the 3d geometry will be considered in the white box modeling and their specific context.

The dataset was then enriched through TABULA which is an archetype European source, specifically designed for the classification of Italian buildings. To consider the renovation conditions of the buildings, the official dataset of the municipality has been regarded as a reliable and updated source. The GIS shape file is then merged into this database and every parcel is associated with the entire buildings of the district. Then, six uncertain parameters were selected to be integrated into geo-referenced data. Table 3.1 shows these parameters.

A monthly thermal simulation will then calculate the energy demand of every archetype code and will provide the required datasets for the Bayesian calibration.

3.6.2 Calibration:

One of the widely employed methods to estimate unknown parameters in inverse problems is the ensemble Kalman Filter (EnKF). Since, EnKF can keep the efficiency in high dimensional parameter spaces such as urban energy modeling (Schillings and Stuart, 2017). In the first step of parameter

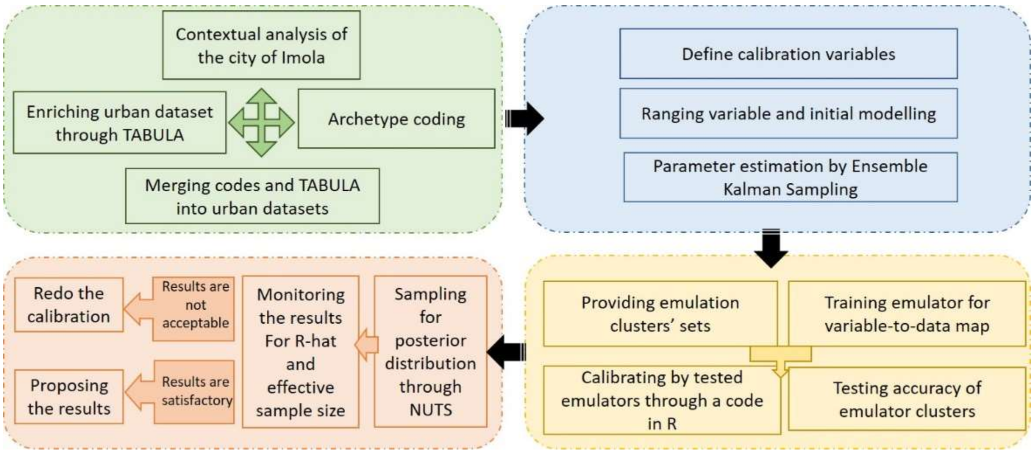

Figure 3.10: The proposed methodology in 4 steps

estimation, the employed equation to achieve the desired posterior distribution is as follows:

$$D\mathcal{G}(u^{(j)}(u^{(k)} \ - \overline{u}) \approx (\mathcal{G}(u^{(k)}) - \mathcal{G}) \qquad (1)$$

Where

$\mathcal{G}$: $R^d \rightarrow R^k$ is a known non-linear forward operator (here is energy modeling process)
u: $\in R^d$ here is the unknown parameter
ū: mean of the unknown parameter
The algorithm introduced by (Kovachki and Stuart, 2019) to create a derivative-free Kalman algorithm for producing samples of the posterior distribution is as the following:

$$\dot{u}^{(j)} = -\frac{1}{J}\sum_{k=1}^{J}\langle \mathcal{G}(u^{(k)}) - \mathcal{G}, \mathcal{G}(u^{(j)}) - y\rangle\, u^{(k)} - C(U)\Gamma_0^{-1}u^{(j)} + \sqrt{2C)U)}\,\dot{W}^{(j)}$$
(2)

Where

$\dot{W}$: is a standard Brownian motion in R^d

Γ: is a known covariance matrix, $\Gamma \in R^{K*K}$

C(U): is the empirical covariance between parameters

To utilize this algorithm for the parameter estimation, based on a linear implicit split-step discretization, the ultimate algorithm that has been employed is as follows:

$$u_{n+1}^{(*,j)} = u_n^{(j)} - \Delta t_n \frac{1}{J}\sum_{k=1}^{J}[\mathcal{G}(u_n^{(k)}) - \mathcal{G}, \mathcal{G}(u_n^{(j)}) - y]\Gamma\, u_n^{(k)} - \Delta t_n C(U)\Gamma_0^{-1}u_{n+1}^{(*,j)} \quad (3)$$

$$u_{n+1}^{(j)} = u_{n+1}^{(*,j)} - \sqrt{2\Delta t_n C(U_n)\xi_n^{(j)}} \quad (4)$$

The pseudo-code for the Ensemble Kalman Sampling (EKS) is taken from a step-by-step algorithm in (Albers et al., 2019)

3.6.3 Emulation:

Due to the complexity of UBEM in iterative calibration, a surrogate is employed to reduce the computation time. GP model has been selected for this step to combine simulated and observed data.

For a GP emulation, a mean (η) and a covariance (δ) functions should be defined for field measured parameters (x) with p number, and the target parameter for calibration (u) with q number. To do so, the equation is:

$$\sum_{\eta,mn} = \frac{1}{\lambda_\eta}\, exp\{-\sum_{k=1}^{p}\beta_\kappa^{\eta}\, |x_{nk} - x_{mk}|^{\alpha} - \sum_{k'=1}^{q}\beta_{p+k\prime}^{\eta}|u_{nk\prime} - u_{mk\prime}|^{\alpha}\}$$
(5)

$$\sum_{\delta,mn} = \frac{1}{\lambda_\delta}\, exp\{-\sum_{k=1}^{p}\beta_k^{\delta}\, |x_{nk} - x_{mk}|^{\alpha}\} \quad (6)$$

Where:

λ_η is the precision hyper-parameter

$\beta_1,\ldots,\beta_{p+q}$ correlation hyper-parameter

The last equation for calculating the relationship between observation parameters (x) and prediction parameters (u) is the vector z with this definition below:

$$\mathcal{L}(z\,|u,\beta^{\eta},\lambda_{\eta},\beta^{\delta},\lambda_{\delta},\lambda_{\varepsilon}) \propto |\Sigma_z|^{-1/2}\exp\left\{-\frac{1}{2}(z-\mu)^T\Sigma_Z^{-1}(z-\mu)\right\}$$
(7)

$$\Sigma_z = \Sigma_\eta + \begin{bmatrix}\Sigma_\delta + \Sigma_y & 0\\ 0 & 0\end{bmatrix} \qquad (8)$$

Σ_η matrix of the mean (η) in the GP which is the output of equation 5

Σ_δ matrix of the covariance δ in the GP which is the output of equation 6

Σ_y is the matrix of observation error

So, the joint posterior probability relies on GP correlation hyper-parameters and precision hyper-parameters, and prediction parameters (Chong and Menberg, 2018).

3.6.4 Sampling:

For posterior distribution to ease sampling No-U-Turn Sampler (NUTS), an extension of the Hamiltonian Monte Carlo (HMC) for the MCMC sampling, has been selected.

In this paper, separate GP models have been employed to emulate the simulator and the discrepancy. The trained emulators will be new clusters for the next step of correlation. The iteration number was set to 40,000 and validation has been proceeded by one data set from the test data and has been considered as the target archetype code.

The assessment was achieved through the Coefficient of Variation of the Root Mean Squared Error (CVRMSE, equation 9) and the Mean Absolute Percentage Error (MAPE, equation 10).

$$CVRMSE = \sqrt{\frac{\frac{\sum_{t=1}^{n_t}(y_t-y_t^*)^2}{n_t}}{\bar{y}}} \times 100\% \qquad (9)$$

$$\text{MAPE}= \frac{\sum_{t=1}^{\boldsymbol{n_t}}\left|\frac{\boldsymbol{y_t}-\boldsymbol{y_t^*}}{\boldsymbol{y_t}}\right|}{\boldsymbol{n_t}} \times 100\% \qquad (10)$$

3.7 Step-wise description of the method implementation in the city of Imola

The proposed method is applied in an urban building stock in the city of Imola, Italy. The input data is collected through the municipality of the city of Bologna, ARPAE Emilia-Romagna (ARPAE, 2020), local weather data, and some other public datasets in urban databases. Buildings are classified in archetypes regarding their characteristic. In this paper, two archetypes are selected for demonstrating the results of the calibration.

Table 3.4:Identification of the 11 defined archetypes based on the property details

Component	Input Parameters	Arch I	Arch II
Envelope	Gross floor area	832	245
	Floor levels	7	2
	Room height	2.8	2.8
	Gross Volume	17871	4076
	Window to wall ratio	20-30%	10-20%
	U-Value floor	2.88	0.4
	Roof	2.88	0.4
	Wall	3.34	0.63
	Windows	2.87	5.05
	Solar heat gain coefficient SHGC	0.35	0.5
HVAC systems	DHW	Individual DHW sys per apartment	Individual DHW sys per apartment
	Heating system	Gas-central heating	Gas-central heating

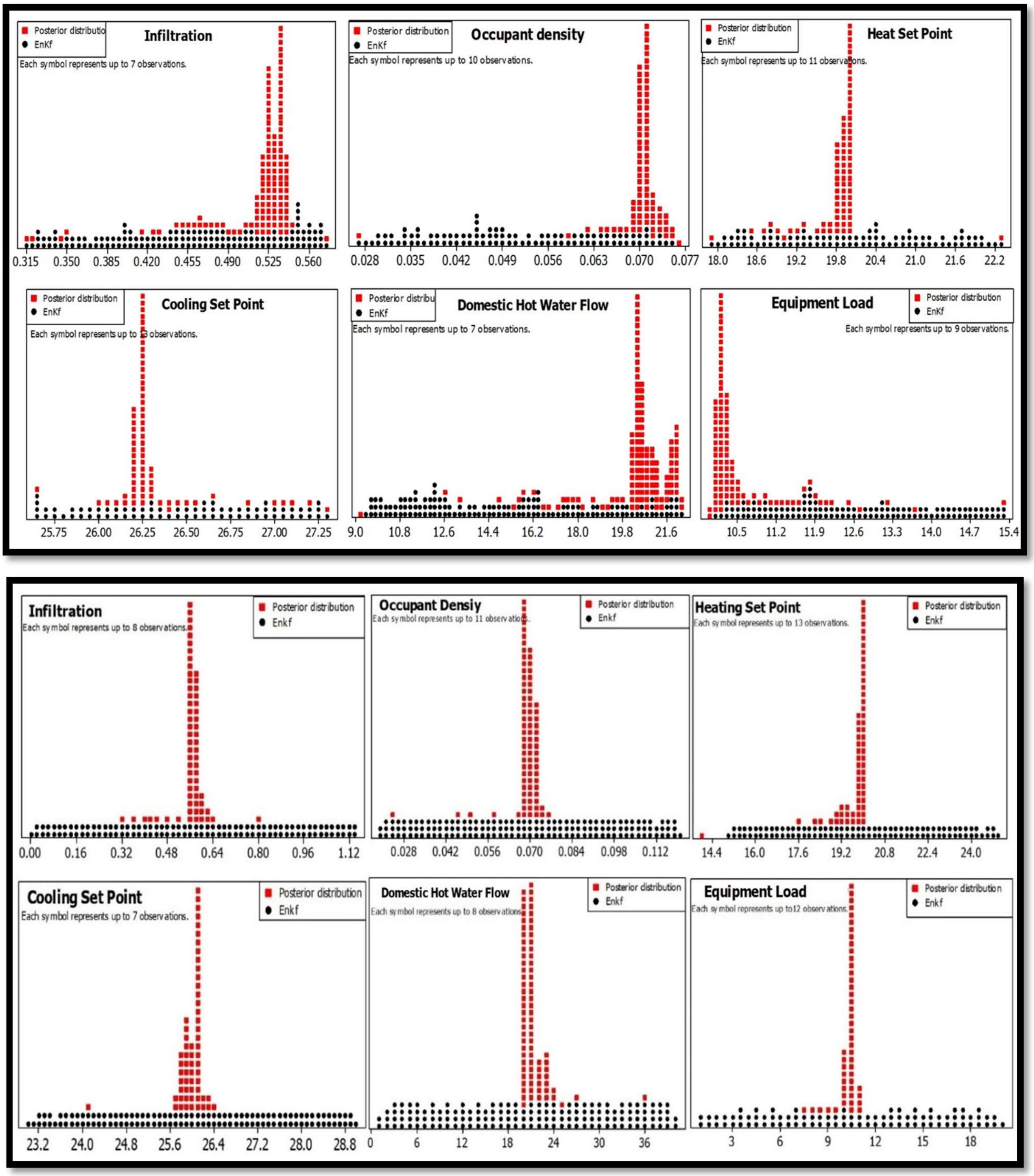

Figure 3.11: Prior and posterior distribution of the archetypes I (above) and II (down), every archetype belongs to a specific built period for the sake of comparison. The X-axes show the value of the variable and the Y-axes show the density of the distribution.

3.7.1 Results:

The calibration process starts with an Ensemble Kalman Sampling method, based on a set of 80 ensemble members out of the last iteration. For emulation, the GP training is used to produce a set of parameter-data particles. The output of this step will be a group of emulators to assess the

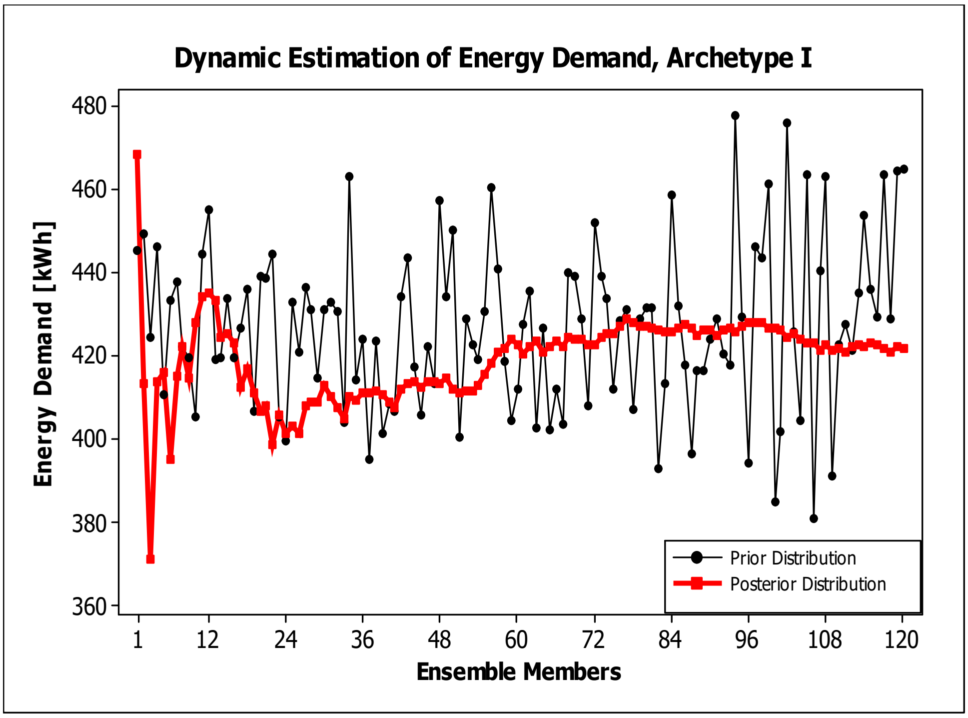

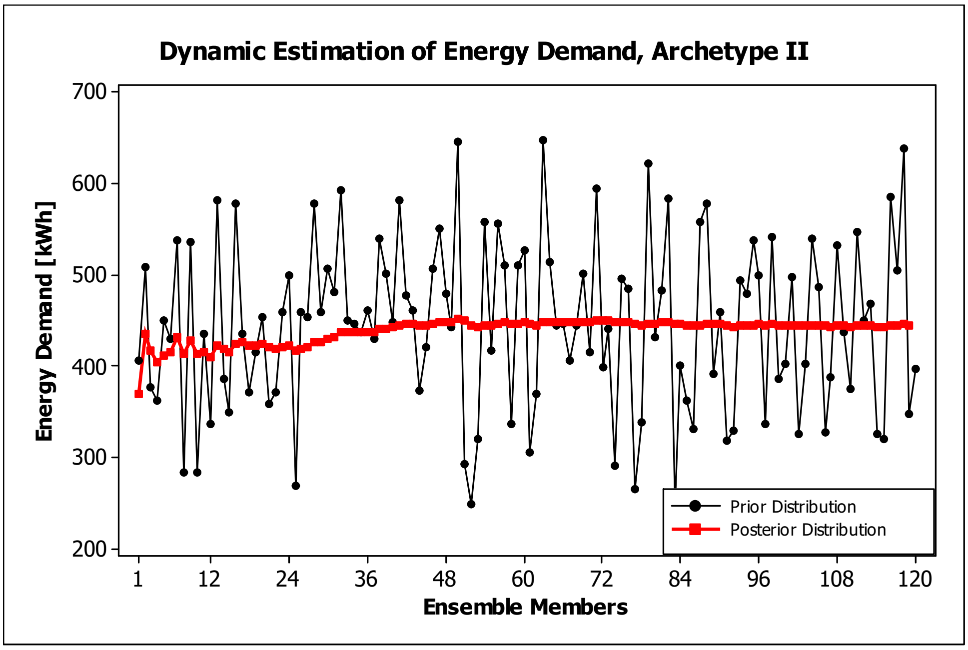

Figure 3.12: Comparison of Energy Demand Estimation in the archetypes

MCMC in the next steps. Following this step, determining the posterior distribution of parameters will get started.

Due to the limit of space in this paper, two archetypes are chosen for detailed analysis. The prior and posterior distributions of six uncertain variables are shown in Fig 3.11. It illustrates the density distribution in both prior and posterior distribution. The black points demonstrate prior distribution and the red points go for the posterior distribution. In general, the variation of posteriors is shrunk. However, the results are varied in two archetypes.

EKS in most of the variables has disseminated the samples accurately where the posterior distribution particles are concentrated. In equipment load and domestic hot water flow, however, the posteriors are close to the end of the ranges in EnKf. In these case studies, Archetype II has shown a clearer distribution, as it is indicated in table 3.3, archetype II is built in the 80^{th} decade and on two floors, while archetype I is a new building and in 7 floors.

The results of the calibration process are shown in Fig 3.12. Each figure shows the value of EUI through 120 prior distribution values of EKS and predictive EUI value estimations (y_{pred}) based on the draws out of the posterior predictive EUI. As it is observable in most of the EKS members the range of the energy estimation is limited to a close range of the posterior distribution for the predictive values of EUI, however, for archetype II the predictive range of EUI (y_{pred}) is disseminated with less variation into the range defined by prior distribution in comparison to the archetype I. One of the possible reasons is the poorly designed excitation signals in the training that can happen in a data-driven model or simply the prior definition of the training that was not compatible with the actual data.

3.8 Evaluation of model performance

The accuracy of the forecasting the EUI corresponded to every archetype was tested through random draws out of the y_{pred} from the posterior distribution. The evaluation for each archetype was performed on its BEM and specific building properties. Every simulation is done through one of the extracts of variables' values. The archetypes are evaluated through two methods, the Coefficient of Variation of the Root Mean Squared Error (CVRMSE) and the Mean Absolute Percentage Error (MAPE) as illustrated respectively in equations 5 and 6.

$$CVRMSE = \sqrt{\frac{\frac{\sum_{t=1}^{n_t}(y_t - y_t^*)^2}{n_t} \times 100\%}{\bar{y}}} \quad (5)$$

$$\text{MAPE} = \frac{\sum_{t=1}^{n_t}\left|\frac{y_t - y_t^*}{y_t}\right|}{n_t} \times 100\% \quad (6)$$

Fig 7 shows how much the energy prediction varies taking the actual values of EUI into account through CVRMSE and MAPE. Archetypes I and II are trained with CVRMSE, archetype II showed less than 0.5%, While Archetype I has shown a bit higher percentage (0.6%) This archetype is a new-built building model that is simulated based on TABULA (Corrado et al., 2012). The reason for this gap could be simply a difference in the defined structure and U-value of the material in practice and simulations or it can be a different assumption on probable input data. The results of MAPE also show the same for Archetypes I (5%) and II (2%).

Investigation of various level of retrofitting strategies

As it has mentioned, the proposed framework aims at reducing the uncertainty for calculating urban building loads and measuring the effects of various retrofitting policies and also accelerate the validation process of the results. For applying the refurbishment measurements on large scale, a series of measurements are considered to examine the energy-saving level. Table 3.1 shows these measurements. Reducing the uncertainty of the unknown parameters gives a database by which modeling any measurement for classified buildings in the urban scale is possible. All three

refurbishment measures have been applied to the model to investigate the results. Fig 3 shows the energy performance of the archetypes in various refurbishing conditions.
To examine the effectiveness of the various retrofitting strategies, energy performance simulations for every strategy have been run based on
the calibrated parameters. Applying the advanced isolation strategy is the most effective retrofitting strategy in reducing heating loads, however, there is no considerable difference in the cooling loads of advanced and standard isolation strategies.

Table 3.5: Retrofitting strategies based on TABULA

Structural section	Standard isolation material	Advanced isolation material	Green materials
Wall	6-11 cm (0.33 W/M2K)	10-15 cm (0.25 W/M2K)	0.60 W/M2K
Roof-ceiling	7-12 cm (0.30 W/M2K)	11-16 cm (0.23 W/M2K)	0.38 W/M2K
Windows/roof replacement	2 W/M2K	1.7 W/M2K	-

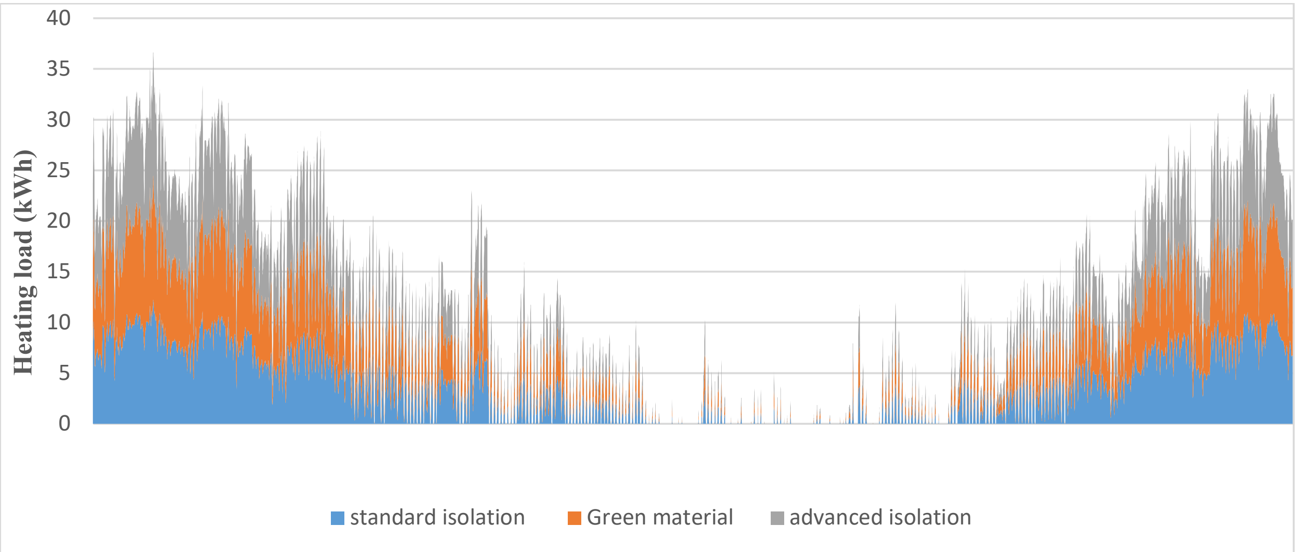

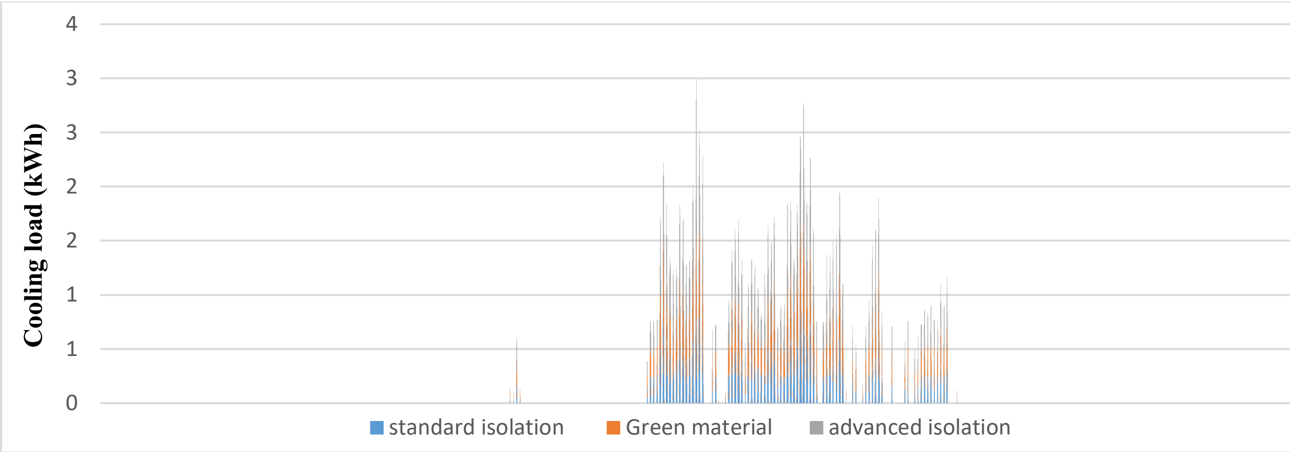

Figure 3.13: Hourly heating and cooling loads of three retrofitting strategies through the calibrated model

3.5 Conclusion:

This chapter proposed two automated calibration methods for long-term energy forecasting at the city scale. The proposed archetype-based energy models have been applied in a neighborhood in the city of Bologna in Italy. The following conclusions can be obtained from this research:

1- The presented archetype-based coding framework for the city of Bologna and imola is based on 7 physical features that can be applied systematically to any urban region for classifying the urban buildings. These seven features are available in most urban databases. Then, the values for six highly uncertain variables (INF, OCC, CSP, HSP, EPD, DHW) are estimated through Bayesian calibration. Therefore, every archetype has been defined based on 7 pre-calibration features and a tight range of six calibrated variables which are the most effective parameters in estimating building energy consumption. The coding framework is flexible and can be applied in any neighborhood containing hundreds of buildings with any uncertain parameters for forecasting energy modeling. This method can be also considered for energy forecasting of unseen buildings.

2- Automated calibration can calculate the importance of parameters concerning building energy consumption. Informative parameters in the calculation of EUI are estimated based on 1000 draws out of the posterior predictive distributions. This method provides a forecasting framework for reliable prediction results.

3- The proposed model has proved a high level of accuracy with almost no bias in almost all the defined archetypes. The evaluation has been calculated both in EUI and also in the 6 highly uncertain variables. The comprehensive investigation in performance metrics clarified the concerned errors in uncertain parameters and the EUI.

The proposed UBEMs prevent monotheism from applying the same strategies in various buildings. The reliability of the model is proven in predicting energy demand based on CVRMSE and MAPE. The model is capable of testing scenarios and recognizing the most effective retrofitting strategies and accelerating the urban-scale calibration. The simple archetype coding makes the method appropriate for energy policymaking on the urban scale and analysis of various retrofitting strategies on large scale for various types of buildings.

Yet, there are many other aspects that this paper did not cover in the calibration of the urban energy forecasting models. Future studies may consider more measures for the robustness of the Bayesian calibration, and also to take into consideration noisy urban datasets in processing hourly and monthly databases and optimize them. Besides, some efforts are needed to extend the functionality of the UBEMs for high-dimensional outputs. Many proposed models on the building-level scale cannot be performed on urban scales due to the required computation time, thus, future studies can explore solutions to eliminate this gap.

Chapter 4 . Analyzing energy performance and thermal behavior of various green buildings

4.1 Summary

This chapter presents a modeling methodology by which a multi-dimensional hygrothermal simulation, based on actual local weather modeling. employing this methodology, a comparison was made between insulation, green roofs, and rooftop greenhouses to analyze energy performance and thermal behavior of buildings. Different aspects of roofing scenarios were analyzed in four parts of energy calculation, the impact of moisture on the thermal behavior of the building, thermal performance of passive-designed rooftop greenhouse, and zero cooling need building. After examining various options for this modeling and considering that roofs must be simulated in one software for a valid comparison, WUFI (Garland and CPHC, 2017) was chosen to perform the simulation. WUFI calculates heat and moisture exchanges between the building envelope and the surroundings. It uses a precise precipitation database to calibrate moisture transport and calculates vapor diffusion and liquid water transport. In this work, air-conditioning in summer always is simulated by an electricity-driven chiller and for the heating system, a gas-fired boiler is performed during all simulations. In every time step, WUFI calculates the hygrothermal loads according to equations based on the Thomas algorithm. Also, WUFI Plus can perform indoor air modeling and model space heating and cooling, which makes it suitable for greenhouse simulation.

4.2 Materials and methodology:

4.2.1 Micro-Climate Modeling

In this chapter, a comprehensive modeling methodology is employed to represent the actual local weather conditions. A localized weather file was used in the modeling, which provided the meteorological, urban morphological, reference site, and urban geometry features for consideration. To accomplish the representation, the Urban Weather Generator (UWG) (Bueno et al., 2013) was employed to generate a weather file including hourly urban canopy air temperatures and a humidity dataset from a regular weather file. It took into consideration the vegetation, urban building and road surface materials, horizontal building density, and vertical-to-horizontal built ratio. The chosen neighborhood for the reference building was in the city of Bologna and was modeled with all the details. The source of this weather file is a close weather station named “urban Bologna”(ARPAE, 2020) and is based on the year of 2018 and 2019. The output of the model showed differences in maximum and minimum temperature and also heating and cooling degree days. Since the precision of every simulation is directly affected by the accuracy of input data, inputting the actual local weather data improves the accuracy of the hygrothermal simulation and the analysis of the results in various scenarios.

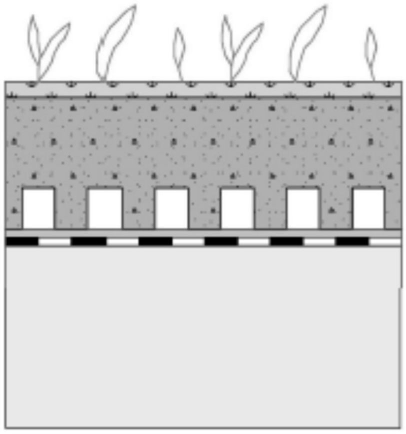

Figure 4.1: System drawing of investigated green roof (image taken form WUFI archive)

4.2.2 Green roof model

In energy modeling, green roofs are generally subdivided into three fundamental components: protection structure, soil, and canopy or vegetation cover (Barrio, 1998). Canopies consist of leaves and also the air between them. Canopies are characterized by two features: the height of the plants and the leaf area index. The soil contains three phases of matter: solid, gas (air and water vapor), and liquid (water). System drawing of the investigated green roof in this study is shown in Figure 4.1 and detailed measures are brought in Table 4.1.

Table 4.1: Hygrothermal properties of the green roof

Hygrothermal parameters	Sedum planting	Substrate	Protection mat
Bulk density kg/m³	1500	405	83
Porosity	0.5	0.82	0.95
Specific heat capacity j/kgK	1000	1000	840
Thermal conductivity, dry, 10 °C/50F W/mk	0.2	0.4	0.035
Water vapor diffusion resistance factor	5	3	1
Typical built-in moisture kg/m³	1	4.2	0.7
Reference water content	12	-	-
Free water saturation	300	-	-
Temp-dep thermal cond.sppliment	2E-4	2E-4	2E-4
Thickness	0.01	0.1	0.02

Green roof modeling can be classified into one-dimensional and multidimensional modeling. One-dimensional modeling simplifies thermal transfer into different layers, which can be simulated faster and are more common in energy modeling (Kumar and Kaushik, 2005). However, multidimensional modeling aims to model thermal effects and geometry inputs more accurately, although the simulation takes a longer time in comparison to the one-dimensional modeling of green roofs and walls. Intersections or curved shapes can only be modeled through two-dimensional modeling, Busser et al. (Busser et al., 2018) have shown that the accuracy of thermal behavior is improved by 30% to 40% in multi-dimensional modeling, especially in contemporary buildings.

The most common model that has been employed to model green roofs is the "Fast All-Season Soil STrength" (Frankenstein and Koenig, 2004). In FASST, there are two distinct equations that calculate the heat flux of soil (Equation 1) and foliage (Equation 2). The heat fluxes in this model consist of absorbed solar radiation, long-wave radiation between leaves, sky, and soil.

$$F_f=\sigma_f[I_s(1 - r_f)+ \varepsilon_f\sigma I_{ir} - \varepsilon_f\sigma T_f^4] + \frac{\sigma_f\varepsilon_g\varepsilon_f\sigma}{\varepsilon_1}(T_g^4 - T_f^4) + H_f + L_f \quad (1)$$

$$F_g= (1-\sigma_f)\ [\ I_s(1 - r_g)+ \varepsilon_g\sigma I_{ir} - \varepsilon_g\sigma T_g^4] + \frac{\sigma_f\varepsilon_g\varepsilon_f\sigma}{\varepsilon_1}(T_g^4 - T_f^4) + H_g + L_g+ k\frac{\partial T_g}{\partial z} \quad (2)$$

While this model has been reliable enough to be employed by EnergyPlus (*EnergyPlus Documentation Engineering Reference*, 1996), it does not take into account the variations in soil thermal properties, including thermal conductivity, specific heat capacity and density, and solar reflection, when calculating. Furthermore, it is not capable of accurately representing the moisture accumulation on roofs. Moreover, the precipitation data provided in the EnergyPlus weather database are considered not accurate for the purposes of this paper. The equation employed in WUFI (Equation 3) included initial temperature, relative humidity (RH), radiation, precipitation, wind speed and direction, and initial construction moisture. A detailed modeling procedure in WUFI is shown in Fig 4.2.

$$\frac{\partial H}{\partial T}.\frac{\partial T}{\partial t}=\nabla.(\lambda\nabla T) + h_v\nabla.(\delta_p\nabla(\emptyset p_{sat})) \quad (3)$$

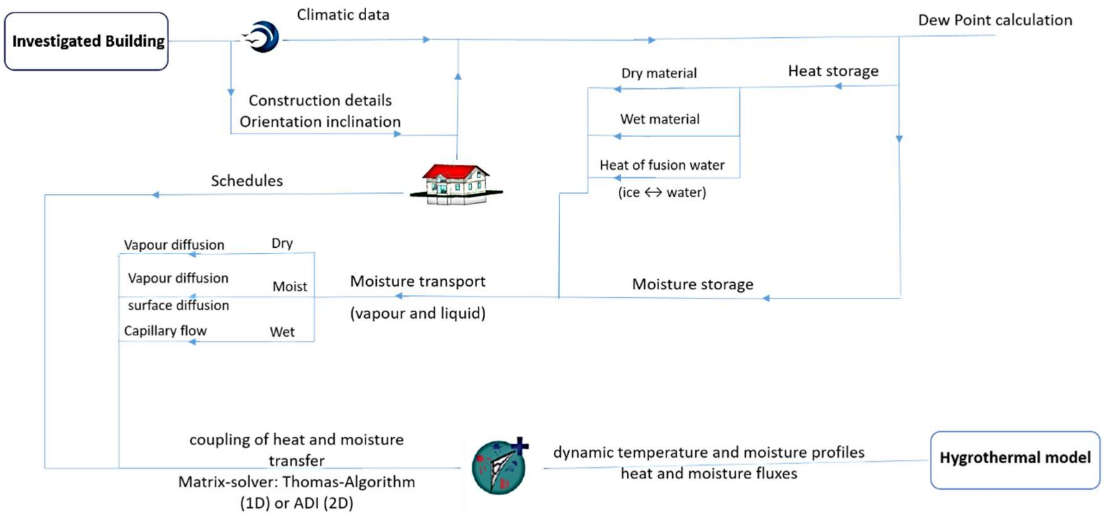

Figure 4.2: The steps of the hygrothermal modeling in WUFI

4.2.3 Rooftop greenhouse model

As a kind of building-integrated agriculture, rooftop greenhouses are kind of cultivation systems which are enclosed to urban rooftops in an environmentally monitored and controlled area. Passive cooling and heating strategies benefit rooftop greenhouses. Rooftop greenhouses can act as a heating system and relive the direct solar gain of the surface of the roof in summer and also in winter to create a monitored space from the cold airflow. The proposed rooftop greenhouse scenario enhances the energy efficiency of buildings by providing a specific design for the shape, openings, and shadings of the greenhouse to take advantage of the green roof and the insulation and can also provide the means of environmentally positive food production. This design is completely in line with passively design strategies in a Mediterranean climate. In this type of climate zone, summers are mostly hot and humid and winters cold. The rooftop greenhouse modeled in this study was 12m wide and 20m long, with windows that could open up to 45 degrees to provide ventilation in the summer. Its structure was made up of wooden frames and glazing glasses with a low-Ɛ coating and a shading coefficient of 0.39. An attached shading cloth covers the east side of the ceiling during summer days. The properties of the rooftop greenhouse are presented in Table 4.2 and 4.3 and Figure 4.3 shows the form details of the proposed rooftop greenhouse.

4.3 Case Study

The methodology was carried out on a two-story residential building in the city of Bologna. The building is modeled based on an Italian national document of typology approach for building stock energy assessment (TABULA) (Corrado et al., 2012) as a representative of Italian building. The modeled parameters of the building are classified and shown in Table 4.3 and figure 4.3. The building was simulated through three roof scenarios: baseline roof, insulated roof, green roof, and a rooftop greenhouse. The building information, including geometry, construction, and schedules, were modeled manually in WUFI.

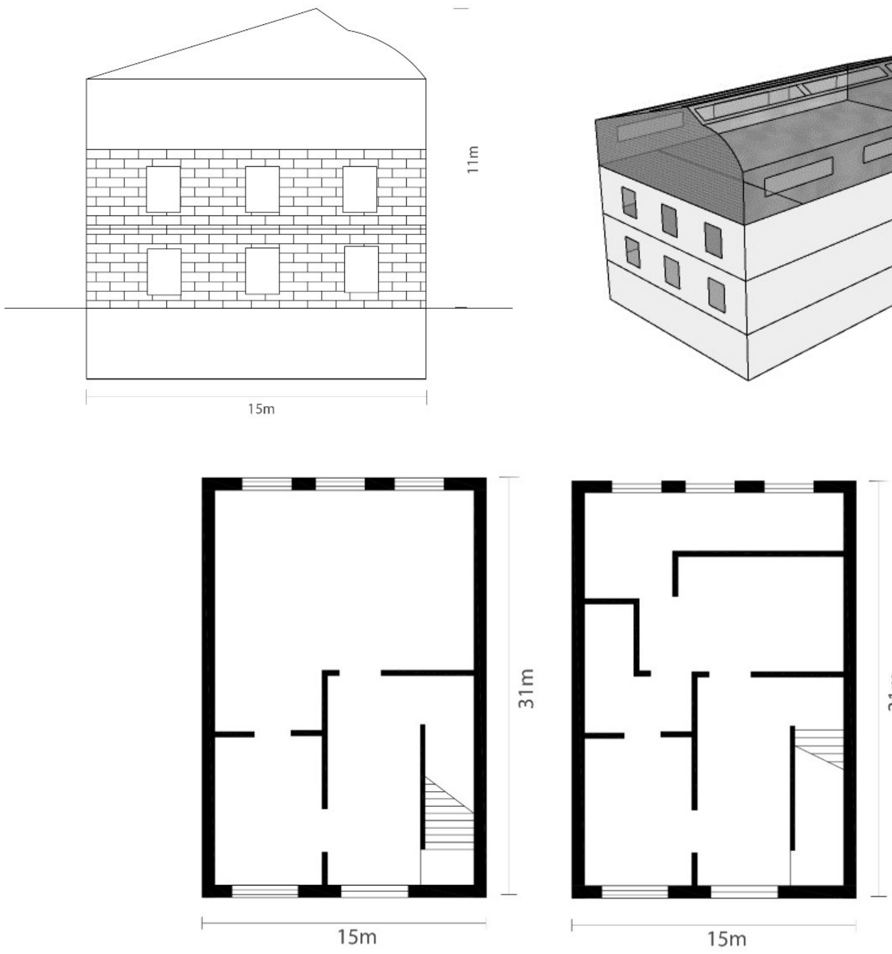

Figure 4.3: Investigated building model

Table 4.2: Thermal properties of ceilings, walls, and structural roof in the investigated buildings

Elements	Thickness (m)	Thermal conductivity (W/m2 K)
Wall	0.265	0.512
Ceiling	0.41	0.970
Roof	0.30	0.523

Table 4.3: Properties of the rooftop greenhouse

Parameters	Value
Gross volume	1060 m^3
Total external surface	302 m^2
Glazed surface	302 m^2
Roof surface	240m^2
Roof surface/total external surface	0.79

4.4 Results and discussion

The building was modeled in WUFI, using three scenarios: an insulated, green roof, and a rooftop greenhouse. The simulations were performed to calculate the annual heating and cooling loads in the same local climate conditions. The energy-saving estimation of the scenarios was extracted and compared to the baseline building design. The simulations were applied in 15-minute steps. The impact of the moisture on the reduction of energy loads and also the possibility of designing a non-cooling building were analyzed.

4.4.1 Energy needs

One of the main advantages of these technologies concerns the improvement of energy-saving during the cooling and heating period of the year. In this paper, this impact will be considered as a primary energy need. During the cooling period, air conditioning is provided with an electrical chiller and during the heating period, heating is provided by a gas boiler. The simulation results show that all roofing solutions reduce the total energy needed for cooling and heating (Figure 4). The best performances came, first, from the insulated roofs with about 20% improvement and, second, the rooftop greenhouse scenario with approximately 15% energy saving in the annual heating and cooling loads of the building. The green roof also has shown 7% improvement in energy saving in comparison to the baseline roof.

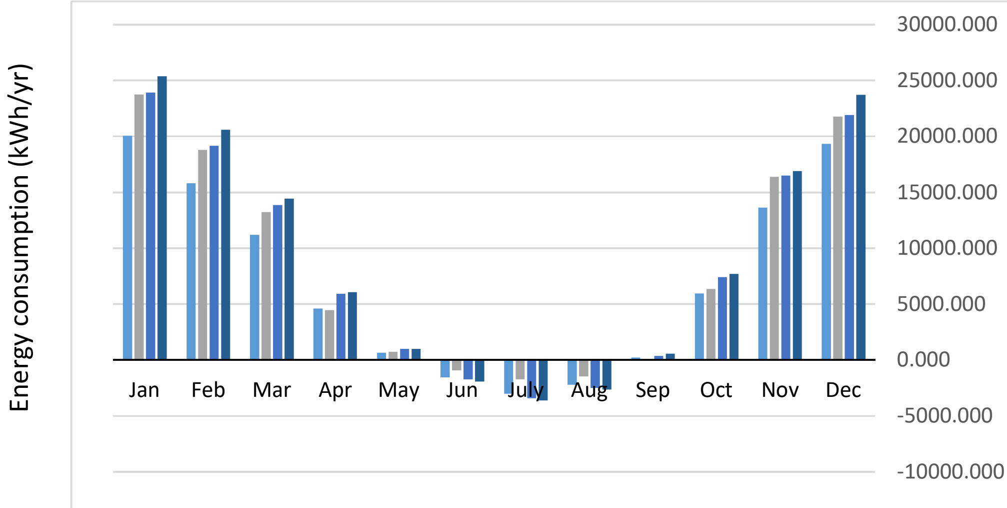

Figure 4.4: Monthly energy consumption of different roof scenarios (kWh /yr)

During heating periods (Nov, Dec, Jan, Feb, March), the best roofing solution is insulated roof and the functionality of green roofs by 5% reduction in heating loads is at the lowest due to the humidity and the moisture that directly affect the heat flux rate, although, in cooling periods, green roofs have a better impact on cooling loads and also the temperature of the roof. Rooftop greenhouse in the heating period shows slightly better than green roofs and it is worth noting that rooftop greenhouse during the heating period is simulated with no opening and shading.

As observed, during the cooling period (Jun, July, August), the performance of the designed rooftop greenhouse is the most effective by 50% reduction since it provides shading, insulation by soil, and also airflow through openings, which consequently leads to a cooler roof surface during the summer. It is a common belief that green coverage always improves energy needs for cooling, nevertheless, the hygrothermal model shows that in a Mediterranean climate the moisture in green roofs can adversely impact the cooling loads, however, in this period insulated and green roofs showed approximately the same improvement in energy needs.

4.4.2 The impact of moisture on the green roof performance

Although modeling results are affected by local microclimates, they are highly dependent on rooftop structures and greening systems. While the structural elements of insulated rooftops are fixed during different seasons (static), green roof elements and, subsequently, their performance are highly dependent on climate conditions (dynamic). The amount of moisture in green roofs affects the level of insulation. Surface wetness is one of the factors that has been, in a limited number of studies, considered in measurements or as a fixed parameter in evaporation efficiency, evaporation ratio, and water vapor conductivity. By increasing the level of water content, thermal conductivity and specific heat of the green roof get enhanced (Figure 4.5). As a matter of fact, when irrigation is applied to the roof, water content is converted and performs as heat (Hirano et al., 2019). Thus, the amount of water needed for evapotranspiration is an important factor in green roof evaluation. In this study, a green roof was modeled on three levels of moisture, namely, actual rainfall, the maximum amount of water, and dry.

Figure 4.6 shows the heating and cooling loads in three configurations during heating and cooling periods. In this case study, due to the Mediterranean climate of Bologna, water can adversely impact the heating load in winter, as the results show the green roof in maximum rainfall in heating period acts nearly equal to baseline roof with more than 6000 Kwh monthly energy consumption. This point is important since it highlights that green coverage of roofs is not always as an energy-saving strategy. The dry green roof, however, achieved the best functionality by 18% improvement in the level of energy load. The reason is that soil acts as an insulation layer in the roof, while the higher the level of moisture in green roofs, the less energy-efficient they become in this climate. On the other hand, in summer, the level of cooling load increases when the wetness of the green roof decreases. This is obviously due to the evaporation of water content that decreases the temperature (endothermic reaction) of the surface and consequently affects the cooling load of the building. It is worth noting that these results are highly variable in various climates.

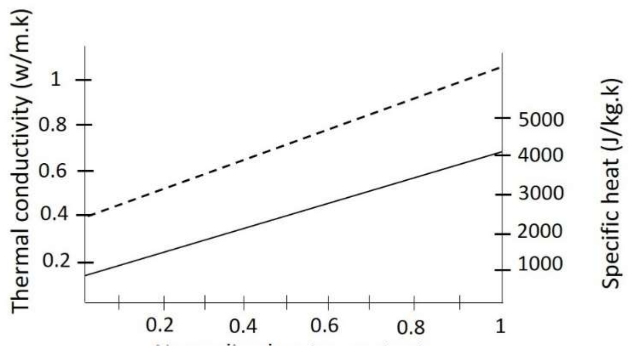

Figure 4.5: moisture dependent properties of the green roof substrate

- - - - - - Thermal conductivity ———— Specific heat

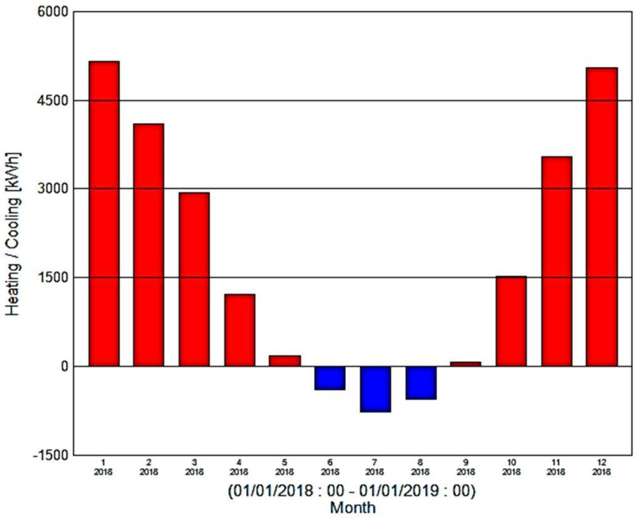

a: Dry green roof

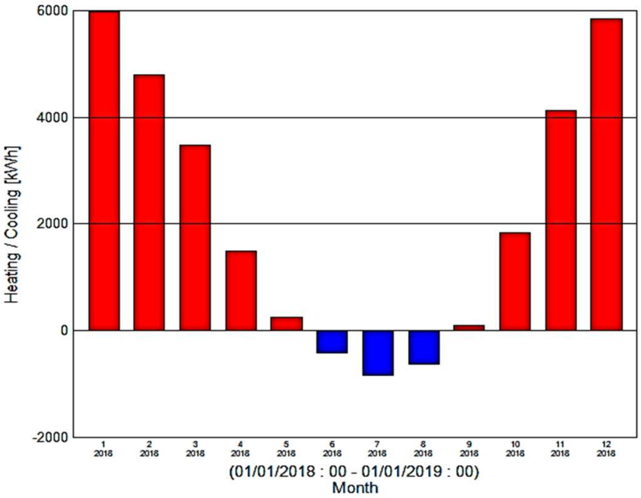

b: Green roof in actual rainfall

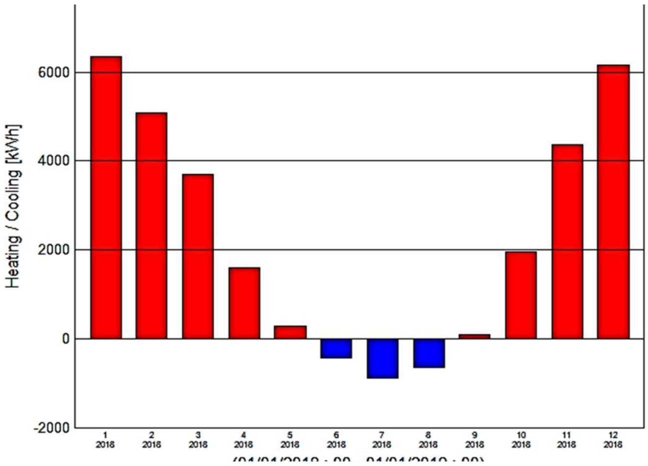

c: Green roof in maximum rainfall

Figure 4.6: Heating and cooling performance of green roofs with different level of moisture, cooling loads are in blue and heating loads are in red, a: Dry; b: actual rainfall; c: maximum rainfall

4.4.3 Rooftop greenhouse space performance

The rooftop greenhouse was explicitly examined for providing an optimal condition (12-26C°) for the thermal needs of a greenhouse and the cultivation conditions. During the heating period, the passively-designed rooftop greenhouse is simulated with opening and shading on the ceiling to limit solar gain while in winter, it is simulated without opening and shading to maximize the solar gain. Table 5 shows the mean, maximum, and minimum monthly temperatures of the rooftop greenhouse and outdoor temperature. In the cooling period of the year, the mean temperature of exterior air was the highest in July at 24°C while the peak temperature was 34°C temperature. The minimum temperature in the cooling period is 6°C in the beginning days of May. The indoor temperature of the rooftop greenhouse in this period showed a maximum of 36°C in July while the mean temperature is still at 25°C.

Outdoor mean air temperature in the heating period varies from 1°C to 13°C. The minimum went down to -12°C and the warmest days are allocated to April and October with a maximum of 23°C. On the other hand, inside the rooftop greenhouse, the average "mean temperature" was 9°C during the heating period, however, it fluctuates between the lowest temperature of -3°C in December and a maximum of 27°C in April.

Table 4.4: Monthly average, minimum, and maximum of rooftop greenhouse and outdoor temperature

Months	The temperature of interior air in the rooftop greenhouse [°C]			The temperature of exterior air [°C]		
	mean	max	min	mean	max	min
Jan	3.22	15.67	-2.15	1.12	10.46	-12.98
Feb	5.62	18.14	-1.48	3.32	15.49	-5.90
March	10.81	23.48	-0.80	8.12	20.69	-1.16
April	14.96	27.00	3.98	12.72	23.16	3.00
May	19.31	30.86	6.67	17.49	27.19	6.49
Jun	23.40	35.83	13.37	21.39	32.99	12.20
July	25.94	36.37	13.39	24.91	34.80	12.03
Aug	25.27	35.01	11.98	23.57	34.80	11.01
Sept	20.88	32.04	9.07	19.70	30.20	8.11
Oct	15.32	25.23	6.87	13.71	23.96	4.43
Nov	10.46	19.01	-0.70	7.22	18.59	-1.70
Dec	6.88	13.83	-3.48	2.64	14.09	-5.16

To assess the indoor climate condition for the thermal needs of a greenhouse, the total hours of overheated and overcooled have been counted. The total hours with a temperature above

27°C constituted less than 7% of the year and total of overcooled hours is up to 28% from which just 6% is the hours with a temperature less than 7°C. Figure 7 shows more detailed weather data of overheated and overcooled hours in the rooftop greenhouse.

Considering cultivation condition, during the overcooled and overheated period, the rooftop greenhouse needs to be controlled in air temperature when it is outside of the 12-26°C range. A functional solution for preventing this drop in temperature during winter nights, as investigated by (Nadal et al., 2017), is installing an air ventilation channel from the heated zone of the building to the greenhouse. This enables the reuse of heated air for the greenhouse.

4.4.4 The possibility of the nearly zero cooling need scenario

Roof configuration is one of the most effective elements in the reduction or even elimination of cooling load in buildings during the period of peak air temperature in summer. Barbaresi et al. (Barbaresi et al., 2017, 2014) examined the possibility of eliminating a conditioning system in a winery and this study uses the same strategy in optimizing or even avoiding conditioning systems. To analyze the feasibility of this scenario, the roof solutions were examined in the operative temperature of residential zones. Figure 8 shows the comparison between the average operative temperatures in the proposed roofing solutions and outdoor temperature in the peak air temperature period in summer. While outdoor mean air temperature is between 32°C and 33°C, the indoor mean air temperature of the building with all the roofing technologies is less than 29°C and the minimum temperature is allocated to rooftop greenhouse which is within the range of 26°C to 28°C. Green roofs with an actual level of rainfall and insulated roofs have shown approximately similar results between 28.5°C and 30°C.

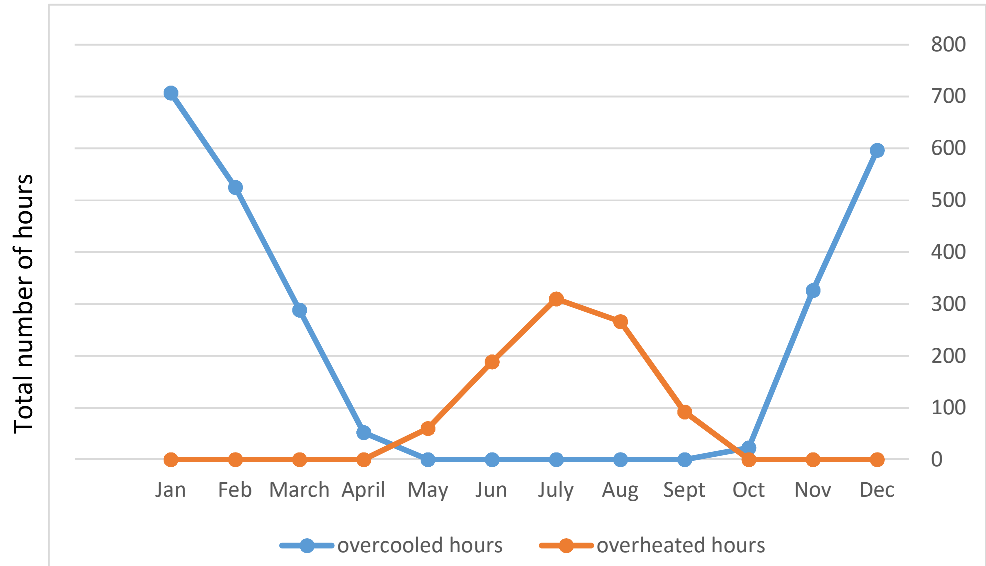

Figure 4.7: Total overheated and overcooled hours of the rooftop greenhouse

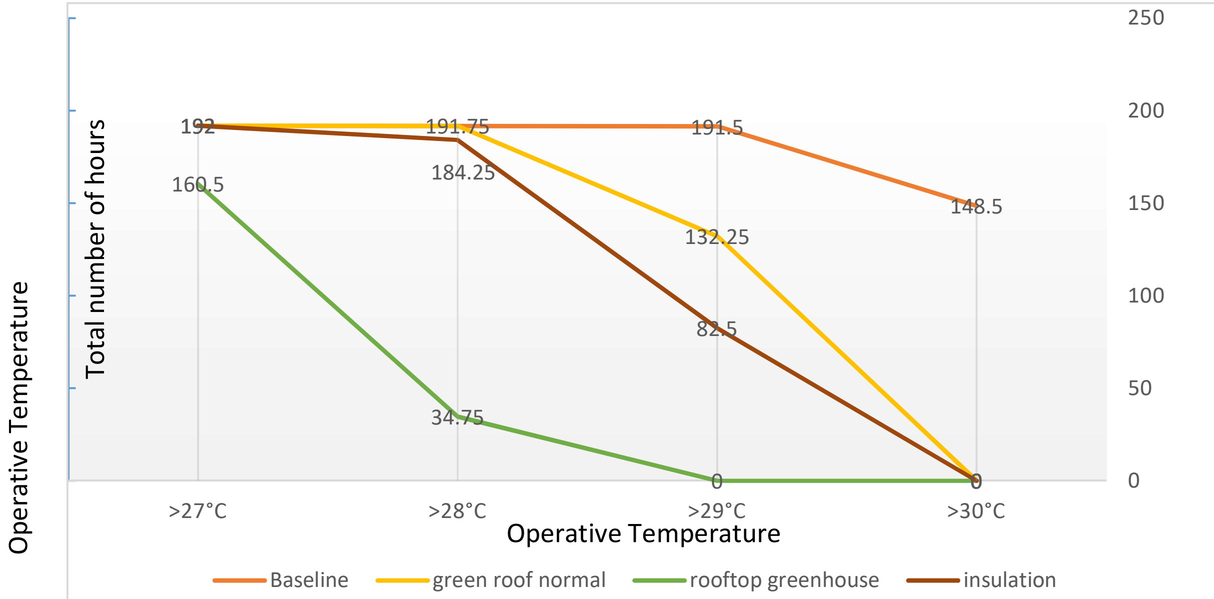

Figure 4.8: Total hours with operative temperature above 26°C in various roofing scenarios during peak air temperature period

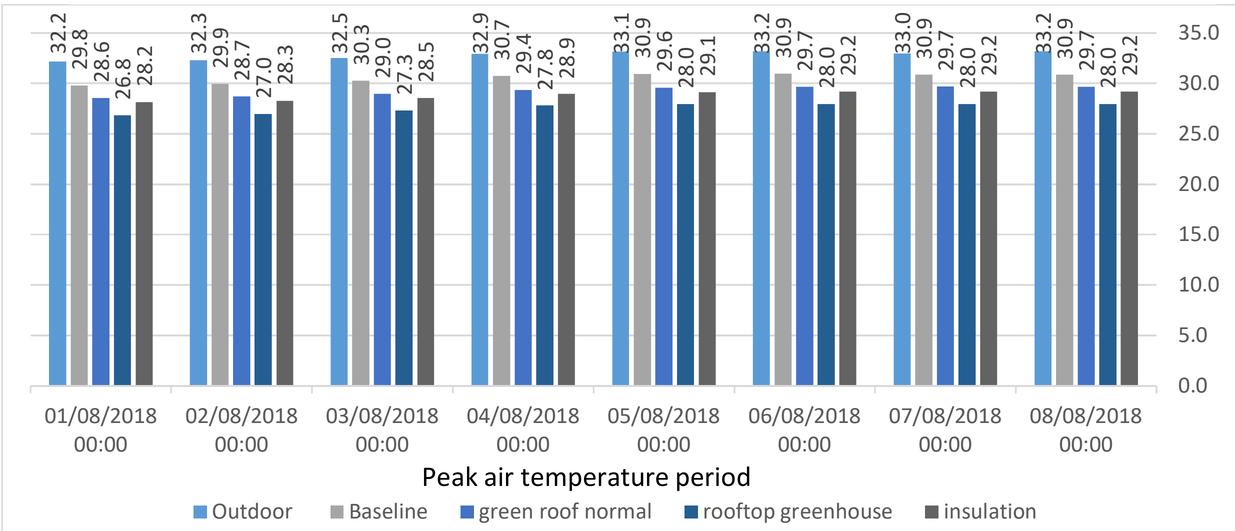

Figure 4.9: Operative temperature in various roofing scenarios during peak air temperature period

Figure 4.8 shows the total hours with an operative temperature above 27°C, 28°C, 29°C, and 30°C. The results from the passive-designed rooftop greenhouse indicate that the percentage of the hours with an operative temperature of more than 28°C were less than 35 which is relatively 18% of the peak period of air temperature. As it has been shown in Figure 8, a passively-designed rooftop greenhouse is by far the most effective and responsive solution to a non-cooling scenario. After the rooftop greenhouse, there is insulated roofs with 184 hours above 28°C and a green roofs with nearly 132 hours above 29°C.

4.5 Conclusion

This chapter aimed to present an accurate methodology for analyzing three roof scenarios, namely insulated roof, green roof, and a rooftop greenhouse. The scenarios were examined through two-dimensional hygrothermal in WUFI simulation on a building in Bologna, Italy. This study specifically focused on refining the methodology for analyzing buildings' energy performance. First, the microclimate of the location was calculated using the Urban Weather Generator to obtain the details of the meteorological features, urban morphology, reference site, and urban geometry parameters as they directly affect building energy loads. Furthermore, a two-dimensional hygrothermal simulation was developed through WUFI, which in comparison to one-dimensional simulations enhances the level of accuracy in simulating thermal behavior, including precipitation effects, the impact of moisture on materials, and special forms of the elements used in buildings. The results of the simulation were examined in 4 topics of a) energy calculation, b) the impact of moisture on the thermal behavior of the building, c) thermal performance of passive-designed rooftop greenhouse, and d) zero cooling need building. The results of the annual energy performance of the building provided interesting findings. In general, roofing scenarios showed different functionality in various conditions. While in the cooling period of the year, the rooftop greenhouse was the most effective solution, during the healing period, the least functionality was shown by the green roof. The developed model proved moisture in green roofs adversely impacts the energy performance of the green roofs in the Mediterranean climate, which means the more the level of the water content of the layers increases, the less energy-saving it gets. Moreover, the specific passive form of the proposed rooftop greenhouse is effectively responsive in controlling indoor thermal behavior to achieve a nearly zero cooling need building.

The present work represents a contribution to plan strategies oriented at reducing the energy consumption at building and urban scales. In fact, the study analyzes scenarios that are considered representative of the investigated area providing researchers and professionals a valid methodology to define the best energy-saving solutions. This work is seen as a baseline for wider research that involves more comprehensive strategies that are not limited to energy reduction but includes also energy production (such as installation of photovoltaic and/or solar panels). All those interventions – active and passive – should be evaluated using the same methodology and taking into account several scenarios. For this reason, future research is needed to apply this methodology to a group of buildings, aimed at showing how a mix of these roofing solutions can work together on a macro scale to create the most responsive solution in an urban context. Finally, a strategy for economic analysis should be identified to complete the study.

Chapter 5 . Urban Microclimate Digital Twin for Developing Green Scenarios

5.1 Summary

This study introduces a Python-enhanced hybrid approach for developing a digital twin pilot for micrometeorological analysis. The digital twin examines the impact of city form and street trees on the Mean Radiant Temperature (MRT) and thermal comfort (Universal Thermal Comfort Index, UTCI) based on a 3D model in Rhino, EnergyPlus, and Ladybug components in grasshopper. The model was tested in two contrasting climates: temperate and humid Imola, Italy, and hot and dry Tempe, Arizona, USA. Model output for Tempe was validated for hot summer days in June 2018 through human biometeorological observations at selected locations on Arizona State University's Tempe campus using the MaRTy cart. Observations across diverse urban forms, sky view factors in two different climate conditions covered a wide range of solar radiation ranges from a minimum TMRT of 28 °C to a maximum of 81 °C. Model generated simulation errors across regimes with RMSE ranging from 5.03 °C to 6.7 °C and 4.1 °C to 8.9 °C in MAE, exceeding a suggested TMRT accuracy of ±5 °C for heat stress studies. Built on open-source software, the model provides a low-cost, computationally efficient solution to assessing neighborhood design strategies for cities.

Abbreviation:

MRT: Mean Radiant Temperature
UTCI: Universal Thermal Comfort Index
DT: Digital Twin

5.2 Materials and methodology

In this chapter, an idealized implementation of a micro-climate digital twin consisting of a physical world, an integrating section, and the digital world is proposed. The main aim of the proposed digital twin is to mirror the physical world in three steps: 1; data collection 2; learning process and analyzing 3; post-implementation processes and decision making. Post-implementation is a validation step that is defined to overcome the consequences of incomplete urban climate data sources and also if a considerable uncertainty cast doubt on the performance of the model. This work is a template that integrates real-time data sources to offline micro-climate simulations and proposes an urban microclimate digital twin. The template also proves how the digital twin can be expanded to include a wide variety of data resources and simulations on various scales and subjects.

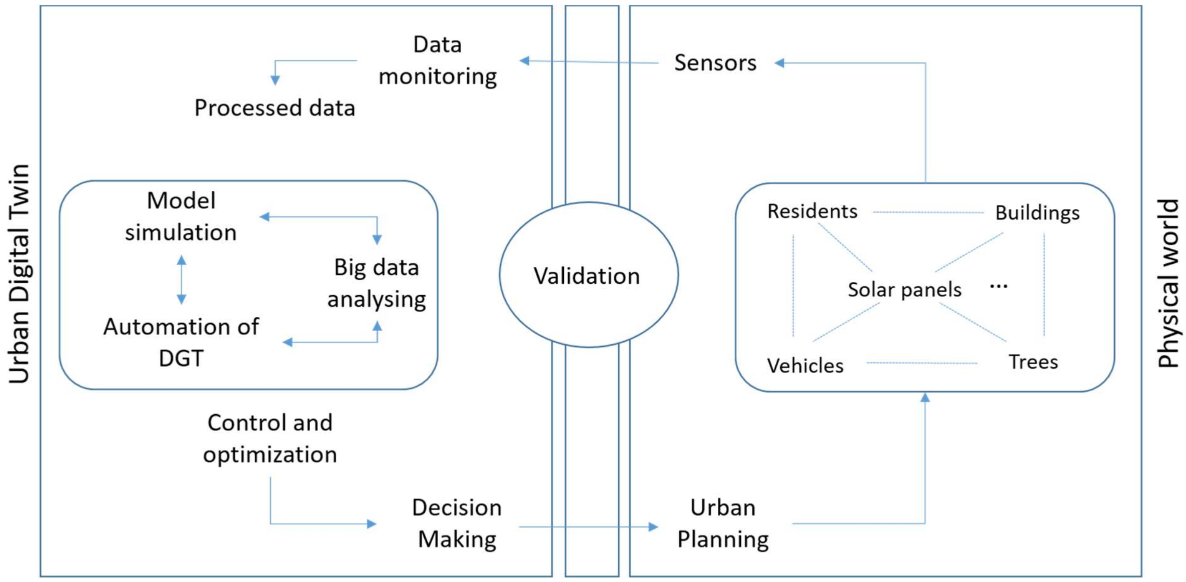

Figure 5.1: Conceptual Framework of an Urban Digital Twin

Overview of Digital Twin

The focus of this microclimate digital twin is to estimate the Mean Radiation Temperature and the Universal Thermal Climate Index (UTCI) which are calculated through a hybrid model based on a Python 3.8.1 code, which simulates each parameter in a separate engine. The interrelations of parameters are coded as a comprehensive Python script to ensure the accuracy of input and output orders in every step and of the outcome of the model in the final step. The model is based on three engines: EnergyPlus, Grasshopper, and OpenFOAM. Figure 5.1 illustrates the interrelations and order of the steps.

Meteorological real-time input data

The first step in developing the microclimate digital twin is a weather data file for short-term forecasting. To accomplish this, a model is developed in grasshopper that aims at regenerating the epw file based on forecasting data. The forecast weather data is acquired from API (OpenWeatherMap) in JSON format that provides short-term forecasting weather data in various time scales. Four elements are required from the API file for the regeneration of the epw file: Dry Bulb Temperature, Relative Humidity, Wind speed, and sky cover. These elements were used to generate hourly dew point temperature, global solar radiation, direct and diffuse decomposition models. Since grasshopper cannot directly interact with EnergyPlus, Honeybee tool was utilized to link open studio, energy plus, radiance, and daysim for an automated process to rewrite an epw file based on the existence epw file. The weather elements were replaced through the automated process in hourly format. This weather file will be used in the next steps for simulations.

Turbulent exchange and wind speed

The airflow patterns were simulated in several computational fluid dynamics (CFD) models to assure the accurate, high-resolution modeling of wind direction (Jörg Franke, Antti Hellsten, Heinke Schlünzen, 2007). The first step was creating a predominately hexahedral mesh with extra refinements at 5 m from the ground and higher density cells at 2 m from the trees to ensure the accuracy of the investigated domain. Wind speed and the mean velocity were obtained by statistical processing of the local weather file. The vertical exchange was designed using a logarithmic law, with a roughness length (z0) of 1 m as the default value. Equation (1) (Mackey et al., 2017) was employed to calculate the turbulence exchange:

$$U(z) = U_{met}\,\frac{\ln(z/z_0)}{\ln(z_{ref}/z_0)} \qquad (1)$$

$U(z)$: the speed at height z

U_{met}: meteorological wind speed

z_{ref}: meteorological reference height

The boundaries were at a height of 300 m twice of Hmax (for the top boundary), and at 400m for the lateral extension that is three-time of Hmax and for simulation of flow re-development a 15x Hmax was chosen. The models were simulated in OpenFOAM (Fiona Robertson; Martin Samy, 2015).

Surface temperature simulation on the pedestrian level

Building and ground surface temperatures were simulated using the EnergyPlus engine. The distribution of solar radiation was re-evaluated by a full exterior reflection setting in a 15-minute time step and in surface models less than 5 × 5 Radiative properties and absorption, albedo (g =

0.25, w = 0.2), and emissivity (εg = 0.95; εw = 0.9) of the urban surfaces. Thermal properties, such as thermal conductivity, thermal diffusivity, and heat capacity, were modeled in EnergyPlus. The process took into account the absorption coefficient for shortwave radiation (k = 0.7) and the skin emissivity of a standing person (εp = 0.95). Surface albedo was set to 0.5 in areas with light grey concrete and shop windows, which are both highly reflective.

Multi-layer radiation temperature matrix

To calculate the MRT, the surface temperature from the previous step was used in Eq. (2), adopted from Thorsson et al. (2007):

$$MRT = \sqrt[4]{[\sum_{i=1}^{N} F_i \ T_I^4]} \qquad (2)$$

F: sky view factor

T: surface temperature

The longwave temperature was calculated by the horizontal infrared radiation, using Eq. (3) (Blazejczyk, 1992):

$$T_{SKY} = \frac{L_a}{\sqrt[4]{(\varepsilon_{person}\sigma)}} \qquad (3)$$

La: the longwave radiation from the sky in W/m2

εperson: the emissivity of the human skin (assumed to be 0.95)

σ is the Stefan–Boltzmann constant (5.667 × 10-8).

For the simulation of the shortwave radiation affecting pedestrians, the model SolarCal was employed to generate the effective radiant field (ERF) and the MRT delta that were later considered in the longwave MRT calculation (Arens et al., 2015). This model was chosen due to features such as applying the seated and standing inputs to variables, which give it an advantage over other models. The SolarCal equation for the ERF is:

$$ERF_{solar} = 0.5 \ f_{eff} f_{svv}((I_{diff} + \ I_{TH} R_{floor}) + A_P f_{bes} I_{dir}/A_D) \ (a_{SW}/a_{LW}) \qquad (4)$$

feff : the fractional of the body that can radiate heat (0.725 for a standing person)

fsvv: sky view factor

fbes: a 1/0 value indicating whether the direct trace vector sun is on the person

Idiff : diffuse sky radiation

ITH: global horizontal radiation

Idir: direct radiation

AP, AD: the geometry coefficients of the human body, which are calculated based on the sun's altitude and azimuth.

Rfloor: the reflectivity of the ground (assumed to be 0.25)

α: the absorptivity and reflectivity of a person's clothing.

The last step was to find the ERF equivalent of the MRT delta, using this equation:

$$ERF = f_{eff} h_r (MRT - T_{LW}) \qquad (5)$$

hr: radiation heat transfer coefficient (W/m2 K)
TLW: base longwave MRT temperature (ºC)

The Universal Thermal Climate Index (UTCI) matrix

The Universal Thermal Climate Index (UTCI) was used for thermal comfort evaluation. The UTCI was introduced in 2011 by the International Society of Biometeorology (ISB) as a new thermal index for outdoor thermal comfort. It evaluates outdoor thermal conditions one-dimensionally in terms of air temperature, wind speed, humidity, and longwave and shortwave radiant heat fluxes. Table 1 shows the categorization of thermal stress based on UTCI ranges. There are different types of UTCI including heat and cold stress, in this paper, we only consider heat stress. This measurement system employs the correlations observed in human adaptive outdoor thermal behavior to predict the clothing of subjects of average age, height, and weight (Jendritzky et al., 2014).

The UTCI considers the wind speed at the standard meteorological height, which is 10 m, while the CFD simulations in this model are performed at the pedestrian level, and that is why some researchers prefer the Physiological Equivalent Temperature (PET) (Rodrigues Prata-Shimomura et al., 2009). This model, however, uses the proportions introduced by Jendritzky et al. (2014) to simply estimate the values of wind speed at the height of 10 m. It also shows that direct beam solar radiation is the dominant control (Park et al., 2014).

Table 5.1: The UTCI assessment scale: the UTCI categorized in terms of thermal stress

UTCI(C) range	Stress category
Above +46	Extreme heat stress
+38 to +46	Very strong heat stress
+32 to +38	Strong heat stress
+26 to +32	Moderate heat stress
+9 to +26	No thermal stress

Fig 5.2 illustrates the development of the urban microclimate digital twin step by step.

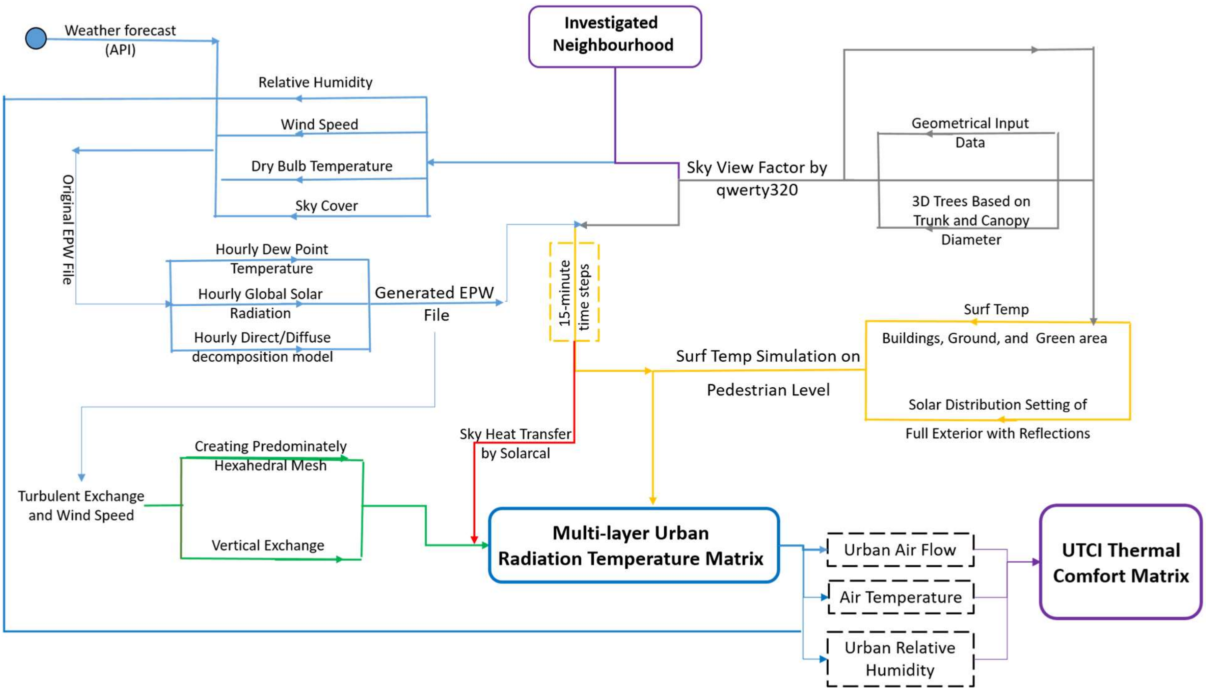

Figure 5.2: Modeling Methodology of the Urban Microclimate Digital Twin

5.3 Digital Twin validation

The field measurements have been conducted in a clear sky in the study area for model validation. Five sample locations are selected for collecting human-bio meteorological data on June 9th, 2018. Observations are conducted hourly from 8 am to 8 pm local standard time in Tempe. The field observation is conducted by a mobile sensor platform MaRTy (Middel et al., 2020; Middel and Krayenhoff, 2019). MaRTy measures georeferenced 6- directional longwave (L) and shortwave (K) radiation flux densities with three Hukseflux 4-Component Net Radiometers, Ta, Ts, v, and RH in 2-s intervals at pedestrian height.

Every sample site is archived through hemispherical 180° photos taken at 1.1 m height with a Canon EOS 6D and Canon EF 8–15-mm f/4 Fisheye USM Ultra-Wide Zoom lens. Table 5.2 illustrates the features related to the five sample locations. Fisheye photo, shade type.

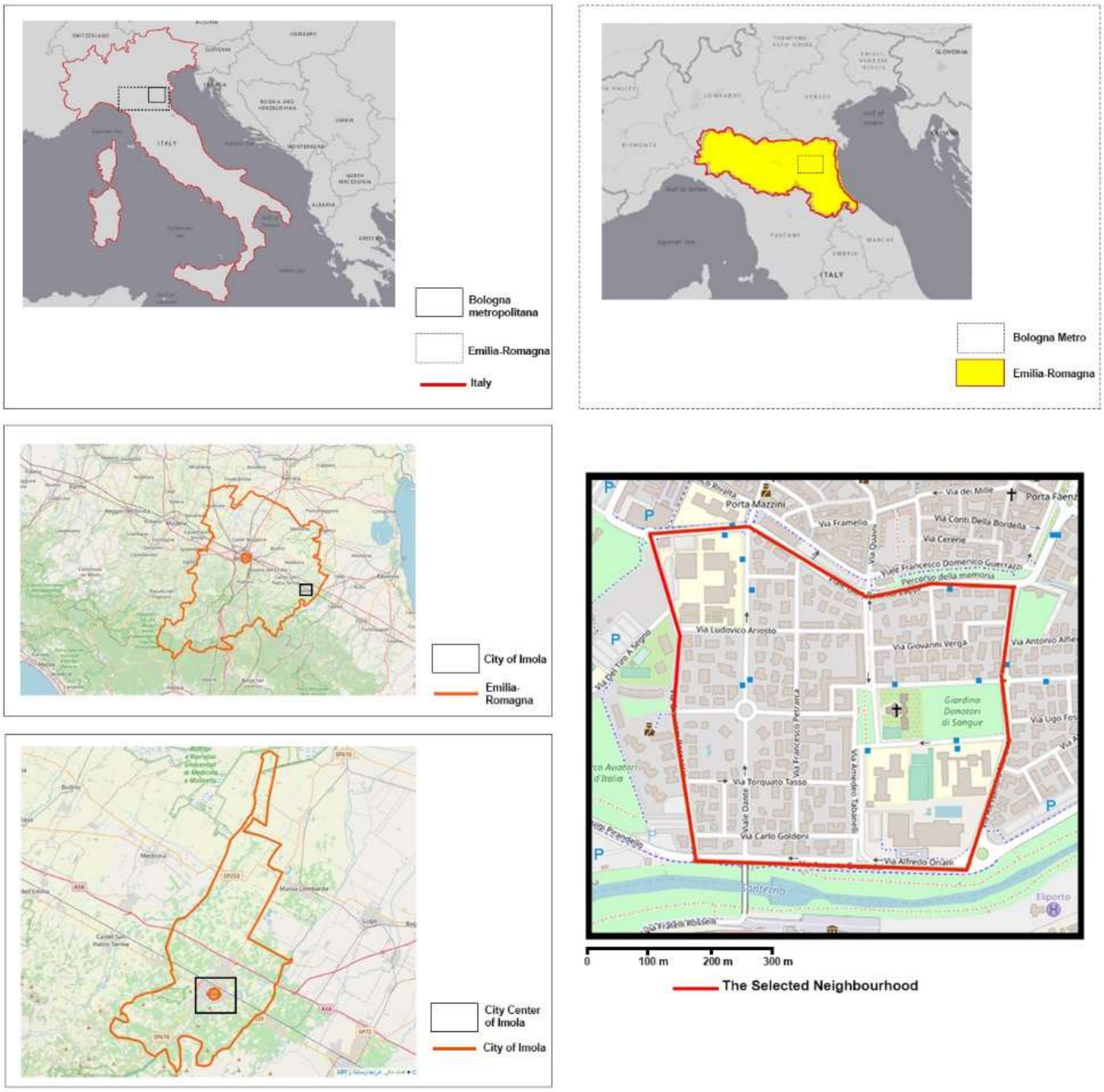

Figure 5.2: Aerial view of the study area in Imola, Italy

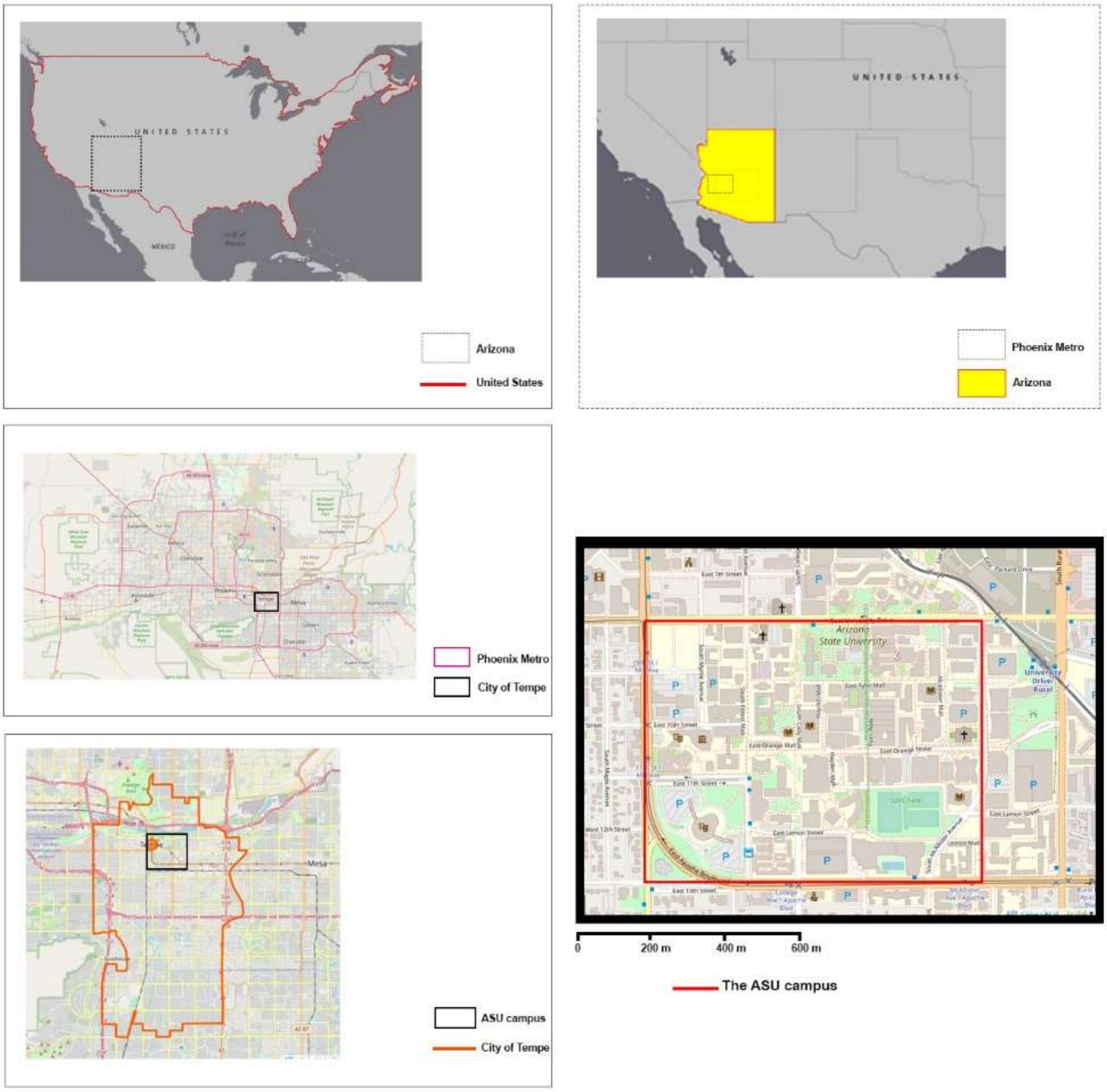

Figure 5.3: Aerial view of the study area in ASU Campus, Tempe, Arizona, USA

Table 5.2: Features of sample points

ID	Fisheye Photo	Shade Type	Ground Surface	Albedo (12:30 LST)	SVF	360° sky fraction	360° tree fraction	360° building fraction	360° imperv. fraction	360° perv. fraction
3100	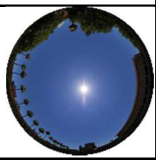	exposed	imperv.	0.20	0.8393	0.2182	0.0988	0.1498	0.1905	0.3410
3840		building canyon	imperv.	-	0.5138	0.0866	0.1681	0.2788	0.4534	0.0009
3041		exposed	imperv.	0.21	0.7681	0.1796	0.1343	0.2281	0.3876	0.0608
3660		PV canopy	imperv.	-	0.0415	0.0208	0.0585	0.4072	0.4714	0.0001
3140		exposed	imperv.	0.17	0.8653	0.2587	0.2669	0.0438	0.3788	0.0389

5.4 Case study: MRT in Imola, Italy, and Tempe, Arizona

The model is implemented in two contrasting climates: temperate and humid Imola, Italy, and hot and dry Tempe, Arizona, USA. Imola (44° 21' 11.0088'' N, 11° 42' 52.9992'' E) is a city in the metropolitan area of Bologna, Italy (Fig 5.3). It covers an area of 204 km2 and has a population of approximately 70,000 inhabitants. According to Koppen climate classification, Imola is in the zone of the humid subtropical climate and relatively continental and four-season version of it. In Imola, the summers are warm and mostly clear and the winters are very cold and partly cloudy. Over the year, the temperature typically varies from -0.5 °C to 31.11° C and is rarely below -5 °C or above 35.5 °C. The city receives approximately 2230 hours of sunlight per year. The selected neighborhood itself has an area of 900 m × 500 m, 9% of which is covered by street tree canopies. The neighborhood consists of detached two to three-story single-buildings with a dense pattern of tree planting in some parts.

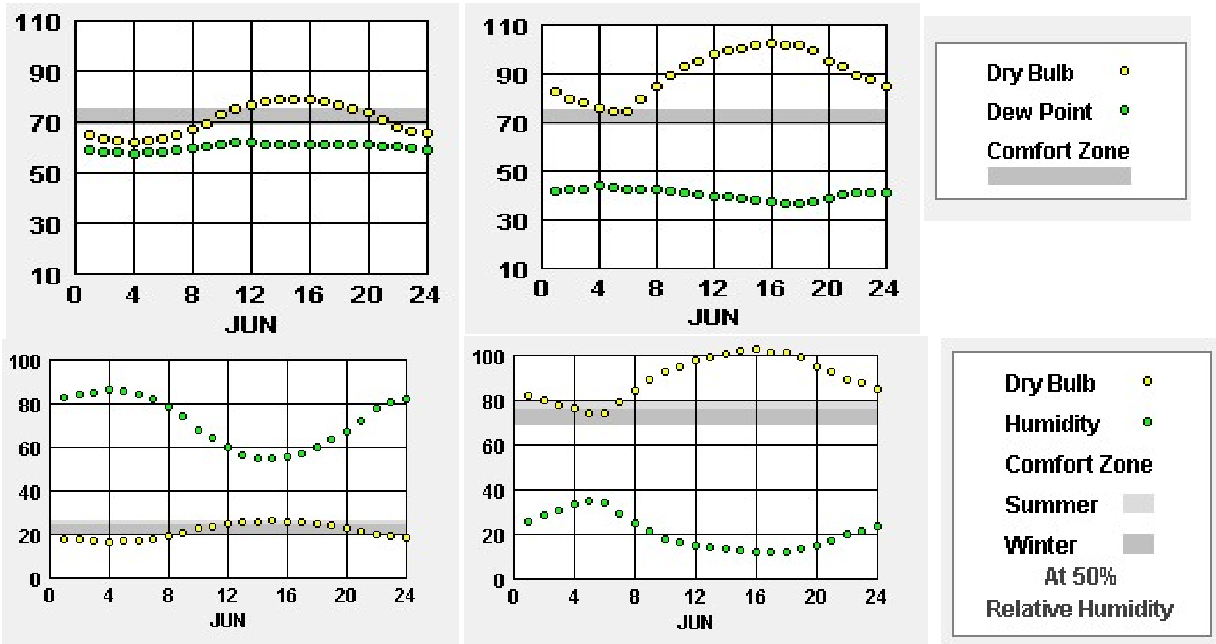

Figure 5.4: Meteorological parameters of Imola and Tempe

Figure 5.5 shows the dew point and dry bulb of Tempe and Imola. Dew point is defined as the temperature that the air requires to become cooled (at constant pressure) to reach a relative humidity (RH) of 100%. So, the Dew point can indicate the real level of feeling of humidity. In Imola the figure shows dew point approximately 15.5 ˚C, which is described as sticky with muggy evenings. In Tempe however, the dew point of 4.4 ˚C can be considered as dry.

Table 5.3: The relatin of Dew Point and Feeling of Humidity

Dew Point	Feeling of Humidity
less than or equal to 12.7 ˚C	dry and comfortable
between 12.7˚C and 18.3 ˚C	becoming sticky" with muggy evenings
greater than or equal to 18.3 ˚C	lots of moisture in the air, becoming oppressive

Tempe (33°25’28.6”N, 111°56’18.6”W), is a city in the East Valley of the Phoenix metropolitan area in Maricopa County, Arizona, USA (Fig. 5.4). With a population of 192,000, Tempe has a subtropical arid climate with a daytime maximum Ta of 50 °C in summer (period of record: 1953–2013). While overnight lows often are between 27 °C and 29 °C (Western Regional Climate Center, 2020). The study area is the campus of Arizona state university in Tempe with three- to four-story office and commercial buildings and mixed-use, high-rise apartments currently under construction, transitioning from an open midrise to an open high-rise zone.

The model is developed for one representative day of summer, the 9th of June 2018 in two cities. The meteorological conditions of the two cities on this day are compared in Fig 5.6.

Fig shows the air temperature, humidity, and wind speed on the daytime on the validation day. The maximum Ta in Imola during the 9th of June was 27 while in Tempe residents experienced a maximum Ta of 42. Besides, there is a considerable difference in relative humidity between these two cities. RH in Tempe shows an approximately steady amount of 10, while in Imola it starts from 60% in the morning and reaches 80 percent after sunset. The wind speed also varies significantly, in Imola it fluctuated between 1 and 4 m/s, and in Tempe, this variation is between 0.3 and 1.7m/s.

Selecting two cities with Ta peaking at 27 and 40 and RH peaking at 12% and 80% in this study allows examining the impacts of various micro-meteorological parameters on MRT.

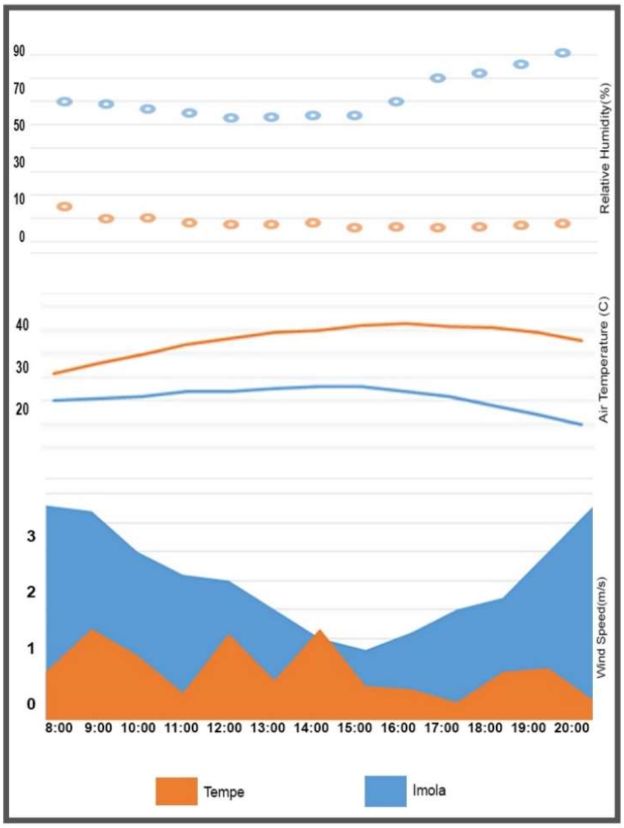

Figure 5.5: comparison of air temperature, humidity, and wind speed of Tempe and Imola

5.5 Results

For quantification of the model accuracy, we measured MBE, CVRMSE, MAE, and Wilmott's index of agreement. MAE demonstrates the Mean Absolute Error while all the points are weighted equally. RMSE gives a relatively high weight to large errors. So RMSE is valuable when large errors are particularly not desirable. RMSE is always larger than MAE, however, the greater the difference is, the more the variance between individual errors is. If in MAE the absolute error is not considered, the output is MBE that is the Mean Bias Error. Thus, MBE should be interpreted carefully, since the positive and negative errors can cancel each other.

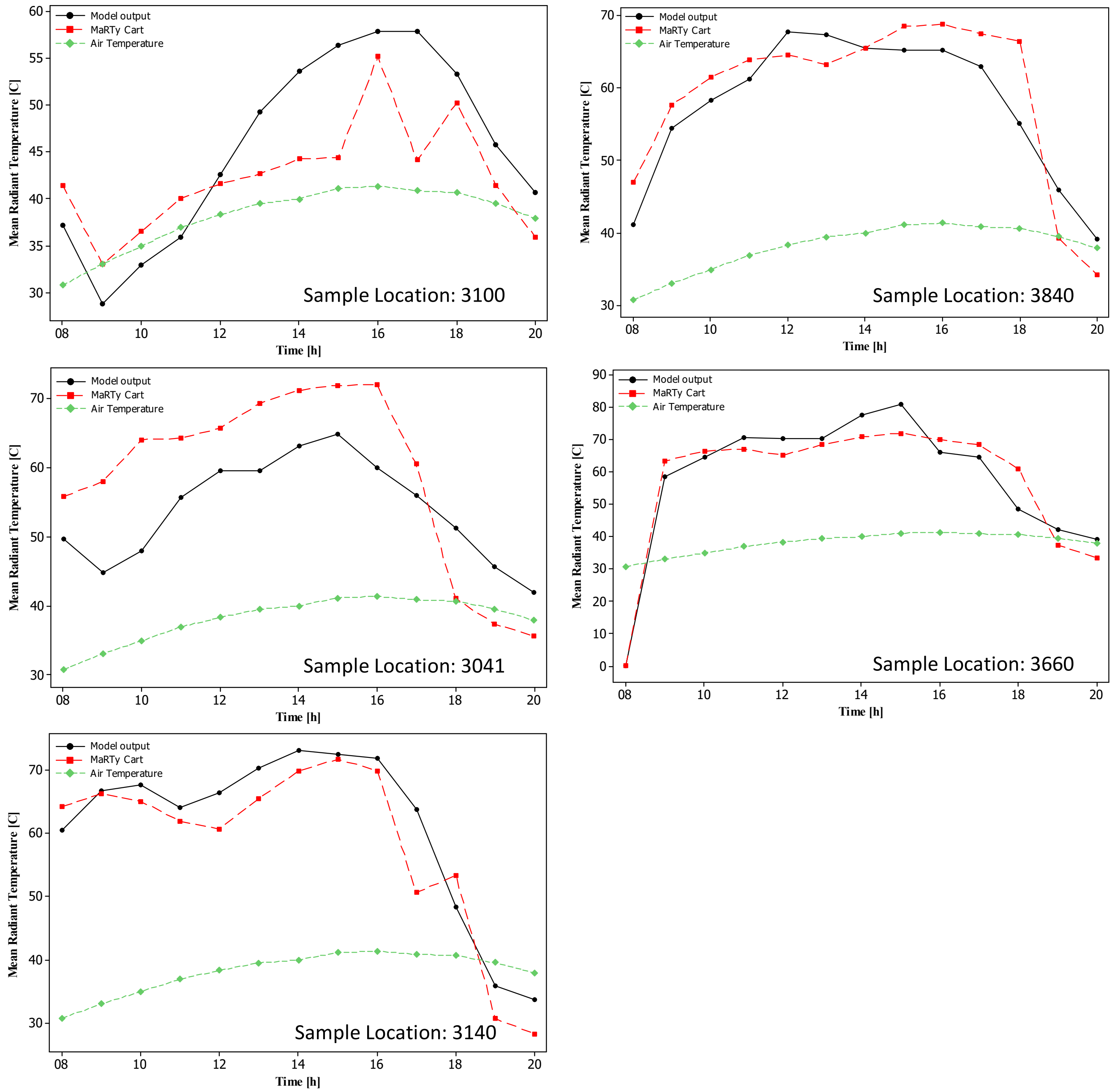

Figure 5.6: Validation of the model's outouts through the measurement by MaRTy Cart on 9th of June, 2018

The highest range of error in all the indexes is related to the sample location 3840 (D). The location is a shaded area and the RMSE is 9.45. however, the lowest amount of error in different error indexes varies. Based on RMSE the most accurate measured location belongs to 3140 (B). This location is sun-exposed with SKV 0.86. MAE shows location 3100 (C) as the best location accompanied with the highest rate of d= 0.961, this means that in location B the variation in MRT during the day is considerable in comparison to location C. On the other hand, MBE estimates location 3041(E) as the best-matched location. The MRT is overpredicted by the model for about 10 degrees, although the SKV for this location is 0.76. the analysis of various error indexes shows RMSE shows a good range for sun-exposed locations with high levels of SKV that a large amount of error is not observed during the day. MBE is not a suitable index for calculating errors when both over and underestimations are observed. Location 3660 (A) is semi-shaded by PV panels and MRT fluctuated from 16 °C to 18 °C due to the various incoming short-wave radiation and RMSE is 6.7 °C.

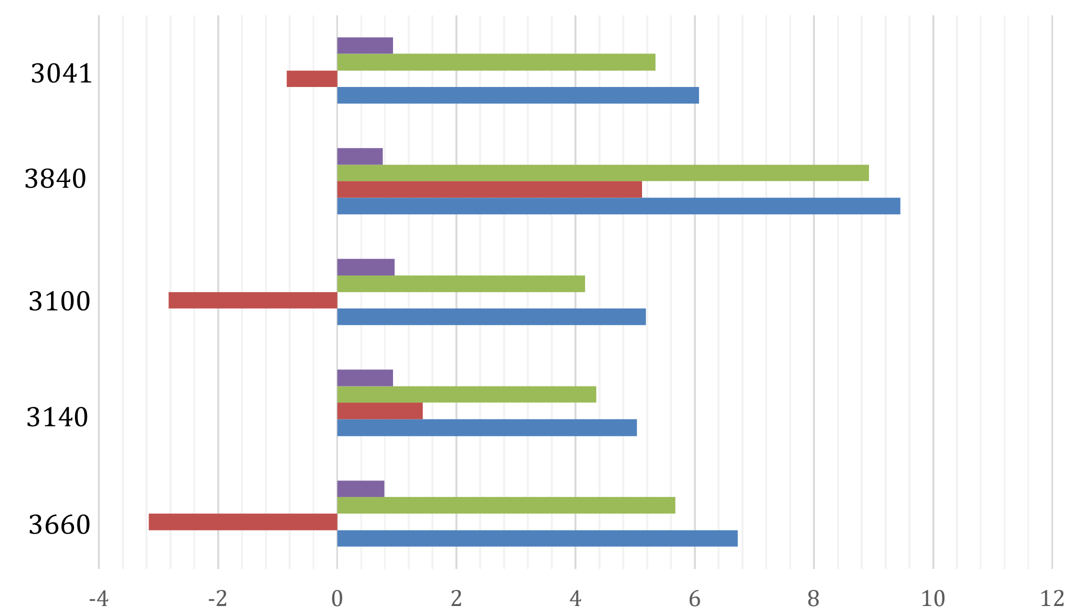

	3660	3140	3100	3840	3041
d:	0.796	0.938	0.961	0.764	0.938
MAE	5.672	4.348	4.164	8.923	5.346
MBE	-3.166	1.44	-2.827	5.115	-0.849
RMSE	6.726	5.03	5.182	9.455	6.072

Figure 5.7: Error indexes

5.5.1 Descriptive Statistics

Due to the short-term forecasting weather data, it can be assured that the discrepancies are not because of weather files but geometry, materials' properties, or the algorithm. The result of the digital twin is presented in the figure 5.9 and 10 which refers to 3 PM local time in both sites. According to the maps, the MRT range of the canyon in Tempe is between 43 °C and 80 °C, while the site in Imola shows a range of 26 °C and 50 °C. A usual tree shade in Tempe can reduce the MRT up to 30 °C, in Imola, however, it can reduce MRT by a maximum of 12 °C.

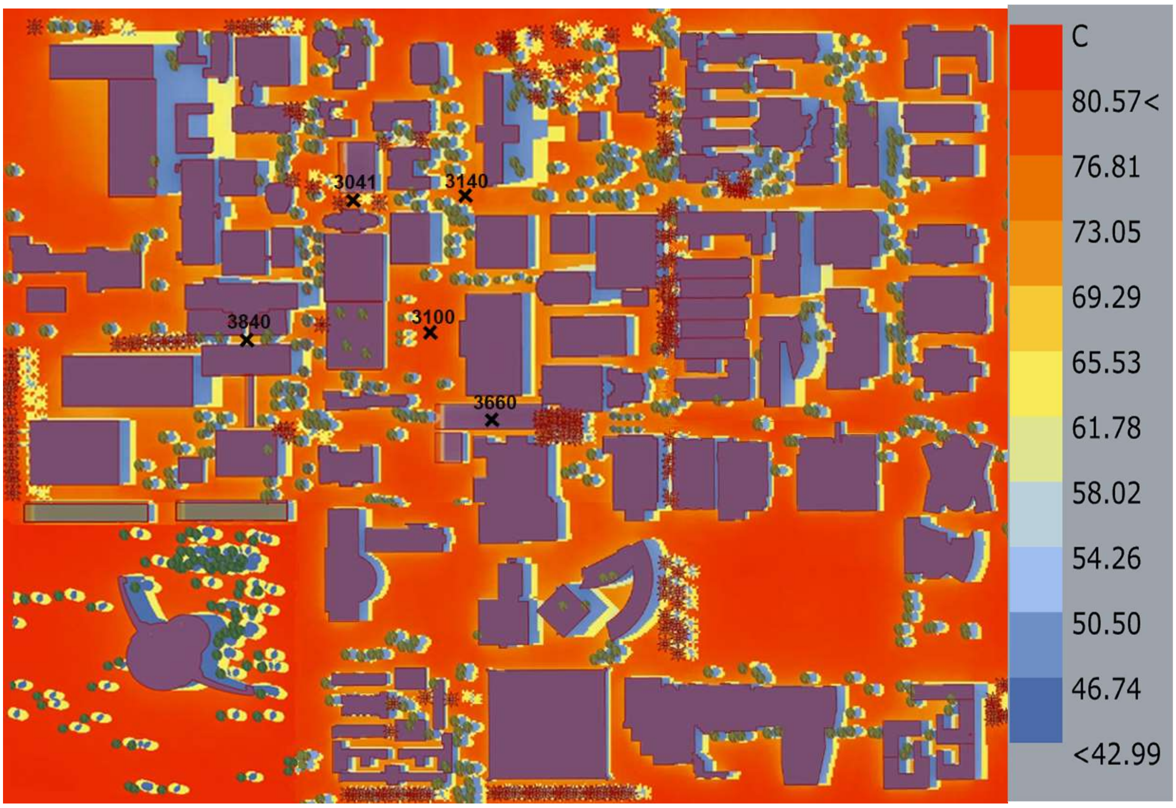

Figure 5.8: Spatial Variation of Mean Radiant Temperature in Tempe, Arizona, The US, on the 9th of June, 2018

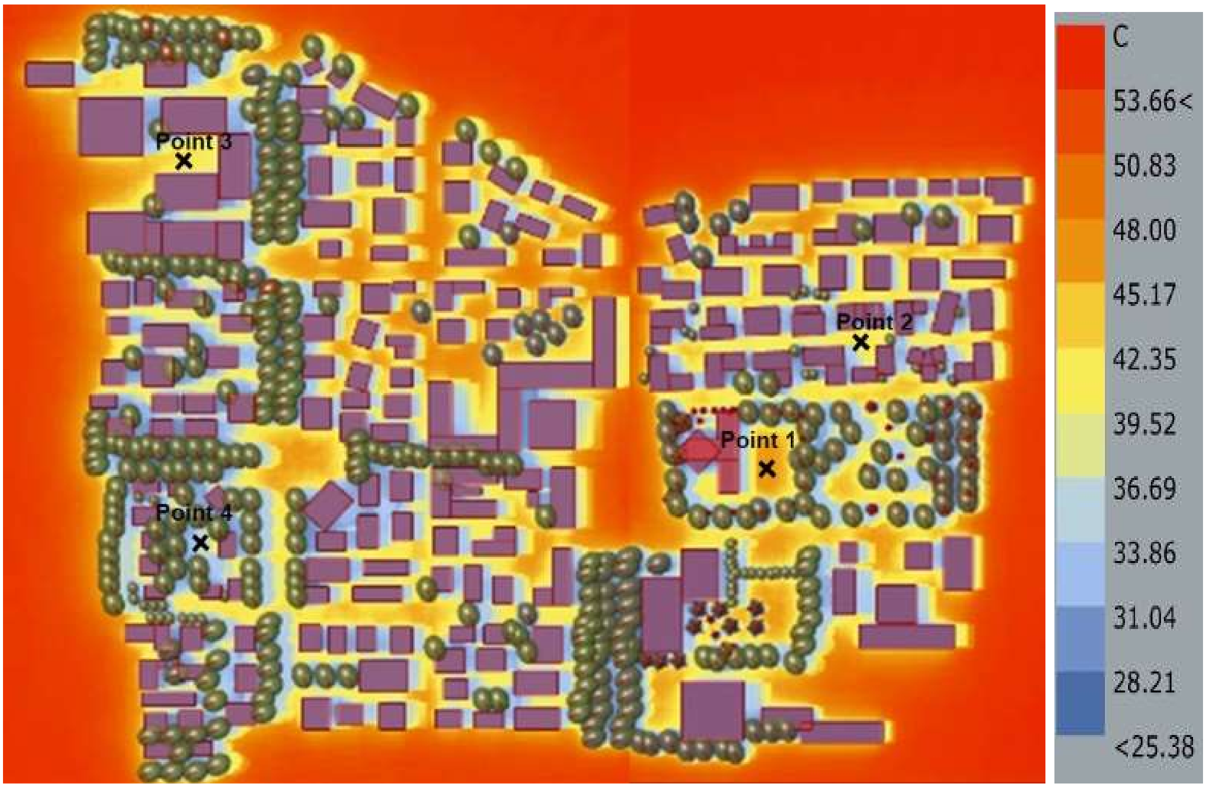

Figure 5.9: Spatial Variation of Mean Radiant Temperature in Imola, on the 9th of June, 2018

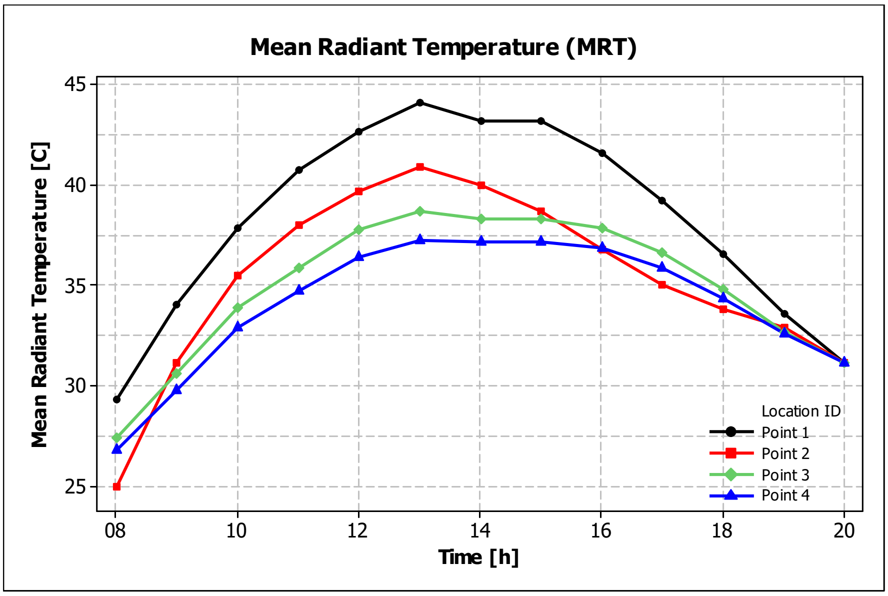

Figure 5.10: Mean Radiant Temperature of the 4 various points in Imola on the 9th of June, 2018

Of the four sample locations in Imola, point 1, which is a small, community-scale park, experienced the highest radiant temperature. As Fig 5.11 shows, during the peak temperature, the MRT reached over 65˚C in this point. The area has a sparse canopy cover, with trees placed at a distance from each other that does not allow them to block shortwave radiation and provide shade to enhance the comfort level of the site. In contrast, point 4 has a high density of buildings and trees, with nearly all of the spaces between the buildings being shaded by trees and geometric surfaces. The MRT in this block on the 9th of June was 43.5˚C, which is approximately 8 degrees lower than that in the sample location 1. As Fig 5.10 shows, the sample location 2 is a good example of the building shade effect in Imola. The dense fabric of the site helps create cool and comfortable pedestrian spaces.

5.5.2 The Universal Thermal Climate Index (UTCI)

Fig 5.11 shows the UTCI map of two case studies on the 9th of June at 3 PM local time. ASU campus is a car-free urban space and specifically is designed for pedestrians. As Fig 5.12 indicates the heat stress in most of the campus areas is in the range of “Extreme Heat Stress”. In Imola, however, the UTCI range is in “Moderate Heat Stress” and this is because of the dense urban context that has provided the area with considerable shaded area. Shade on ASU campus during the peak period can reduce MRT by 16 ˚C (81 to 65 ˚C) and UTCI by 6 ˚C (46 to 52 ˚C). In Imola this reduction in MRT is 13 ˚C (41- 54 ˚C) and 3 ˚C (28 - 25 ˚C) in UTCI.

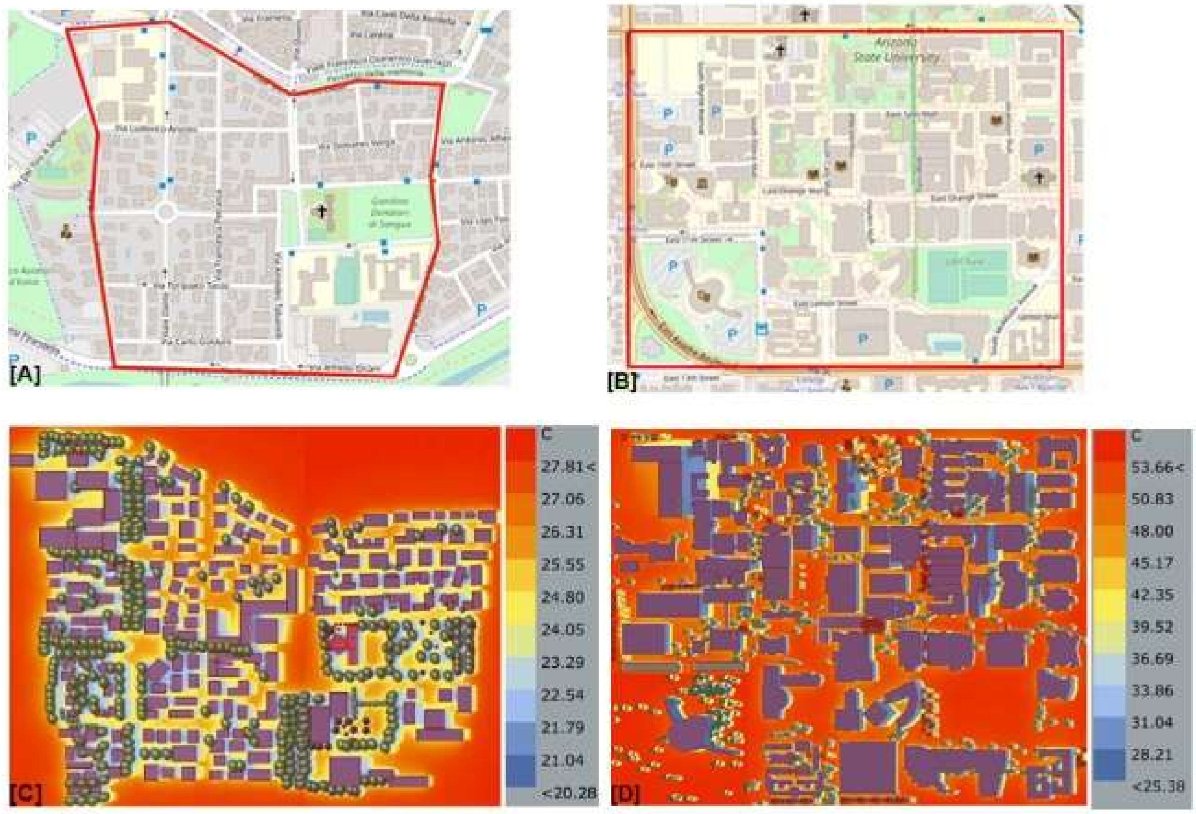

Figure 5.11: Spatial Variation of Universal Thermal Climate Index in Tempe [B]&[D] and Imola [A]&[C] on the 9th of June, 2018

5.6 Discussion

MRT differs significantly by location and time from a minimum of 25 °C (Imola, Jun 9th, 8 AM CET) to a maximum of 44 °C (Imola, Jun 9th, 1 PM CET). In Tempe, however, the range of MRT is higher (41 °C, Jun 9th, 8 AM; 81 °C, Jun 9th, 3 PM). MRT mostly depends on short wave radiation (Middel and Krayenhoff, 2019). So the most highlighted difference between Ta and MRT is the Tempe, point 3100, Jun 9th, 9:30 AM.

There are several models for simulating MRT; Rayman (Matzarakis et al., 2009) takes very simple environments, and also shortwave and longwave radiation are simplified. Rayman calculates the MRT from the Stefan-Boltzmann radiation law. ENVI-met (Bruse, 2004) is a three-dimensional microclimate model, Envi met MRT is defined by the equation of Bruse. It takes into account building ground, vegetation, and water entities. Ground evaporation and vegetation's transpiration are considered. Ladybug and Honeybee(Roudsari and Pak, 2013) can model complex environments. They simulate MRT by computing a long-wave MRT based on surface temperatures received from EnergyPlus and factored by View Factors studied with Raytracing. AUTODESK CFD (Autodesk, 2021) provides computational fluid dynamics and thermal simulation; it calculates MRT based on Finite Element Methods (FEM), and surface properties and radiation wavelength is roughly estimated. Citysim pro(Robinson et al., 2009) simulates and optimizes the sustainability of urban settlements by predicting energy fluxes at various scales the model considers ground evaporation and transpiration of vegetation entities. With a complete definition of building ground vegetation entities. MRT calculation is based on the integral radiation measurement defined by Hoppe. Solar and Long Wave Environmental Irradiance Geometry SOLWEIG (Lindberg et al., 2008) derives MRT by modeling shortwave and longwave radiation fluxes in six directions (upward, downward and from the four cardinal points) and angular factors.

Envi-met is the most-employed model in the last decade, however, the excessive simulating time that envi-met requires is a drawback of it. Ladybug tools can simulate various complex geometries while reduces simulating time. The proposed method has been run for an area of 650*800 on a computer intel core i5, 16 GB memory, and CPU 1.8 GHz. The simulation has been done in approximately 5 days. While similar simulation in Envi-met takes roughly 14 days. The accuracy of methods has varied in different studies depends on the input data, simulation engines, and complexity of the built environment. Aghamolaei et al. (Aghamolaei et al., 2020) investigated the Thermal comfort of three different morphological characters in Tehran through Ladybug. The model is validated by globe temperatures and RMSE range is reported. Evola et al. (Evola et al., 2020) validated the outdoor MRT through Ladybug tools and the results show that in the sun-exposed area the workflow overestimates MRT and it is more reliable in the shaded reference points and range of RMSE is between -0.6 to 0.3.

Naboni et al. (naboni et al., 2020) employed a parametric method in Ladybug for modeling indoor and outdoor MRT and calibrated the model through a test room. Crank et al. (Crank et al., 2020) have validated Envi-met and Rayman and the results demonstrated that none of these models are reliable due to the large range of errors spatially for enclosed and complex urban forms. In contrast to similar studies, validation in this study showed a different range of errors. RMSE differs from 5 °C to 9 °C. for this validation, TMRT was observed using the 6-directional method with MaRTy. The authors recommended that these methods should not be employed without in-situ validation.

On top of all the existing challenges in the adaptation of simulations and built environments, climate inconstancy induces large uncertainties in the assessments. Most of the simulations employ Typical Meteorology Year (TMY) weather data files. These weather data sets are mostly representatives of the typical condition of a climate zone based on 30 years of weather data sets. These files neglect climate variations, irregularities, and extreme conditions. The proposed method in this study is based on short-term weather predictions by taking the advantage of real-time weather generating methodology for considering future climate uncertainties.

5.6.1 Application of the cooling scenario

In order to evaluate the model's efficiency in quantifying the effect of increases in trees on neighborhoods, the study employed a strategy scenario that involved adding trees in specific places as well as optimizing the number of trees in public spaces. Several studies have investigated how urban surfaces affect the spatial variation of radiant temperature by creating shade (Thorsson et al., 2011). Trees and the spatial localization of additional trees play equally important roles in reducing the MRT on a small scale. The first step in adding trees in ideal spots requires creating a precise map of each block's climate comfort based on the UTCI to determine the priority of each parcel to receive additional trees (Figure 5.12).

Archetype HR-MCC in Bologna

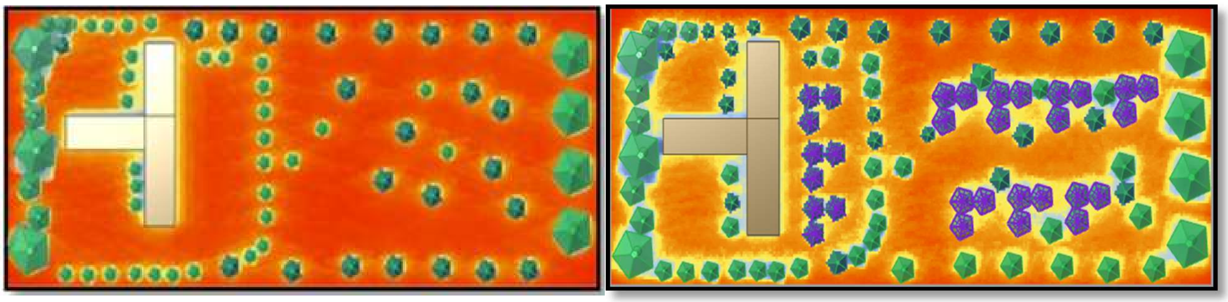

Archetype LR-LCC in Imola

Figure 5.12: Spatial variations in UTCI of cooling scenario by additional trees in Bologna and Imola

Two observations from prior studies were considered in testing the scenarios: First, trees are more effective at reducing the MRT as clusters rather than individually (Streiling and Matzarakis, 2003); and second, as Konarska et al. (2014) and Shahidan (2015) have shown, high-density tree canopies prevent more solar radiation from reaching the ground, thereby reducing land surface temperature and the MRT. Two blocks with the highest MRT in Bologna and Imola were selected to serve as settings for the tree addition cooling scenario. Figure 10 shows the MRT following the addition of street trees and the resulting reductions at each site.

Ten clusters of trees with a height of 10 m and a canopy width of 7 m were added in each site (additional trees are highlighted in blue). No changes were made to the current design of the sites so that the results are relevant for the development of effective retrofitting strategies. As the MRT of the Bologna archetype HR-MCC shows in Figure 10, during the hottest hours of the year, the cooling scenario can lower the radiant temperature by 9˚C and improve the climate comfort of the neighborhood by up to 35%. In Imola, the archetype LR-HCC, which was modeled with the same number of trees as the HR-MCC, showed a higher level of radiant temperature improvement. The cooling strategy reduced the temperature by up to 13˚C during the hottest hour of the year.

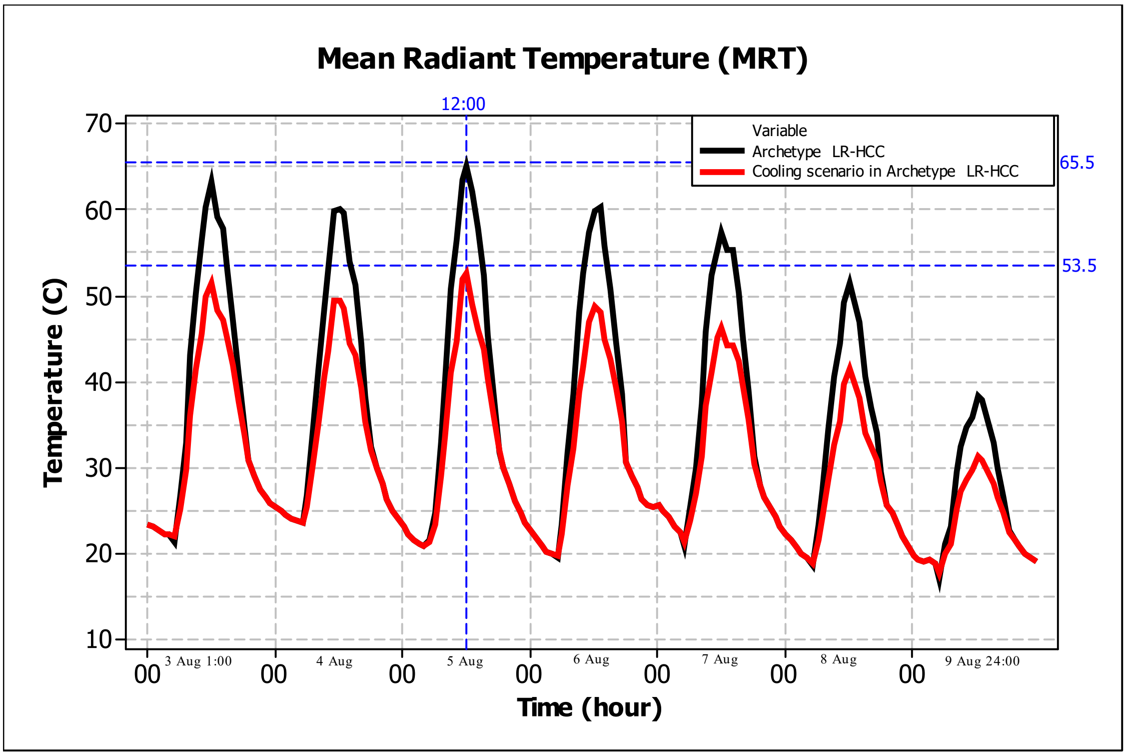

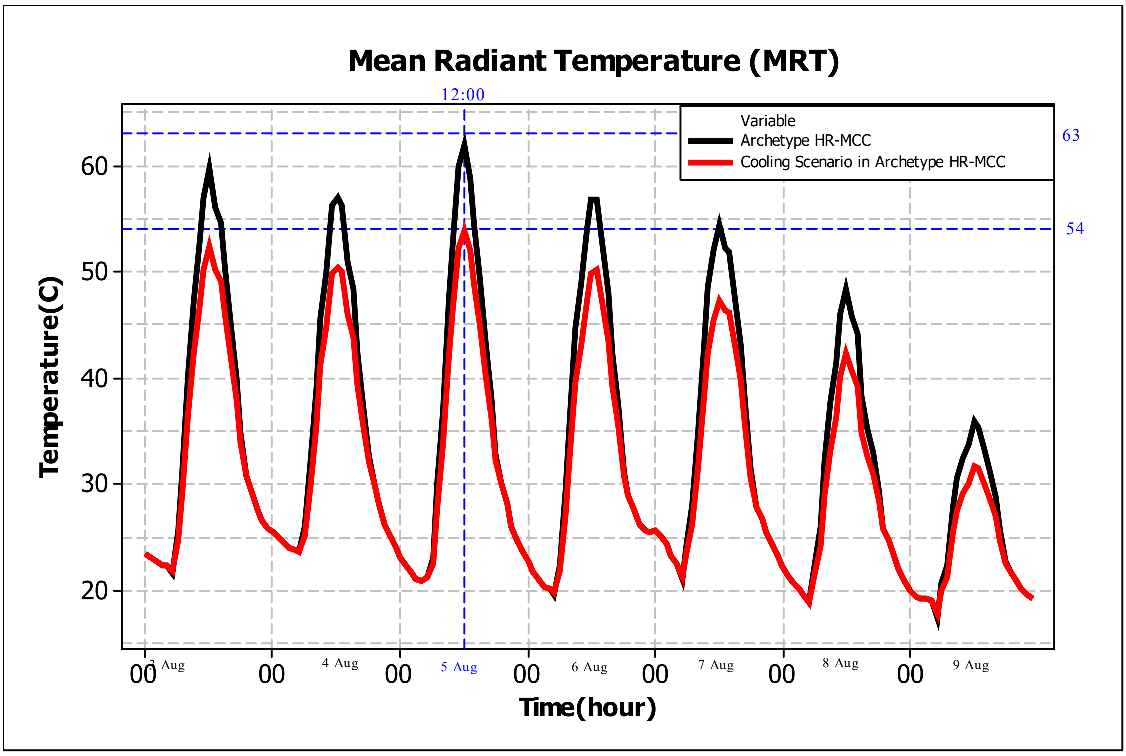

Figure 5.13: UTCI of cooling scenario by additional trees in Bologna (above) and Imola (below)

5.6.2 Sensitivity of the model to tree height and canopy density

The model was employed to investigate the relationship between tree height and total leaf area and thermal comfort. The streets of Bologna were modeled once with a scenario involving 15 m trees and another time involving trees with a canopy diameter of 10 m. The trees were all shorter than the buildings and each was modeled once with a low and again with a high leaf area index (LAI = 0.50, 1.50). The low and high LAIs were half and twice that of an average tree in the neighborhood, respectively. Thermal comfort modeling is the temperature relevant to the surfaces and the air above the ground. To evaluate the sensitivity of the model to tree characteristics, the MRT and UTCI in the scenarios were calculated on August 5, the hottest day of the year. The trees were added along the streets with enough distance from each other to enhance the effects. Figure 5.13 shows the results.

The first difference was observed at 7:00 AM, with the figures showing various behaviors. Having the lowest MRT, the scenario with extra-wide canopies (greater LAI) remained the coolest. The difference reached its peak at 1:00 PM, when the wide canopies reduced the radiant temperature from 57˚C to 45˚C. In the scenario with tall trees, this value was 50˚C, which decreased in the afternoon. The difference between all the simulations completely disappeared after sunset. The relative UTCI figures also showed a similar behavior in all the scenarios, although the difference between the scenarios was minimized to just 1˚C. These evaluations demonstrate the effectiveness of tree foliage in daytime cooling, in terms of both the MRT and UTCI, on the pedestrian level (1.1 m high) and show that tree height is not a leading factor in comparison to the LAI. Figure 5.14 illustrates the spatial variation of the MRT and the climate comfort level of the scenarios.

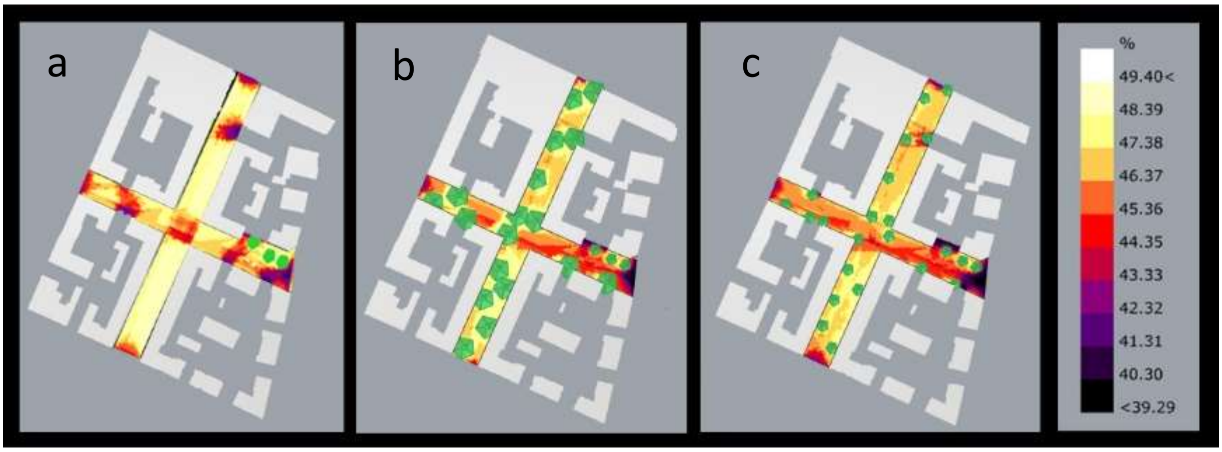

Figure 5.14: Spatial variation of MRT (above) and climate comfort percentage (below) for neighborhoods with differing tree height and density, current situation(a), the scenario of additional wide-foliage trees(b), the scenario of additional tall trees(c)

5.7 Conclusions

Today, the increase in urban population has led to global environmental and economic issues that negatively impact cities and, consequently, urban planning procedures. In recent decades, urban planning and design have increasingly been involved in decreasing carbon emissions. The retrofitting strategy of redesigning urban trees is one of the ways of achieving low-carbon cities. Digital twins stand for one of the latest technology trends for planning future cities. In this chapter, we set out to propose a digital twin prototype including a real-time climate model in complex 3-dimensional models of cities. The proposed digital twin simplifies complex concepts and key steps for the development of an urban microclimate digital twin, it includes a hybrid model that takes a novel approach to MRT modeling. First, it is a cohesive approach that minimizes miscalculation by employing various engines and using the output of one step as input for the next step in an integrated fashion. Second, it uses an accurate 3D model of geometric properties of buildings and trees, accompanied by DSMs from existing case studies. In addition, a procedure for generating real-time weather data files is proposed for the experiment day for analyzing surface temperatures to generate accurate hourly outputs. Lastly, the hierarchical structure of the proposed model not only enables it to overcome the issues of previous models regarding modeling thermally comfortable urban environments, but also makes it faster, more accurate, and higher in quality by combining various, highly efficient engines into an integrated set of 3D visualization and mapping methods.

Street trees are now more than ever valuable for our urban environments given how extreme heat in cities has reached concerning levels in recent decades. Overall, the number of trees must increase to prevent this effect, and urban design principles are essential for optimizing the distribution and placement of trees. Moreover, a balance must also be created between urban management and urban engineering to maximize the benefits of trees in retrofitting strategies. This digital twin can provide urban planners and policymakers with a precise and useful methodology for simulating the effects of trees on urban-scale, pedestrian-level thermal comfort and also help them guarantee the functionality of policies in different urban settings.

Chapter 6 . Concluding remarks

In this section, I synthesize the encompassing perspectives from the 5 chapters, make judgments as to what can be learned from them collectively, relate these to the previous literature, and reflect on new questions that emerge. Before this discussion, this section returns to the four inter-related research questions posed at the beginning:

The main research question of the thesis: how can we employ green adaptation for moving toward a zero impact or even positive environmental impact neighborhood and upscale it to cities?

The main question of this thesis concerns the possibility of developing zero impact neighborhoods through green adaptation strategies . This thesis has proposed conceptual and practical approaches for addressing green adaptation in different urban planning aspects, throughout adaptability of approaches and guidelines. A toolchain to evaluate how well every policy can affect a neighborhood in terms of sustainability (**Chapters 3 & 5**). There are various dimensions for evaluating green adaptability at the neighborhood scale. Policymakers vitally need to understand the consequences of potential courses in terms of costs and benefits (**Chapter 4**). Besides, uncertainties in calculating adaptivity impacts on a large scale are another layer of complicated decision-making and evaluation of green strategies in existing urban contexts. In addition to all the evaluation approaches that are proposed as part of this thesis, there are some points that I would like to mention in this section.

First, any urban context has its specific microclimate regarding the built environment, solar radiation, topography, shading, and air pollution. These factors are essential in estimating city heat gain and loss, optimizing energy balance, and developing neighborhoods with positive environmental impacts. Evaluating the green adaptivity of a neighborhood differs depending on the characteristics of the site. Evaluation methods identify the full advantages of every geographical location and develop climate-responsive green strategies. Second, the green adaptation policies differ from building to building depending on passive design principles. These principles include optimizing building energy usage, retrofitting of building stock, improvement of urban green space at low cost. This thesis argues that the city as a whole is more important than single buildings and principles should consider renewing the city through energy-efficient green architecture. Lastly, a green city requires to mitigate urban heat island (UHI) and introduce green strategies such as green roofs, inner green spaces, street tree planting. Evaluating the green adaptivity of a city is assessing the potential of urban cooling through increasing the percentage of green spaces and re-engineering the urban space to enhance the resilience of the urban ecosystem and as a comprehensive strategy contributes both and jointly to mitigating and adaptating approaches to climate change.

RQ 1: How to make the most effective retrofitting policies for buildings stock?

The first question regards the decision-making process of green adaptivity of building stock. I discussed the most common approaches in predicting the energy demand of building stock in **chapter 2 (Section 2.1.1)**. The main contribution of this chapter is to give a critical understanding of the state of the art of energy demand forecasting techniques. **Chapter 3** involves developing a comprehensive method for forecasting and calibrating energy demand and unknown parameters for being able to propose more accurate retrofitting scenarios for building stocks. Municipalities need to have a database of buildings to define the objectives of the interventions at building stocks, this database will give a broad perspective of the building stocks and their renovation potentials. Based on this database, the methodology can forecast the energy demand of buildings based on their features. Policymakers prioritize the retrofitting strategies for a cost-effective renovation and every building archetype in a building stock will have a specific renovation plan based on an ideal target of saving energy potential.

RQ 2: How can we evaluate the thermal behavior of buildings for green roofing scenarios?

The second question of this thesis seeks the energy efficiency of residential buildings after applying different roofing scenarios. After reviewing existing methods in the **chapter 2 (section 2.3)**, **Chapter 4** is explicitly allocated to the evaluation of various roofing scenarios. Analysing green adaptation strategies in buildings, sometimes, can be complicated, due to the humidity and water content in green roofs. In **chapter 4**, I developed a multidimensional hygrothermal model to simulate the energy performance of a two-story building. Three roofing scenarios including an insulated, green roof, and a rooftop greenhouse are selected for evaluation. The method shows the impact of water in the green roofs is extremely impacting on the thermal behavior of buildings. Simulations indicate the negative impact of moisture in green roofs and more importantly, the possibility of developing nearly-zero cooling buildings in the case studies by applying rooftop greenhouses.

RQ 3: How to develop a real-time model of the urban spaces to monitor pedestrian climate comfort in the neighbourhood through various greening scenarios?

The third question raises concerns regarding the urban spaces and using green adaptation to reduce heat stress. In response to this question, first, I analysed the atate of the art in **chapter 2, section 2.4**, based on this section, I decided to develop an urban microclimate digital twin. This digital twin is a set of urban-level simulations to model the thermal comfort and specify tempo-spatial MRT. I discussed the functionality of the proposed digital twin in **chapter 5**. It is worth mentioning that in this thesis I only studied green strategies in terms of street trees as it is the most effective factor in pedestrian comfort in different scenarios.

I considered time and space as the two main factors in generating this microclimate digital twin. It allows the users to perform real-time what-if analysis in urban green scenarios. Another feature of the digital twin is an automated workflow for generating weather files in a real-time modeling procedure. Identifying time as a variable in the development of the digital twin contributed to the real-time spatial data input to the model. My procedure recognizes the urban area as a space-time zone and eventually, it leads to location-specified heat mitigation strategies. We concluded that the proposed workflow is an appropriate methodology for neighborhood-scale green adaptation planning.

Fo what concerns the foreseeing methods for examining the impacts of green policies. The proposed urban microclimate digital twin in **chapter 5** can be employed to assess the impacts of implemented urban climate adaptation strategies. Analyzing the scenarios through the digital twin indicates the correlation between the size and shape of green spaces is not linear. The impact of the spatial layout of trees on mitigation urban heat islands mostly relies on shading and evapotranspiration processes. Thus, tree species, microclimate, and spatial scale are important factors. The main advantage of the proposed methodology is developing and testing synthetic green scenarios for urban spaces in real-time.

Within **chapter 5**, I explored the future green scenarios, strategic planning for greener urban environments. The outcome of the digital twin for the scenarios offers decision support for policymaking. For instance, in Imola, I declared the desired locations for green developments. Furthermore, the real-time simulation enhances the possibility of involving stakeholders in future urban developments. I consider digital twins as the assessment tool for future sustainable land use demands.

By linking the perceptions of green adaptation and planning practices, three main themes have been proposed and analyzed within this thesis. However, this research can be extended in various directions and paths to provide further data to support its development conceptually and in practice. First, developing a more detailed and diverse perspective toward green adaptation is necessary to meet challenges of climate change. Second, Real-time assessments should be developed at all levels to provide an in-depth understanding of the social and economic aspects of policies. Third, Identifying uncertainties and predictions in all the sources and their impacts in technical socio-economic models.

This Ph.D. dissertation has drawn on a deeper understanding of green adaptation planning in the urban built environment and offers a comprehensive framework for built communities. Responding to research questions has led the thesis to emphasize two vital dimensions. First, it highlights the role of uncertainty in modeling green adaptation policies. I discussed that when we develop a model from buildings to urban spaces, uncertainty is unavoidable. Unquestionably, uncertainty is an important part of examining climate change impacts. Uncertainties in green adaptation policies can be considered in predicting impacts of climate change or complexity in green adaptation measurements. Despite all the possible uncertainties in the prediction of adaptation policies, there is often enough certainty to identify action plans for green adaptation rather than postponing to gain more accuracy. The second dimension is the joint consideration of the problems, unifying multidisciplinary issues into one single procedure. The growing interest in green adaptation planning on large scales has led to research and action plans in a wide variety of topics. From architecture to ecology urbanism there are diverse approaches and theories which prove the complexity of green adaptation planning as the multidisciplinary, interdisciplinary, and transdisciplinary nature of this topic. This has made this thesis an opportunity for generating a comprehensive framework capable of guiding policymakers toward a fundamental transformation.

List of figures

List of tables

References:

Abdel-Aal, R.E., Al-Garni, A.Z., 1997. Forecasting monthly electric energy consumption in eastern Saudi Arabia using univariate time-series analysis. Energy 22, 1059–1069. https://doi.org/10.1016/s0360-5442(97)00032-7

Afshar, K., Bigdeli, N., 2011. Data analysis and short term load forecasting in Iran electricity market using singular spectral analysis ({SSA}). Energy 36, 2620–2627. https://doi.org/10.1016/j.energy.2011.02.003

Aghamolaei, R., Azizi, M.M., Aminzadeh, B., Mirzaei, P.A., 2020. A tempo-spatial modelling framework to assess outdoor thermal comfort of complex urban neighbourhoods. Urban Clim. 33, 100665. https://doi.org/10.1016/j.uclim.2020.100665

Aigner, D.J., Sorooshian, C., Kerwin, P., 1984. Conditional Demand Analysis for Estimating Residential End-Use Load Profiles. Energy J. 5. https://doi.org/10.5547/issn0195-6574-ej-vol5-no3-6

Akay, D., Atak, M., 2007. Grey prediction with rolling mechanism for electricity demand forecasting of Turkey. Energy 32, 1670–1675. https://doi.org/10.1016/j.energy.2006.11.014

Al-Ghandoor, A., Al-Hinti, I., Jaber, J.O., Sawalha, S.A., 2008. Electricity consumption and associated {GHG} emissions of the Jordanian industrial sector: Empirical analysis and future projection. Energy Policy 36, 258–267. https://doi.org/10.1016/j.enpol.2007.09.020

Al-Iriani, M.A., 2006. Energy{\textendash}{GDP} relationship revisited: An example from {GCC} countries using panel causality. Energy Policy 34, 3342–3350. https://doi.org/10.1016/j.enpol.2005.07.005

Albers, D.J., Blancquart, P.-A., Levine, M.E., Seylabi, E.E., Stuart, A., 2019. Ensemble Kalman Methods With Constraints.

Alcántara, V., del R\'\io, P., Hernández, F., 2010. Structural analysis of electricity consumption by productive sectors. The Spanish case. Energy 35, 2088–2098. https://doi.org/10.1016/j.energy.2010.01.027

AlRashidi, M.R., EL-Naggar, K.M., 2010. Long term electric load forecasting based on particle swarm optimization. Appl. Energy 87, 320–326. https://doi.org/10.1016/j.apenergy.2009.04.024

AMARAWICKRAMA, H., HUNT, L., 2008. Electricity demand for Sri Lanka: A time series analysis. Energy 33, 724–739. https://doi.org/10.1016/j.energy.2007.12.008

Amjady, N., 2001. Short-term hourly load forecasting using time-series modeling with peak load estimation capability. {IEEE} Trans. Power Syst. 16, 798–805.

https://doi.org/10.1109/59.962429

An Energy Use Model of the Residential Sector, 1980. . {IEEE} Trans. Syst. Man, Cybern. 10, 749–755. https://doi.org/10.1109/tsmc.1980.4308396

Ang, B.W., 1995a. Decomposition methodology in industrial energy demand analysis. Energy 20, 1081–1095. https://doi.org/10.1016/0360-5442(95)00068-r

Ang, B.W., 1995b. Multilevel decomposition of industrial energy consumption. Energy Econ. 17, 39–51. https://doi.org/10.1016/0140-9883(95)98905-j

Ang, B.W., Lee, P.W., 1996. Decomposition of industrial energy consumption: The energy coefficient approach. Energy Econ. 18, 129–143. https://doi.org/10.1016/0140-9883(95)00049-6

Ang, J.B., 2007. {CO}2 emissions, energy consumption, and output in France. Energy Policy 35, 4772–4778. https://doi.org/10.1016/j.enpol.2007.03.032

ARAS, H., ARAS, N.I.L., 2004. Forecasting Residential Natural Gas Demand. Energy Sources 26, 463–472. https://doi.org/10.1080/00908310490429740

Arbex, M., Perobelli, F.S., 2010. Solow meets Leontief: Economic growth and energy consumption. Energy Econ. 32, 43–53. https://doi.org/10.1016/j.eneco.2009.05.004

Arens, E., Hoyt, T., Zhou, X., Huang, L., Zhang, H., Schiavon, S., 2015. Title: Modeling the comfort effects of short-wave solar radiation indoors MODELING THE COMFORT EFFECTS OF SHORT-WAVE SOLAR RADIATION INDOORS 88, 1. https://doi.org/10.1016/j.buildenv.2014.09.004

ARPAE, 2020. Hydro-Weather-Climate, dexter system.

Arsenault, E., Bernard, J.-T., Carr, C.W., Genest-Laplante, E., 1995. A total energy demand model of Québec. Energy Econ. 17, 163–171. https://doi.org/10.1016/0140-9883(94)00003-y

Asadi, E., Gameiro, M., Henggeler, C., Dias, L., Glicksman, L., 2014. Multi-objective optimization for building retrofit : A model using genetic algorithm and artificial neural network and an application. Energy Build. 81, 444–456. https://doi.org/10.1016/j.enbuild.2014.06.009

Asadi, S., Mostavi, E., Boussaa, D., Indaganti, M., 2019. Building energy model calibration using automated optimization-based algorithm. Energy Build. 198, 106–114. https://doi.org/10.1016/j.enbuild.2019.06.001

Ascione, F., Bianco, N., De’ Rossi, F., Turni, G., Vanoli, G.P., 2013. Green roofs in European climates. Are effective solutions for the energy savings in air-conditioning? https://doi.org/10.1016/j.apenergy.2012.11.068

Ascione, F., Bianco, N., Stasio, C. De, Mauro, G.M., Vanoli, G.P., 2016. A Methodology to Assess and Improve the Impact of Public Energy Policies for Retrofitting the Building Stock: Application to Italian Office Buildings. Int. J. Heat Technol. 34, S277--S286. https://doi.org/10.18280/ijht.34s213

Astee, L.Y., Kishnani, N.T., 2010. Building integrated agriculture utilising rooftops for sustainable food crop cultivation in Singapore. J. Green Build. 5, 105–113. https://doi.org/10.3992/jgb.5.2.105

Austin, M., Delgoshaei, P., Coelho, M., Heidarinejad, M., 2020. Architecting Smart City Digital Twins: Combined Semantic Model and Machine Learning Approach. J. Manag. Eng. 36, 04020026. https://doi.org/10.1061/(asce)me.1943-5479.0000774

Autodesk, 2021. CFD 2016 Help: Physical Models [WWW Document]. Autodesk CFD 2016. URL http://help.autodesk.com/view/SCDSE/2016/ENU/?guid=GUID-3FCD44C0-8AAC-4826-B199-9D1C299F7165 (accessed 8.17.21).

Ávila-Hernández, A., Simá, E., Xamán, J., Hernández-Pérez, I., Téllez-Velázquez, E., Chagolla-Aranda, M.A., 2020. Test box experiment and simulations of a green-roof: Thermal and energy performance of a residential building standard for Mexico. Energy Build. 209, 109709. https://doi.org/10.1016/j.enbuild.2019.109709

Awad, M., Khanna, R., 2015. Support Vector Regression, in: Efficient Learning Machines. Apress, pp. 67–80. https://doi.org/10.1007/978-1-4302-5990-9_4

Aydinalp-Koksal, M., Ugursal, V.I., 2008. Comparison of neural network, conditional demand analysis, and engineering approaches for modeling end-use energy consumption in the residential sector. Appl. Energy 85, 271–296. https://doi.org/10.1016/j.apenergy.2006.09.012

Aydinalp, M., Ugursal, V.I., Fung, A.S., 2004. Modeling of the space and domestic hot-water heating energy-consumption in the residential sector using neural networks. Appl. Energy 79, 159–178. https://doi.org/10.1016/j.apenergy.2003.12.006

Aydinalp, M., Ugursal, V.I., Fung, A.S., 2003. Effects of socioeconomic factors on household appliance, lighting, and space cooling electricity consumption. Int. J. Glob. Energy Issues 20, 302. https://doi.org/10.1504/ijgei.2003.003969

Aydinalp, M., Ugursal, V.I., Fung, A.S., 2002. Modeling of the appliance, lighting, and space-cooling energy consumptions in the residential sector using neural networks. Appl. Energy 71, 87–110. https://doi.org/10.1016/s0306-2619(01)00049-6

Azadeh, A., Ghaderi, S.F., Sohrabkhani, S., 2007. Forecasting electrical consumption by integration of Neural Network, time series and {ANOVA}. Appl. Math. Comput. 186, 1753–1761. https://doi.org/10.1016/j.amc.2006.08.094

Balaras, C.A., Gaglia, A.G., Georgopoulou, E., Mirasgedis, S., Sarafidis, Y., Lalas, D.P., 2007. European residential buildings and empirical assessment of the Hellenic building stock, energy consumption, emissions and potential energy savings. Build. Environ. 42, 1298–1314. https://doi.org/10.1016/j.buildenv.2005.11.001

Ballarini, I., Corgnati, S.P., Corrado, V., 2014. Use of reference buildings to assess the energy saving potentials of the residential building stock: The experience of {TABULA} project. Energy Policy 68, 273–284. https://doi.org/10.1016/j.enpol.2014.01.027

Barbaresi, A., Dallacasa, F., Torreggiani, D., Tassinari, P., 2017. Retrofit interventions in non-conditioned rooms: calibration of an assessment method on a farm winery. J. Build. Perform. Simul. 10, 91–104. https://doi.org/10.1080/19401493.2016.1141994

Barbaresi, A., Torreggiani, D., Benni, S., Tassinari, P., 2014. Underground cellar thermal simulation: Definition of a method for modelling performance assessment based on experimental calibration. Energy Build. 76, 363–372. https://doi.org/10.1016/j.enbuild.2014.03.008

Barrio, E.P. Del, 1998. Analysis of the green roofs cooling potential in buildings. Energy Build. 27, 179–193. https://doi.org/10.1016/s0378-7788(97)00029-7

Bartels, R., Fiebig, D.G., 2000. Residential End-Use Electricity Demand: Results from a Designed Experiment. Energy J. 21. https://doi.org/10.5547/issn0195-6574-ej-vol21-no2-3

Bartels, R., Fiebig, D.G., 1990. Integrating Direct Metering and Conditional Demand Analysis for Estimating End-Use Loads. Energy J. 11. https://doi.org/10.5547/issn0195-6574-ej-vol11-no4-5

Benaouda, D., Murtagh, F., Starck, J.-L., Renaud, O., 2006. Wavelet-based nonlinear multiscale decomposition model for electricity load forecasting. Neurocomputing 70, 139–154. https://doi.org/10.1016/j.neucom.2006.04.005

Benni, S., Tassinari, P., Barbaresi, A., Torreggiani, D., 2016. Efficacy of greenhouse natural ventilation : Environmental monitoring and CFD simulations of a study case Efficacy of greenhouse natural ventilation : environmental monitoring and CFD simulations of a study case. Energy Build. https://doi.org/10.1016/j.enbuild.2016.05.014

Bentzen, J., Engsted, T., 2001. A revival of the autoregressive distributed lag model in estimating energy demand relationships. Energy 26, 45–55. https://doi.org/10.1016/s0360-5442(00)00052-9

Bertrand Iooss, A., Da Veiga, S., Janon, A., Pujol, G., contribu-tions from Baptiste Broto, with, Boumhaout, K., Delage, T., El Amri, R., Fruth, J., Gilquin, L., Guillaume, J., Le Gratiet, L., Lemaitre, P., Marrel, A., Mey-naoui, A., Nelson, B.L., Monari, F., Oomen, R., Rakovec, O., Ramos, B., Roustant, O., Song, E., Staum, J., Sueur, R., Touati, T., Weber, F., 2020. Package “sensitivity” Title Global Sensitivity Analysis of Model Outputs.

Betancourt, M., 2018. A Conceptual Introduction to Hamiltonian Monte Carlo.

Bianco, V., Manca, O., Nardini, S., Minea, A.A., 2010. Analysis and forecasting of nonresidential electricity consumption in Romania. Appl. Energy 87, 3584–3590. https://doi.org/10.1016/j.apenergy.2010.05.018

Blazejczyk, K., 1992. MENEX· mE MAN-ENVIRONMENT HEAT EXCHANGE MODEL AND ITS APPLICATIONS IN BIOCLIMATOLOGY.

Bodger, P.S., Tay, H.S., 1987. Logistic and energy substitution models for electricity forecasting: A comparison using New Zealand consumption data. Technol. Forecast. Soc. Change 31, 27–48. https://doi.org/10.1016/0040-1625(87)90021-7

Booth, A.T., Choudhary, R., 2013. Decision making under uncertainty in the retrofit analysis of the UK housing stock: Implications for the Green Deal. Energy Build. 64, 292–308. https://doi.org/10.1016/j.enbuild.2013.05.014

Booth, A.T., Choudhary, R., Spiegelhalter, D.J., 2013. A hierarchical bayesian framework for calibrating micro-level models with macro-level data. J. Build. Perform. Simul. 6, 293–318. https://doi.org/10.1080/19401493.2012.723750

Booth, A.T., Choudhary, R., Spiegelhalter, D.J., 2012. Handling uncertainty in housing stock models. Build. Environ. 48, 35–47. https://doi.org/10.1016/j.buildenv.2011.08.016

Boroojeni, K.G., Amini, M.H., Bahrami, S., Iyengar, S.S., Sarwat, A.I., Karabasoglu, O., 2017. A novel multi-time-scale modeling for electric power demand forecasting: From short-term to medium-term horizon. Electr. Power Syst. Res. 142, 58–73. https://doi.org/10.1016/j.epsr.2016.08.031

Bowler, D.E., Buyung-Ali, L., Knight, T.M., Pullin, A.S., 2010. Urban greening to cool towns and cities: A systematic review of the empirical evidence. Landsc. Urban Plan. https://doi.org/10.1016/j.landurbplan.2010.05.006

Bruse, M., 2004. ENVI-met 3.0: Updated Model Overview.

Bueno, B., Norford, L., Hidalgo, J., Pigeon, G., 2013. The urban weather generator. J. Build. Perform. Simul. 6, 269–281. https://doi.org/10.1080/19401493.2012.718797

Busser, T., Berger, J., Piot, A., Pailha, M., Woloszyn, M., Experimental, M.W., 2018. Experimental validation of hygrothermal models for building materials and walls: an analysis of recent trends. https://doi.org/hal-01678857

Capasso, A., Grattieri, W., Lamedica, R., Prudenzi, A., 1994. A bottom-up approach to residential load modeling. {IEEE} Trans. Power Syst. 9, 957–964. https://doi.org/10.1109/59.317650

Caplow, T., Nelkin, J., 2007. Building-integrated greenhouse systems for low energy cooling. 2nd

PALENC Conf. 28th AIVC Conf. Build. Low Energy Cool. Adv. Vent. Technol. 21st Century 1, 172–176.

Carbonaro, A., Maniezzo, V., 2003. The Ant Colony Optimization Paradigm for Combinatorial Optimization, in: Natural Computing Series. Springer Berlin Heidelberg, pp. 539–557. https://doi.org/10.1007/978-3-642-18965-4_21

Carlo, J., Ghisi, E., Lamberts, R., Para, N., Ahorro, E.L., 2003. THE USE OF COMPUTER SIMULATION TO ESTABLISH ENERGY EFFICIENCY PARAMETERS FOR A BUILDING CODE OF A CITY IN BRAZIL LabEEE – Energy Efficiency in Buildings Laboratory Federal University of Santa Catarina. Methodology 131–138.

Cascone, S., Coma, J., Gagliano, A., Pérez, G., 2019. The evapotranspiration process in green roofs: A review. Build. Environ. https://doi.org/10.1016/j.buildenv.2018.10.024

Caves, D.W., Herriges, J.A., Train, K.E., Windle, R.J., 1987. A Bayesian Approach to Combining Conditional Demand and Engineering Models of Electricity Usage. Rev. Econ. Stat. 69, 438. https://doi.org/10.2307/1925531

Cerezo, C., Dogan, T., Reinhart, C.F., 2014. TOWARDS STANDARIZED BUILDING PROPERTIES TEMPLATE FILES FOR EARLY DESIGN ENERGY MODEL GENERATION Massachusetts Institute of Technology , Cambridge , MA.

Cerezo Davila, C., Reinhart, C.F., Bemis, J.L., 2016. Modeling Boston: A workflow for the efficient generation and maintenance of urban building energy models from existing geospatial datasets. Energy 117, 237–250. https://doi.org/10.1016/j.energy.2016.10.057

Cetin, K.S., Tabares-Velasco, P.C., Novoselac, A., 2014. Appliance daily energy use in new residential buildings: Use profiles and variation in time-of-use. Energy Build. 84, 716–726. https://doi.org/10.1016/j.enbuild.2014.07.045

Ceylan, H., Ozturk, H.K., 2004. Estimating energy demand of Turkey based on economic indicators using genetic algorithm approach. Energy Convers. Manag. 45, 2525–2537. https://doi.org/10.1016/j.enconman.2003.11.010

Ceylan, Huseyin, Ceylan, Halim, Haldenbilen, S., Baskan, O., 2008. Transport energy modeling with meta-heuristic harmony search algorithm, an application to Turkey. Energy Policy 36, 2527–2535. https://doi.org/10.1016/j.enpol.2008.03.019

Changhong, C., Bingyan, W., Qingyan, F., Green, C., Streets, D.G., 2006. Reductions in emissions of local air pollutants and co-benefits of Chinese energy policy: a Shanghai case study. Energy Policy 34, 754–762. https://doi.org/10.1016/j.enpol.2004.07.007

Charytoniuk, W., Chen, M.S., Olinda, P. Van, 1998. Nonparametric regression based short-term load forecasting. {IEEE} Trans. Power Syst. 13, 725–730. https://doi.org/10.1109/59.708572

Chaudhary, G., New, J., Sanyal, J., Im, P., O'Neill, Z., Garg, V., 2016. Evaluation of "Autotune" calibration against manual calibration of building energy models. Appl. Energy 182, 115–134. https://doi.org/10.1016/j.apenergy.2016.08.073

Chavez, S.G., Bernat, J.X., Coalla, H.L., 1999. Forecasting of energy production and consumption in Asturias (northern Spain). Energy 24, 183–198. https://doi.org/10.1016/s0360-5442(98)00099-1

Chemisana, D., Lamnatou, C., 2014. Photovoltaic-green roofs: An experimental evaluation of system performance. Appl. Energy 119, 246–256. https://doi.org/10.1016/j.apenergy.2013.12.027

Chen, J., Gao, X., Hu, Y., Zeng, Z., Liu, Y., 2019a. A meta-model-based optimization approach for fast and reliable calibration of building energy models. Energy 188, 116046. https://doi.org/10.1016/j.energy.2019.116046

Chen, J., Gao, X., Hu, Y., Zeng, Z., Liu, Y., 2019b. A meta-model-based optimization approach for fast and reliable calibration of building energy models. Energy 188, 116046. https://doi.org/10.1016/j.energy.2019.116046

Chen, P.-F., Lee, C.-C., 2007. Is energy consumption per capita broken stationary? New evidence from regional-based panels. Energy Policy 35, 3526–3540. https://doi.org/10.1016/j.enpol.2006.12.027

Chen, W., 2005. The costs of mitigating carbon emissions in China: findings from China {MARKAL}-{MACRO} modeling. Energy Policy 33, 885–896. https://doi.org/10.1016/j.enpol.2003.10.012

Chong, A., Menberg, K., 2018. Guidelines for the Bayesian calibration of building energy models. Energy Build. 174, 527–547. https://doi.org/10.1016/j.enbuild.2018.06.028

Christodoulakis, N.M., Kalyvitis, S.C., Lalas, D.P., Pesmajoglou, S., 2000. Forecasting energy consumption and energy related {CO}2 emissions in Greece. Energy Econ. 22, 395–422. https://doi.org/10.1016/s0140-9883(99)00040-7

Cinar, D., Kayakutlu, G., Daim, T., 2010. Development of future energy scenarios with intelligent algorithms: Case of hydro in Turkey. Energy 35, 1724–1729. https://doi.org/10.1016/j.energy.2009.12.025

Cioara, T., Anghel, I., Antal, M., Salomie, I., Antal, C., Ioan, A.G., 2021. An Overview of Digital Twins Application Domains in Smart Energy Grid. undefined.

Clarke, J.A., Johnstone, C.M., Kim, J.M., Tuohy, P.G., 2009. Energy, Carbon and Cost Performance of Building Stocks: Upgrade Analysis, Energy Labelling and National Policy Development. Adv. Build. Energy Res. 3, 1–20. https://doi.org/10.3763/aber.2009.0301

Coelho, M., Austin, M., Blackburn, M., 2017. Semantic Behavior Modeling and Event-Driven Reasoning for Urban System of Systems. Int. J. Adv. Intell. Syst. 10, 365–382.

Collins, S., Kotze, D.J., Lü, X., Kuoppam, K., 2017. Thermal behavior of green roofs under Nordic winter conditions 122, 206–214. https://doi.org/10.1016/j.buildenv.2017.06.020

Congedo, P.M., Baglivo, C., Centonze, G., 2020. Walls comparative evaluation for the thermal performance improvement of low-rise residential buildings in warm Mediterranean climate. J. Build. Eng. 28, 101059. https://doi.org/10.1016/j.jobe.2019.101059

Corrado, V., Ballarini, I., Corgnati, S.P., 2012. Typology Approach for Building Stock National scientific report on the TABULA activities in Italy.

Costanzo, V., Evola, G., Marletta, L., 2016. Energy savings in buildings or UHI mitigation ? Comparison between green roofs and cool roofs. Energy Build. 114, 247–255.

Crank, P.J., Middel, A., Wagner, M., Hoots, D., Smith, M., Brazel, A., 2020. Validation of seasonal mean radiant temperature simulations in hot arid urban climates. Sci. Total Environ. 749, 141392. https://doi.org/10.1016/j.scitotenv.2020.141392

Crompton, P., Wu, Y., 2005. Energy consumption in China: past trends and future directions. Energy Econ. 27, 195–208. https://doi.org/10.1016/j.eneco.2004.10.006

Dai, H., Xie, X., Xie, Y., Liu, J., Masui, T., 2016. Green growth: The economic impacts of large-scale renewable energy development in China. Appl. Energy 162, 435–449. https://doi.org/10.1016/j.apenergy.2015.10.049

Deb, K., Pratap, A., Agarwal, S., Meyarivan, T., 2002. A fast and elitist multiobjective genetic algorithm: NSGA-II. IEEE Trans. Evol. Comput. 6, 182–197. https://doi.org/10.1109/4235.996017

Developer Raises the Bar in the Bronx | Architect Magazine [WWW Document], n.d. URL https://www.architectmagazine.com/technology/developer-raises-the-bar-in-the-bronx_o (accessed 12.6.19).

Doan, T., Litterman, R., Sims, C., 1984. Forecasting and conditional projection using realistic prior distributions. Econom. Rev. 3, 1–100. https://doi.org/10.1080/07474938408800053

Douthitt, R.A., 1989. An economic analysis of the demand for residential space heating fuel in Canada. Energy 14, 187–197. https://doi.org/10.1016/0360-5442(89)90062-5

Ediger, V. \cS., Akar, S., 2007. {ARIMA} forecasting of primary energy demand by fuel in Turkey. Energy Policy 35, 1701–1708. https://doi.org/10.1016/j.enpol.2006.05.009

Ediger, V. \cS., Tatl\idil, H., 2002. Forecasting the primary energy demand in Turkey and analysis of cyclic patterns. Energy Convers. Manag. 43, 473–487. https://doi.org/10.1016/s0196-

8904(01)00033-4

Egelioglu, F., Mohamad, A.A., Guven, H., 2001. Economic variables and electricity consumption in Northern Cyprus. Energy 26, 355–362. https://doi.org/10.1016/s0360-5442(01)00008-1

Ekonomou, L., 2010. Greek long-term energy consumption prediction using artificial neural networks. Energy 35, 512–517. https://doi.org/10.1016/j.energy.2009.10.018

El-Telbany, M., El-Karmi, F., 2008. Short-term forecasting of Jordanian electricity demand using particle swarm optimization. Electr. Power Syst. Res. 78, 425–433. https://doi.org/10.1016/j.epsr.2007.03.011

Energy Agency, I., 2021. Review 2021 Assessing the effects of economic recoveries on global energy demand and CO 2 emissions in 2021 Global Energy.

Energy Information Administration, U., 2020. Residential Demand Module of the National Energy Modeling System: Model Documentation 2020.

EnergyPlus Documentation Engineering Reference, 1996.

Erdogdu, E., 2010. Natural gas demand in Turkey. Appl. Energy 87, 211–219. https://doi.org/10.1016/j.apenergy.2009.07.006

Ermis, K., Midilli, A., Dincer, I., Rosen, M.A., 2007. Artificial neural network analysis of world green energy use. Energy Policy 35, 1731–1743. https://doi.org/10.1016/j.enpol.2006.04.015

Evins, R., Orehounig, K., Dorer, V., 2016. Variability between domestic buildings: the impact on energy use. J. Build. Perform. Simul. 9, 162–175. https://doi.org/10.1080/19401493.2015.1006526

Evola, G., Costanzo, V., Magrì, C., Margani, G., Marletta, L., Naboni, E., 2020. A novel comprehensive workflow for modelling outdoor thermal comfort and energy demand in urban canyons: Results and critical issues. Energy Build. 216, 109946. https://doi.org/10.1016/j.enbuild.2020.109946

Fan, J.Y., McDonald, J.D., 1994. A real-time implementation of short-term load forecasting for distribution power systems. {IEEE} Trans. Power Syst. 9, 988–994. https://doi.org/10.1109/59.317646

Fan, S., Chen, L., Lee, W.-J., 2008. Machine learning based switching model for electricity load forecasting. Energy Convers. Manag. 49, 1331–1344. https://doi.org/10.1016/j.enconman.2008.01.008

Fan, Y., Liao, H., Wei, Y.-M., 2007. Can market oriented economic reforms contribute to energy efficiency improvement? Evidence from China. Energy Policy 35, 2287–2295.

https://doi.org/10.1016/j.enpol.2006.07.011

Fang, T., Lahdelma, R., 2016. Evaluation of a multiple linear regression model and {SARIMA} model in forecasting heat demand for district heating system. Appl. Energy 179, 544–552. https://doi.org/10.1016/j.apenergy.2016.06.133

Farahbakhsh, H., Ugursal, V.I., Fung, A.S., 1998. A residential end-use energy consumption model for Canada. Int. J. Energy Res. 22, 1133–1143. https://doi.org/10.1002/(sici)1099-114x(19981025)22:13<1133::aid-er434>3.0.co;2-e

Fernández, M., Conde, B., Eguía, P., Granada, E., 2018. Parameter identification of a round-robin test box model using a deterministic and probabilistic methodology. J. Build. Perform. Simul. 11, 623–638. https://doi.org/10.1080/19401493.2017.1420824

Ferrante, P., La Gennusa, M., Peri, G., Scaccianoce, G., Sorrentino, G., 2015. Comparison between conventional and vegetated roof by means of a dynamic simulation, in: Energy Procedia. Elsevier Ltd, pp. 2917–2922. https://doi.org/10.1016/j.egypro.2015.11.667

Fiona Robertson; Martin Samy, 2015. Factors Affecting the Diffusion of Integrated Reporting – A UK FTSE 100 perspective. Sustainability Accounting. Manag. Policy J. 6, 1–39.

Forbes, D., 2011. Planning Sustainable Cities: Global Report on Human Settlements 2009 - By United Nations Human Settlements Programme. Geogr. Res. 49, 447–448. https://doi.org/10.1111/j.1745-5871.2010.00677.x

Forouzanfar, M., Doustmohammadi, A., Menhaj, M.B., Hasanzadeh, S., 2010. Modeling and estimation of the natural gas consumption for residential and commercial sectors in Iran. Appl. Energy 87, 268–274. https://doi.org/10.1016/j.apenergy.2009.07.008

Fouquet, R., Pearson, P., Hawdon, D., Robinson, C., Stevens, P., 1997. The future of {UK} final user energy demand. Energy Policy 25, 231–240. https://doi.org/10.1016/s0301-4215(96)00109-7

Francis, B.M., Moseley, L., Iyare, S.O., 2007. Energy consumption and projected growth in selected Caribbean countries. Energy Econ. 29, 1224–1232. https://doi.org/10.1016/j.eneco.2007.01.009

Frankenstein, S., Koenig, G.G., 2004. Fast All-season Soil STrength (FASST).

Fumo, N., Biswas, M.A.R., 2015. Regression analysis for prediction of residential energy consumption. Renew. Sustain. Energy Rev. 47, 332–343. https://doi.org/10.1016/j.rser.2015.03.035

Fung, A.S.L., Aydinalp, M., Ugursal, V.I., Data, C.R.E.E., Centre, A., Efficiency, C., Branch, A.E., 1999. Econometric Models for Major Residential Energy End-uses. CREEDAC, Dalhousie University.

Galindo, L.M., 2005. Short- and long-run demand for energy in Mexico: a cointegration approach. Energy Policy 33, 1179–1185. https://doi.org/10.1016/j.enpol.2003.11.015

Garc\'\ia-Ascanio, C., Maté, C., 2010. Electric power demand forecasting using interval time series: A comparison between {VAR} and {iMLP}. Energy Policy 38, 715–725. https://doi.org/10.1016/j.enpol.2009.10.007

Gareta, R., Romeo, L.M., Gil, A., 2006. Forecasting of electricity prices with neural networks. Energy Convers. Manag. 47, 1770–1778. https://doi.org/10.1016/j.enconman.2005.10.010

Garland, J., CPHC, L.W., 2017. WUFI [WWW Document]. ASHRAE Stand. 140-2017. URL https://www.phius.org/Tools-Resources/TechCorner/WUFI Passive Validation using ASHRAE 140-2017.pdf (accessed 1.30.22).

Gholami, M., Barbaresi, A., Torreggiani, D., Tassinari, P., 2020. Upscaling of spatial energy planning, phases, methods, and techniques: A systematic review through meta-analysis. Renew. Sustain. Energy Rev. https://doi.org/10.1016/j.rser.2020.110036

Gielen, D., Changhong, C., 2001. The {CO}2 emission reduction benefits of Chinese energy policies and environmental policies: Ecol. Econ. 39, 257–270. https://doi.org/10.1016/s0921-8009(01)00206-3

Gil-Alana, L.A., Loomis, D., Payne, J.E., 2010. Does energy consumption by the {US} electric power sector exhibit long memory behavior? Energy Policy 38, 7512–7518. https://doi.org/10.1016/j.enpol.2010.07.018

Glasure, Y.U., 2002. Energy and national income in Korea: further evidence on the role of omitted variables. Energy Econ. 24, 355–365. https://doi.org/10.1016/s0140-9883(02)00036-1

Gonzalez-Romera, E., Jaramillo-Moran, M.A., Carmona-Fernandez, D., 2006. Monthly Electric Energy Demand Forecasting Based on Trend Extraction. {IEEE} Trans. Power Syst. 21, 1946–1953. https://doi.org/10.1109/tpwrs.2006.883666

González-Romera, E., Jaramillo-Morán, M.A., Carmona-Fernández, D., 2008. Monthly electric energy demand forecasting with neural networks and Fourier series. Energy Convers. Manag. 49, 3135–3142. https://doi.org/10.1016/j.enconman.2008.06.004

González-Romera, E., Jaramillo-Morán, M.Á., Carmona-Fernández, D., 2007. Forecasting of the electric energy demand trend and monthly fluctuation with neural networks. Comput. Ind. Eng. 52, 336–343. https://doi.org/10.1016/j.cie.2006.12.010

GORI, F., LUDOVISI, D., CERRITELLI, P., 2007. Forecast of oil price and consumption in the short term under three scenarios: Parabolic, linear and chaotic behaviour. Energy 32, 1291–1296. https://doi.org/10.1016/j.energy.2006.07.005

Gotham Greens: Brooklyn's New High-Tech Rooftop Farm [WWW Document], n.d. URL https://www.fastcompany.com/1678197/gotham-greens-brooklyns-new-high-tech-rooftop-farm (accessed 2.17.20).

Guler, B., Ugursal, V.I., Fung, A.S., Koksal, M.A., 2008. Impact of energy efficiency upgrade retrofits on the residential energy consumption and Greenhouse Gas emissions in Canada. Int. J. Environ. Technol. Manag. 9, 434. https://doi.org/10.1504/ijetm.2008.019464

Hagan, M.T., Behr, S.M., 1987. The Time Series Approach to Short Term Load Forecasting. {IEEE} Trans. Power Syst. 2, 785–791. https://doi.org/10.1109/tpwrs.1987.4335210

Haida, T., Muto, S., 1994. Regression based peak load forecasting using a transformation technique. {IEEE} Trans. Power Syst. 9, 1788–1794. https://doi.org/10.1109/59.331433

Hamzaçebi, C., 2007. Forecasting of Turkey{\textquotesingle}s net electricity energy consumption on sectoral bases. Energy Policy 35, 2009–2016. https://doi.org/10.1016/j.enpol.2006.03.014

Hamzacebi, C., Es, H.A., 2014. Forecasting the annual electricity consumption of Turkey using an optimized grey model. Energy 70, 165–171. https://doi.org/10.1016/j.energy.2014.03.105

Harris, J.L., Liu, L.-M., 1993. Dynamic structural analysis and forecasting of residential electricity consumption. Int. J. Forecast. 9, 437–455. https://doi.org/10.1016/0169-2070(93)90072-u

Hasan, A., 1999. Optimizing insulation thickness for buildings using life cycle cost. Appl. Energy 63, 115–124. https://doi.org/10.1016/S0306-2619(99)00023-9

Heo, Y., Augenbroe, G., Graziano, D., Muehleisen, R.T., Guzowski, L., 2015. Scalable methodology for large scale building energy improvement: Relevance of calibration in model-based retrofit analysis. Build. Environ. 87, 342–350. https://doi.org/10.1016/j.buildenv.2014.12.016

Hirano, Y., Ihara, T., Gomi, K., Fujita, T., 2019. Simulation-based evaluation of the effect of Green Roofs in Office Building Districts on Mitigating the Urban Heat Island effect and reducing CO2 emissions. Sustain. 11. https://doi.org/10.3390/SU11072055

Hirst, E., 1978. A model of residential energy use. Simulation 30, 69–74. https://doi.org/10.1177/003754977803000301

Hirst, E., Goeltz, R., White, D., 1986. Determination of household energy using `fingerprints' from energy billing data. Int. J. Energy Res. 10, 393–405. https://doi.org/10.1002/er.4440100410

Hondroyiannis, G., Lolos, S., Papapetrou, E., 2002. Energy consumption and economic growth: assessing the evidence from Greece. Energy Econ. 24, 319–336. https://doi.org/10.1016/s0140-9883(02)00006-3

Hong, W.-C., 2010. Application of chaotic ant swarm optimization in electric load forecasting. Energy Policy 38, 5830–5839. https://doi.org/10.1016/j.enpol.2010.05.033

Hong, W.-C., 2009. Electric load forecasting by support vector model. Appl. Math. Model. 33, 2444–2454. https://doi.org/10.1016/j.apm.2008.07.010

Hoos, T., Merzkirch, A., Maas, S., Scholzen, F., 2016. Energy consumption of non-retrofitted institutional building stock in Luxembourg and the potential for a cost-efficient retrofit. Energy Build. 123, 162–168. https://doi.org/10.1016/j.enbuild.2016.03.065

Hsiao, C., Mountain, C., Illman, K.H., 1995. A Bayesian Integration of End-Use Metering and Conditional-Demand Analysis. J. Bus. Econ. Stat. 13, 315. https://doi.org/10.2307/1392191

Hsu, C.-C., Chen, C.-Y., 2003. Regional load forecasting in Taiwan{\textendash}{\textendash}applications of artificial neural networks. Energy Convers. Manag. 44, 1941–1949. https://doi.org/10.1016/s0196-8904(02)00225-x

Huang, P., Huang, G., Wang, Y., 2015. HVAC system design under peak load prediction uncertainty using multiple-criterion decision making technique. Energy Build. 91, 26–36. https://doi.org/10.1016/j.enbuild.2015.01.026

Huang, Y., Chen, C., Liu, W., 2018. Thermal performance of extensive green roofs in a subtropical metropolitan area 159, 39–53.

Huang, Y.J., Brodrick, J., 2000. A Bottom-Up Engineering Estimate of the Aggregate Heating and Cooling Loads of the Entire US Building Stock Prototypical Residential Buildings. 2000 ACEEE Summer Study Energy Effic. Build. 135–148.

Huang, Z., Yu, H., Peng, Z., Zhao, M., 2015. Methods and tools for community energy planning: A review. Renew. Sustain. Energy Rev. 42, 1335–1348. https://doi.org/10.1016/j.rser.2014.11.042

Hunt, L.C., Judge, G., Ninomiya, Y., 2003. Underlying trends and seasonality in {UK} energy demand: a sectoral analysis. Energy Econ. 25, 93–118. https://doi.org/10.1016/s0140-9883(02)00072-5

Hunt, L.C., Ninomiya, Y., 2005. Primary energy demand in Japan: an empirical analysis of long-term trends and future {CO}2 emissions. Energy Policy 33, 1409–1424. https://doi.org/10.1016/j.enpol.2003.12.019

Issa, R.R.A., Flood, I., Asmus, M., n.d. Development of a Neural Network to Predict Residential Energy Consumption, in: Proceedings of the Sixth International Conference on the Application of Artificial Intelligence to Civil and Structural Engineering. Civil-Comp Press. https://doi.org/10.4203/ccp.74.28

Jaffal, I., Ouldboukhitine, S., 2012. A comprehensive study of the impact of green roofs on building energy performance 43. https://doi.org/10.1016/j.renene.2011.12.004

Jain, A., Srinivas, E., Rauta, R., 2009. Short term load forecasting using fuzzy adaptive inference and similarity, in: 2009 World Congress on Nature & Biologically Inspired Computing ({NaBIC}). IEEE. https://doi.org/10.1109/nabic.2009.5393627

Jannuzzi, G.D.M., Schipper, L., 1991. The structure of electricity demand in the Brazilian household sector. Energy Policy 19, 879–891. https://doi.org/10.1016/0301-4215(91)90013-e

Jendritzky, Gerd, Havenith, George, Batchvarova, Ekaterina, Jendritzky, G, Havenith, G, Weihs, P., Batchvarova, E, Dedear, R., Inst Meteorology, N., Střelcová, al, Hazards, N., 2014. The universal thermal climate index UTCI Á goal and state of COST Action 730 The Universal Thermal Climate Index UTCI Goal and state of COST Action 730.

Jonas Tornberg, L.T.A., 2012. A GIS energy model for the building stock of Goteborg Jonas.

Jónsson, T., Pinson, P., Madsen, H., 2010. On the market impact of wind energy forecasts. Energy Econ. 32, 313–320. https://doi.org/10.1016/j.eneco.2009.10.018

Jörg Franke, Antti Hellsten, Heinke Schlünzen, B.C., 2007. Best Practice Guideline for the Cfd Simulation of Flows in the Urban Environment. Cost 732: Quality Assurance and Improvement of Microscale Meteorological Models, BEST PRACTICE GUIDELINE FOR THE CFD SIMULATION OF FLOWS IN THE URBAN ENVIRONMENT, COST Action 732.

Jungels, J., Rakow, D.A., Allred, S.B., Skelly, S.M., 2013. Attitudes and aesthetic reactions toward green roofs in the Northeastern United States. Landsc. Urban Plan. 117, 13–21. https://doi.org/10.1016/j.landurbplan.2013.04.013

JW, S., 2002. Energy demand in the fifteen European Union countries by 2010 {\textemdash} a forecasting model based on the decomposition approach. Fuel Energy Abstr. 43, 220. https://doi.org/10.1016/s0140-6701(02)86023-4

Kadian, R., Dahiya, R.P., Garg, H.P., 2007. Energy-related emissions and mitigation opportunities from the household sector in Delhi. Energy Policy 35, 6195–6211. https://doi.org/10.1016/j.enpol.2007.07.014

Kalmár, F., 2016. Summer operative temperatures in free running existing buildings with high glazed ratio of the facades. J. Build. Eng. 6, 236–242. https://doi.org/10.1016/j.jobe.2016.04.003

Kan, H., Chen, B., Chen, C., Fu, Q., Chen, M., 2004. An evaluation of public health impact of ambient air pollution under various energy scenarios in Shanghai, China. Atmos. Environ. 38, 95–102. https://doi.org/10.1016/j.atmosenv.2003.09.038

Kankal, M., Akp\inar, A., Kömürcü, M.\. I., Öz\csahin, T. \cSükrü, 2011. Modeling and forecasting of Turkey’s energy consumption using socio-economic and demographic variables. Appl. Energy 88, 1927–1939. https://doi.org/10.1016/j.apenergy.2010.12.005

Kannan, R., Ekins, P., Strachan, N., n.d. The Structure and Use of the {UK} {MARKAL} Model. https://doi.org/10.4337/9781849801997.00017

Kannan, R., Strachan, N., 2009. Modelling the {UK} residential energy sector under long-term decarbonisation scenarios: Comparison between energy systems and sectoral modelling approaches. Appl. Energy 86, 416–428. https://doi.org/10.1016/j.apenergy.2008.08.005

Kennedy, M.C., Hagan, A.O., 2001. Bayesian calibration of computer models. J. R. Stat. Soc. B 425–465.

Kiartzis, S.J., Bakirtzis, A.G., Theocharis, J.B., Tsagas, G., n.d. A fuzzy expert system for peak load forecasting. Application to the Greek power system, in: 2000 10th Mediterranean Electrotechnical Conference. Information Technology and Electrotechnology for the Mediterranean Countries. Proceedings. {MeleCon} 2000 (Cat. No.00CH37099). IEEE. https://doi.org/10.1109/melcon.2000.879726

Kim, J.-H., Augenbroe, G., Suh, H.-S., Wang, Q., 2015. DOMESTIC BUILDING ENERGY PREDICTION IN DESIGN STAGE UTILIZING LARGE-SCALE CONSUMPTION DATA FROM REALIZED PROJECTS.

Kohler, N., Schwaiger, B., Barth, B., Koch, M., 1999. Mass flow, energy flow and costs of the German building stock. Karlsruhe.

Kontokosta, C.E., Tull, C., 2017. A data-driven predictive model of city-scale energy use in buildings. Appl. Energy 197, 303–317. https://doi.org/10.1016/j.apenergy.2017.04.005

Kovachki, N.B., Stuart, A.M., 2019. Ensemble Kalman inversion: A derivative-free technique for machine learning tasks. Inverse Probl. 35. https://doi.org/10.1088/1361-6420/ab1c3a

Kucukali, S., Baris, K., 2010. Turkey’s short-term gross annual electricity demand forecast by fuzzy logic approach. Energy Policy 38, 2438–2445. https://doi.org/10.1016/j.enpol.2009.12.037

Kumar, R., Kaushik, S.C., 2005. Performance evaluation of green roof and shading for thermal protection of buildings. Build. Environ. 40, 1505–1511. https://doi.org/10.1016/j.buildenv.2004.11.015

Kumar, S., Madlener, R., 2016. {CO}2 emission reduction potential assessment using renewable energy in India. Energy 97, 273–282. https://doi.org/10.1016/j.energy.2015.12.131

Kumar, U., Jain, V.K., 2010. Time series models (Grey-Markov, Grey Model with rolling mechanism and singular spectrum analysis) to forecast energy consumption in India. Energy 35, 1709–1716. https://doi.org/10.1016/j.energy.2009.12.021

Labandeira, X., Labeaga, J.M., Rodr\'\iguez, M., 2006. A Residential Energy Demand System for Spain. Energy J. 27. https://doi.org/10.5547/issn0195-6574-ej-vol27-no2-6

Lafrance, G., Perron, D., 1994. Evolution of Residential Electricity Demand by End-Use in Quebec 1979-1989: A Conditional Demand Analysis. Energy Stud. Rev. 6. https://doi.org/10.15173/esr.v6i2.334

Lam, J.C., Tang, H.L., Li, D.H.W., 2008. Seasonal variations in residential and commercial sector electricity consumption in Hong Kong. Energy 33, 513–523. https://doi.org/10.1016/j.energy.2007.10.002

Lamnatou, C., Chemisana, D., 2015. A critical analysis of factors affecting photovoltaic-green roof performance. Renew. Sustain. Energy Rev. https://doi.org/10.1016/j.rser.2014.11.048

Larsen, B.M., Nesbakken, R., 2004. Household electricity end-use consumption: results from econometric and engineering models. Energy Econ. 26, 179–200. https://doi.org/10.1016/j.eneco.2004.02.001

Lean, H.H., Smyth, R., 2009. Long memory in {US} disaggregated petroleum consumption: Evidence from univariate and multivariate {LM} tests for fractional integration. Energy Policy 37, 3205–3211. https://doi.org/10.1016/j.enpol.2009.04.017

Lee, C.-C., Chang, C.-P., 2007. The impact of energy consumption on economic growth: Evidence from linear and nonlinear models in Taiwan. Energy 32, 2282–2294. https://doi.org/10.1016/j.energy.2006.01.017

Lee, C.-C., Chien, M.-S., 2010. Dynamic modelling of energy consumption, capital stock, and real income in G-7 countries. Energy Econ. 32, 564–581. https://doi.org/10.1016/j.eneco.2009.08.022

Lee, S.-C., Shih, L.-H., 2011. Forecasting of electricity costs based on an enhanced gray-based learning model: A case study of renewable energy in Taiwan. Technol. Forecast. Soc. Change 78, 1242–1253. https://doi.org/10.1016/j.techfore.2011.02.009

Lee, Y.-S., Tong, L.-I., 2011. Forecasting energy consumption using a grey model improved by incorporating genetic programming. Energy Convers. Manag. 52, 147–152. https://doi.org/10.1016/j.enconman.2010.06.053

Li, H., Li, X., Qi, M., 2014. Field testing of natural ventilation in college student dormitories (Beijing, China). Build. Environ. 78, 36–43. https://doi.org/10.1016/j.buildenv.2014.04.009

Li, W., Tian, Z., Lu, Y., Fu, F., 2018. Stepwise calibration for residential building thermal performance model using hourly heat consumption data. Energy Build. 181, 10–25. https://doi.org/10.1016/j.enbuild.2018.10.001

Liang, Q.-M., Fan, Y., Wei, Y.-M., 2007. Multi-regional input{\textendash}output model for regional energy requirements and {CO}2 emissions in China. Energy Policy 35, 1685–1700. https://doi.org/10.1016/j.enpol.2006.04.018

Lim, H., Zhai, Z. (John), 2018. Influences of energy data on Bayesian calibration of building energy model. Appl. Energy 231, 686–698. https://doi.org/10.1016/j.apenergy.2018.09.156

Lim, H., Zhai, Z.J., 2017. Comprehensive evaluation of the influence of meta-models on Bayesian calibration. Energy Build. 155, 66–75. https://doi.org/10.1016/j.enbuild.2017.09.009

Limanond, T., Jomnonkwao, S., Srikaew, A., 2011. Projection of future transport energy demand of Thailand. Energy Policy 39, 2754–2763. https://doi.org/10.1016/j.enpol.2011.02.045

Lin, B., Moubarak, M., 2014. Estimation of energy saving potential in China{\textquotesingle}s paper industry. Energy 65, 182–189. https://doi.org/10.1016/j.energy.2013.12.014

Lindberg, F., Holmer, B., Thorsson, S., 2008. SOLWEIG 1.0 – Modelling spatial variations of 3D radiant fluxes and mean radiant temperature in complex urban settings. Int. J. Biometeorol. 2008 527 52, 697–713. https://doi.org/10.1007/S00484-008-0162-7

Lise, W., Montfort, K. Van, 2007. Energy consumption and {GDP} in Turkey: Is there a co-integration relationship? Energy Econ. 29, 1166–1178. https://doi.org/10.1016/j.eneco.2006.08.010

Litterman, R.B. (Federa. R.B. of M., 1979. Techniques of forecasting using vector autoregressions.

Liu, H.-T., Guo, J.-E., Qian, D., Xi, Y.-M., 2009. Comprehensive evaluation of household indirect energy consumption and impacts of alternative energy policies in China by input{\textendash}output analysis. Energy Policy 37, 3194–3204. https://doi.org/10.1016/j.enpol.2009.04.016

Liu, Y., 2009. Exploring the relationship between urbanization and energy consumption in China using {ARDL} (autoregressive distributed lag) and {FDM} (factor decomposition model). Energy 34, 1846–1854. https://doi.org/10.1016/j.energy.2009.07.029

Lu, I.J., Lewis, C., Lin, S.J., 2009. The forecast of motor vehicle, energy demand and {CO}2 emission from Taiwan{\textquotesingle}s road transportation sector. Energy Policy 37, 2952–2961. https://doi.org/10.1016/j.enpol.2009.03.039

Lu, I.J., Lin, S.J., Lewis, C., 2008. Grey relation analysis of motor vehicular energy consumption in Taiwan. Energy Policy 36, 2556–2561. https://doi.org/10.1016/j.enpol.2008.03.015

Lu, W., Ma, Y., 2004. Image of energy consumption of well off society in China. Energy Convers. Manag. 45, 1357–1367. https://doi.org/10.1016/j.enconman.2003.09.005

Mabel, M.C., Fernandez, E., 2008. Growth and future trends of wind energy in India. Renew. Sustain. Energy Rev. 12, 1745–1757. https://doi.org/10.1016/j.rser.2007.01.016

MacGregor, W.A., Hamdullahpur, F., Ugursal, V.I., 1993. Space heating using small-scale fluidized beds: A technoeconomic evaluation. Int. J. Energy Res. 17, 445–466. https://doi.org/10.1002/er.4440170602

Mackey, C., Galanos, T., Norford, L., Roudsari, M.S., Bhd, N.S., 2017. Wind , Sun , Surface Temperature , and Heat Island : Critical Variables for High-Resolution Outdoor Thermal Comfort Payette Architects , United States of America Massachusetts Institute of Technology , United States of America University of Pennsylvania ,. Proc. 15th IBPSA Conf. 985–993.

Maia, A.S., Carvalho, F.A. t. De, Ludermir, T., 2006. Symbolic interval time series forecasting using a hybrid model, in: 2006 Ninth Brazilian Symposium on Neural Networks ({SBRN}{\textquotesingle}06). IEEE. https://doi.org/10.1109/sbrn.2006.41

Mamlook, R., Badran, O., Abdulhadi, E., 2009. A fuzzy inference model for short-term load forecasting. Energy Policy 37, 1239–1248. https://doi.org/10.1016/j.enpol.2008.10.051

Manfren, M., Aste, N., Moshksar, R., 2013. Calibration and uncertainty analysis for computer models - A meta-model based approach for integrated building energy simulation. Appl. Energy 103, 627–641. https://doi.org/10.1016/j.apenergy.2012.10.031

Masih, A.M.M., Masih, R., 1996. Energy consumption, real income and temporal causality: results from a multi-country study based on cointegration and error-correction modelling techniques. Energy Econ. 18, 165–183. https://doi.org/10.1016/0140-9883(96)00009-6

Mathworks, 2017. Matlab R2017b [WWW Document].

Matzarakis, A., Rutz, F., Mayer, H., 2009. Modelling radiation fluxes in simple and complex environments: basics of the RayMan model. Int. J. Biometeorol. 2009 542 54, 131–139. https://doi.org/10.1007/S00484-009-0261-0

McNeel, R. and others, 2021. Rhinoceros 3D, Version 7.0. Robert McNeel \& Assoc. Seattle, WA.

Middel, A., AlKhaled, S., Schneider, F.A., Hagen, B., Coseo, P., 2021. 50 Grades of Shade. Bull. Am. Meteorol. Soc. 1–35. https://doi.org/10.1175/BAMS-D-20-0193.1

Middel, A., Krayenhoff, E.S., 2019. Micrometeorological determinants of pedestrian thermal exposure during record-breaking heat in Tempe, Arizona: Introducing the MaRTy observational platform. Sci. Total Environ. 687, 137–151. https://doi.org/10.1016/J.SCITOTENV.2019.06.085

Middel, A., Turner, V.K., Schneider, F.A., Zhang, Y., Stiller, M., 2020. Solar reflective pavements—A policy panacea to heat mitigation? Environ. Res. Lett. 15, 064016.

https://doi.org/10.1088/1748-9326/AB87D4

Mihalakakou, G., Santamouris, M., Tsangrassoulis, A., 2002. On the energy consumption in residential buildings. Energy Build. 34, 727–736. https://doi.org/10.1016/s0378-7788(01)00137-2

Miranda-Agrippino, S., Ricco, G., 2018. Bayesian Vector Autoregressions. {SSRN} Electron. J. https://doi.org/10.2139/ssrn.3253086

Miranda, V., Monteiro, C., n.d. Fuzzy inference in spatial load forecasting, in: 2000 {IEEE} Power Engineering Society Winter Meeting. Conference Proceedings (Cat. No.00CH37077). IEEE. https://doi.org/10.1109/pesw.2000.850087

Mirlatifi, A.M., Egelioglu, F., Atikol, U., 2015. An econometric model for annual peak demand for small utilities. Energy 89, 35–44. https://doi.org/10.1016/j.energy.2015.06.119

Model documentation report: Residential sector demand module of the national energy modeling system, 1998. . Office of Scientific and Technical Information ({OSTI}). https://doi.org/10.2172/563838

Moghadam, S.T., Toniolo, J., Mutani, G., Lombardi, P., 2018. A {GIS}-statistical approach for assessing built environment energy use at urban scale. Sustain. Cities Soc. 37, 70–84. https://doi.org/10.1016/j.scs.2017.10.002

Moghram, I., Rahman, S., 1989. Analysis and evaluation of five short-term load forecasting techniques. {IEEE} Trans. Power Syst. 4, 1484–1491. https://doi.org/10.1109/59.41700

Mu, H., Kondou, Y., Tonooka, Y., Sato, Y., Zhou, W., Ning, Y., Sakamoto, K., 2004. Grey relative analysis and future prediction on rural household biofuels consumption in China. Fuel Process. Technol. 85, 1231–1248. https://doi.org/10.1016/j.fuproc.2003.10.018

Mu, T., Xia, Q., Kang, C., 2010. Input-output table of electricity demand and its application. Energy 35, 326–331. https://doi.org/10.1016/j.energy.2009.09.024

naboni, emanuele, meloni, marco, makey, chris, kaempf, jerome, 2020. The Simulation of Mean Radiant Temperature in Outdoor Conditions: A review of Software Tools Capabilities. Proc. Build. Simul. 2019 16th Conf. IBPSA 16, 3234–3241. https://doi.org/10.26868/25222708.2019.210301

Nadal, A., Llorach-Massana, P., Cuerva, E., López-Capel, E., Montero, J.I., Josa, A., Rieradevall, J., Royapoor, M., 2017. Building-integrated rooftop greenhouses: An energy and environmental assessment in the mediterranean context. Appl. Energy 187, 338–351. https://doi.org/10.1016/j.apenergy.2016.11.051

Nadal, A., Rodríguez-Cadena, D., Pons, O., Cuerva, E., Josa, A., Rieradevall, J., 2019. Feasibility assessment of rooftop greenhouses in Latin America. The case study of a social neighborhood in Quito, Ecuador. Urban For. Urban Green. 44, 126389. https://doi.org/10.1016/j.ufug.2019.126389

Nagpal, S., Mueller, C., Aijazi, A., Reinhart, C.F., 2019. A methodology for auto-calibrating urban building energy models using surrogate modeling techniques. J. Build. Perform. Simul. 12, 1–16. https://doi.org/10.1080/19401493.2018.1457722

Narayan, S., 2016. Predictability within the energy consumption{\textendash}economic growth nexus: Some evidence from income and regional groups. Econ. Model. 54, 515–521. https://doi.org/10.1016/j.econmod.2015.12.037

NASA, 2022. Mitigation and Adaptation | Solutions – Climate Change: Vital Signs of the Planet [WWW Document]. URL https://climate.nasa.gov/solutions/adaptation-mitigation/ (accessed 1.31.22).

Nesbakken, R., 1999. Price sensitivity of residential energy consumption in Norway. Energy Econ. 21, 493–515. https://doi.org/10.1016/s0140-9883(99)00022-5

Nilsson, K., Söderström, M., 1993. Industrial applications of production planning with optimal electricity demand. Appl. Energy 46, 181–192. https://doi.org/10.1016/0306-2619(93)90067-y

Nishio, K., Asano, H., 2006. A residential end-use demand model for analyzing the energy conservation potential of new energy efficient technologies. Proc. energy Effic. Domest. appliances Light.

Nocera, F., Gagliano, A., Detommaso, M., Evola, G., 2016. Thermal Behavior of an Extensive Green Roof: Numerical Simulations and Experimental Investigations INTERNATIONAL JOURNAL OF HEAT AND TECHNOLOGY A publication of IIETA. Artic. Int. J. Heat Technol. 34, 226–234. https://doi.org/10.18280/ijht.34S206

Nogales, F.J., Contreras, J., Conejo, A.J., Espinola, R., 2002. Forecasting next-day electricity prices by time series models. {IEEE} Trans. Power Syst. 17, 342–348. https://doi.org/10.1109/tpwrs.2002.1007902

NYC Rooftop Hydroponic Garden Classroom Urban Farm Greenhouse [WWW Document], n.d. URL https://www.urbangardensweb.com/2011/11/16/nyc-classroom-in-an-urban-rooftop-farm/ (accessed 12.6.19).

O'Neill, B.C., Desai, M., 2005. Accuracy of past projections of {US} energy consumption. Energy Policy 33, 979–993. https://doi.org/10.1016/j.enpol.2003.10.020

Odhiambo, N.M., 2009. Energy consumption and economic growth nexus in Tanzania: An {ARDL} bounds testing approach. Energy Policy 37, 617–622. https://doi.org/10.1016/j.enpol.2008.09.077

Ouldboukhitine, S.E., Belarbi, R., Sailor, D.J., 2014. Experimental and numerical investigation of urban street canyons to evaluate the impact of green roof inside and outside buildings. Appl. Energy 114, 273–282. https://doi.org/10.1016/j.apenergy.2013.09.073

Ozturk, H.K., Ceylan, H., Canyurt, O.E., Hepbasli, A., 2005. Electricity estimation using genetic algorithm approach: a case study of Turkey. Energy 30, 1003–1012. https://doi.org/10.1016/j.energy.2004.08.008

Ozturk, H.K., Ceylan, H., Hepbasli, A., Utlu, Z., 2004. Estimating petroleum exergy production and consumption using vehicle ownership and {GDP} based on genetic algorithm approach. Renew. Sustain. Energy Rev. 8, 289–302. https://doi.org/10.1016/j.rser.2003.10.004

Padmakumari, K., Mohandas, K.P., Thiruvengadam, S., 1999. Long term distribution demand forecasting using neuro fuzzy computations. Int. J. Electr. Power Energy Syst. 21, 315–322. https://doi.org/10.1016/s0142-0615(98)00056-8

Palermo, S.A., Turco, M., Principato, F., Piro, P., 2019. Hydrological Effectiveness of an Extensive Green Roof in Mediterranean Climate. Water 11, 1378. https://doi.org/10.3390/w11071378

Palmer, J., Boardman, B., Bottrill, C., Darby, S., Hinnells, M., Killip, G., Layberry, R., Lovell, H., 2006. Reducing the environmental impact of housing Final Report Consultancy study in support of the Royal Commission on Environmental Pollution's 26 th Report on the Urban Environment.

Pao, H.-T., Tsai, C.-M., 2011. Modeling and forecasting the {CO}2 emissions, energy consumption, and economic growth in Brazil. Energy 36, 2450–2458. https://doi.org/10.1016/j.energy.2011.01.032

PAO, H., 2006. Comparing linear and nonlinear forecasts for Taiwan{\textquotesingle}s electricity consumption. Energy 31, 2129–2141. https://doi.org/10.1016/j.energy.2005.08.010

Pao, H.T., 2009. Forecasting energy consumption in Taiwan using hybrid nonlinear models. Energy 34, 1438–1446. https://doi.org/10.1016/j.energy.2009.04.026

Papalexopoulos, A.D., Hesterberg, T.C., 1990. A regression-based approach to short-term system load forecasting. {IEEE} Trans. Power Syst. 5, 1535–1547. https://doi.org/10.1109/59.99410

Park, S., Tuller, S.E., Jo, M., 2014. Application of Universal Thermal Climate Index (UTCI) for microclimatic analysis in urban thermal environments. Landsc. Urban Plan. 125, 146–155. https://doi.org/10.1016/j.landurbplan.2014.02.014

Parti, M., Parti, C., 1980. The Total and Appliance-Specific Conditional Demand for Electricity in the Household Sector. Bell J. Econ. 11, 309. https://doi.org/10.2307/3003415

Petersdorff, C., Boermans, T., Harnisch, J., 2006. Mitigation of {CO}2 Emissions from the {EU}-15 Building Stock. Beyond the {EU} Directive on the Energy Performance of Buildings (9 pp). Environ. Sci. Pollut. Res. - Int. 13, 350–358. https://doi.org/10.1065/espr2005.12.289

Qi, Q., Tao, F., 2018. Digital Twin and Big Data Towards Smart Manufacturing and Industry 4.0: 360 Degree Comparison. IEEE Access 6, 3585–3593. https://doi.org/10.1109/ACCESS.2018.2793265

Raffio, G., Isambert, O., Mertz, G., Schreier, C., Kissock, K., 2007. Targeting Residential Energy Assistance, in: {ASME} 2007 Energy Sustainability Conference. ASME. https://doi.org/10.1115/es2007-36080

Raghuvanshi, S.P., Chandra, A., Raghav, A.K., 2006. Carbon dioxide emissions from coal based power generation in India. Energy Convers. Manag. 47, 427–441. https://doi.org/10.1016/j.enconman.2005.05.007

Ramirez, R., Sebold, F., Mayer, T., Ciminelli, M., Abrishami, M., 2005. A BUILDING SIMULATION PALOOZA : THE CALIFORNIA CEUS PROJECT AND D R CEUS Itron , Inc ., Consulting and Analysis Services 1003–1010.

Reinhart, C.F., Cerezo Davila, C., 2016. Urban building energy modeling - A review of a nascent field. Build. Environ. https://doi.org/10.1016/j.buildenv.2015.12.001

Rini, D.P., Shamsuddin, S.M., Yuhaniz, S.S., 2011. Particle Swarm Optimization: Technique, System and Challenges. Int. J. Comput. Appl. 14, 19–27. https://doi.org/10.5120/1810-2331

Robinson, D., Haldi, F., Kämpf, J., Leroux, P., Perez, D., Rasheed, A., Wilke, U., 2009. Citysim: Comprehensive micro-simulation of resource flows for sustainable urban planning. IBPSA 2009 - Int. Build. Perform. Simul. Assoc. 2009 1083–1090.

Rodrigues Prata-Shimomura, A., Marques, L., Anésia, M.;, Frota, B., 2009. PHYSIOLOGICAL EQUIVALENT TEMPERATURE INDEX APPLIED TO WIND TUNNEL EROSION TECHNIQUE PICTURES FOR THE ASSESSMENT OF PEDESTRIAN THERMAL COMFORT.

Roudsari, M.S., Pak, M., 2013. LADYBUG: A PARAMETRIC ENVIRONMENTAL PLUGIN FOR GRASSHOPPER TO HELP DESIGNERS CREATE AN ENVIRONMENTALLY-CONSCIOUS DESIGN, in: Building Performance Simulation Association. Chambery, France.

Rout, U.K., Vo$\upbeta$, A., Singh, A., Fahl, U., Blesl, M., Gallachóir, B.P.Ó., 2011. Energy and emissions forecast of China over a long-time horizon. Energy 36, 1–11. https://doi.org/10.1016/j.energy.2010.10.050

Saab, S., Badr, E., Nasr, G., 2001. Univariate modeling and forecasting of energy consumption:

the case of electricity in Lebanon. Energy 26, 1–14. https://doi.org/10.1016/s0360-5442(00)00049-9

Sadaei, H.J., Enayatifar, R., Abdullah, A.H., Gani, A., 2014. Short-term load forecasting using a hybrid model with a refined exponentially weighted fuzzy time series and an improved harmony search. Int. J. Electr. Power Energy Syst. 62, 118–129. https://doi.org/10.1016/j.ijepes.2014.04.026

Saddler, H., Diesendorf, M., Denniss, R., 2007. Clean energy scenarios for Australia. Energy Policy 35, 1245–1256. https://doi.org/10.1016/j.enpol.2006.03.013

Sadorsky, P., 2009. Renewable energy consumption, {CO}2 emissions and oil prices in the G7 countries. Energy Econ. 31, 456–462. https://doi.org/10.1016/j.eneco.2008.12.010

SAHA, G., STEPHENSON, J., 1980. A model of residential energy use in New Zealand. Energy 5, 167–175. https://doi.org/10.1016/0360-5442(80)90005-5

Saidur, R., Masjuki, H.H., Jamaluddin, M.Y., 2007. An application of energy and exergy analysis in residential sector of Malaysia. Energy Policy 35, 1050–1063. https://doi.org/10.1016/j.enpol.2006.02.006

Sailor, D.J., 2008. A green roof model for building energy simulation programs. Energy Build. 40, 1466–1478. https://doi.org/10.1016/j.enbuild.2008.02.001

Samouilidis, J.-E., Mitropoulos, C.S., 1984. Energy and economic growth in industrializing countries. Energy Econ. 6, 191–201. https://doi.org/10.1016/0140-9883(84)90016-1

Sanstad, A.H., McMenamin, S., Sukenik, A., Barbose, G.L., Goldman, C.A., 2014. Modeling an aggressive energy-efficiency scenario in long-range load forecasting for electric power transmission planning. Appl. Energy 128, 265–276. https://doi.org/10.1016/j.apenergy.2014.04.096

Sari, R., Soytas, U., 2004. Disaggregate energy consumption, employment and income in Turkey. Energy Econ. 26, 335–344. https://doi.org/10.1016/j.eneco.2004.04.014

Schillings, C., Stuart, A.M., 2017. Analysis of the ensemble Kalman filter for inverse problems. SIAM J. Numer. Anal. 55, 1264–1290. https://doi.org/10.1137/16M105959X

Shailza, 2018. ENERGY MODELING OF MULTI-STORIED RESIDENTIAL BUILDINGS-A MANUAL CALIBRATION APPROACH, in: 2018 Building Performance Analysis Conference and SimBuild Co-Organized by ASHRAE and IBPSA-USA. Chicago, IL.

Sharma, D.P., Nair, P.S.C., Balasubramanian, R., 2002. Demand for commercial energy in the state of Kerala, India: an econometric analysis with medium-range projections. Energy Policy 30, 781–791. https://doi.org/10.1016/s0301-4215(01)00138-0

Shimoda, Y., Fujii, T., Morikawa, T., Mizuno, M., 2004. Residential end-use energy simulation at city scale. Build. Environ. 39, 959–967. https://doi.org/10.1016/j.buildenv.2004.01.020

Shipley, D., Todesco, G., Adelaar Ottawa, ON (Canada)], M. [Marbek R.C., 2002. Modelling a nation of buildings : estimating energy efficiency potential for large building samples. International Building Performance Simulation Association, Canadian Chapter, Ottawa, ON (Canada), Canada.

Siller, T., Kost, M., Imboden, D., 2007. Long-term energy savings and greenhouse gas emission reductions in the Swiss residential sector. Energy Policy 35, 529–539. https://doi.org/10.1016/j.enpol.2005.12.021

Silva, C.M., Gomes, M.G., Silva, M., 2016. Green roofs energy performance in Mediterranean climate. Energy Build. 116, 318–325. https://doi.org/10.1016/j.enbuild.2016.01.012

Sisman, N., Kahya, E., Aras, N., Aras, H., 2007. Determination of optimum insulation thicknesses of the external walls and roof (ceiling) for Turkey's different degree-day regions. Energy Policy 35, 5151–5155. https://doi.org/10.1016/j.enpol.2007.04.037

Sky Vegetables [WWW Document], n.d. URL http://www.skyvegetables.com/ (accessed 12.6.19).

Snäkin, J.P., 2000. An engineering model for heating energy and emission assessment. The case of North Karelia, Finland. Appl. Energy 67, 353–381. https://doi.org/10.1016/S0306-2619(00)00035-0

Sokol, J., Cerezo Davila, C., Reinhart, C.F., 2017. Validation of a Bayesian-based method for defining residential archetypes in urban building energy models. Energy Build. 134, 11–24. https://doi.org/10.1016/j.enbuild.2016.10.050

Song, K.-B., Baek, Y.-S., Hong, D.H., Jang, G., 2005. Short-Term Load Forecasting for the Holidays Using Fuzzy Linear Regression Method. {IEEE} Trans. Power Syst. 20, 96–101. https://doi.org/10.1109/tpwrs.2004.835632

Sözen, A., 2009. Future projection of the energy dependency of Turkey using artificial neural network. Energy Policy 37, 4827–4833. https://doi.org/10.1016/j.enpol.2009.06.040

Sözen, A., Arcaklio\uglu, E., Özalp, M., Kanit, E.G., 2005a. Solar-energy potential in Turkey. Appl. Energy 80, 367–381. https://doi.org/10.1016/j.apenergy.2004.06.001

Sözen, A., Arcaklio\uglu, E., Özkaymak, M., 2005b. Turkey's net energy consumption. Appl. Energy 81, 209–221. https://doi.org/10.1016/j.apenergy.2004.07.001

Sözen, A., Gülseven, Z., Arcaklio\uglu, E., 2007. Forecasting based on sectoral energy consumption of {GHGs} in Turkey and mitigation policies. Energy Policy 35, 6491–6505. https://doi.org/10.1016/j.enpol.2007.08.024

Steenhof, P.A., Fulton, W., 2007. Scenario development in China{\textquotesingle}s electricity sector. Technol. Forecast. Soc. Change 74, 779–797. https://doi.org/10.1016/j.techfore.2006.09.004

Steiner, F., 2014. Frontiers in urban ecological design and planning research. Landsc. Urban Plan. 125, 304–311. https://doi.org/10.1016/j.landurbplan.2014.01.023

Streiling, S., Matzarakis, A., 2003. Influence of single and small clusters of trees on the bioclimate of a city: A case study [WWW Document]. J. Arboric.

Suganthi, L., Samuel, A.A., 2012. Energy models for demand forecasting{\textemdash}A review. Renew. Sustain. Energy Rev. 16, 1223–1240. https://doi.org/10.1016/j.rser.2011.08.014

Sumer, K.K., Goktas, O., Hepsag, A., 2009. The application of seasonal latent variable in forecasting electricity demand as an alternative method. Energy Policy 37, 1317–1322. https://doi.org/10.1016/j.enpol.2008.11.014

Summerfield, A.J., Lowe, R.J., Oreszczyn, T., 2010. Two models for benchmarking {UK} domestic delivered energy. Build. Res. Inf. 38, 12–24. https://doi.org/10.1080/09613210903399025

Surhone, L.M., Timpledon, M.T., Marseken, S.F., 2010. Sustainable landscape architecture: sustainable design, sustainable urban drainage systems, fauna, flora, green roof, roof garden, context theory. Betascript Publishing, Beau Bassin, Mauritius.

Swan, L.G., Ugursal, V.I., 2009. Modeling of end-use energy consumption in the residential sector: A review of modeling techniques. Renew. Sustain. Energy Rev. 13, 1819–1835. https://doi.org/10.1016/j.rser.2008.09.033

Swan, L.G., Ugursal, V.I., Beausoleil-Morrison, I., 2009. A database of house descriptions representative of the Canadian housing stock for coupling to building energy performance simulation. J. Build. Perform. Simul. 2, 75–84. https://doi.org/10.1080/19401490802491827

Taheri, M., Kingdom, U., Tahmasebi, F., 2013. A Case Study of Optimization-Aided Thermal Building Performance Simulation Calibration A CASE STUDY OF OPTIMIZATION-AIDED THERMAL BUILDING PERFORMANCE SIMULATION CALIBRATION Mahnameh Taheri , Farhang Tahmasebi , Ardeshir Mahdavi Vienna University of Techn.

Tang, L., Wu, Y., Yu, L., 2018. A randomized-algorithm-based decomposition-ensemble learning methodology for energy price forecasting. Energy 157, 526–538. https://doi.org/10.1016/j.energy.2018.05.146

The Vinegar Factory - Eli Zabar EliZabar.com [WWW Document], n.d. URL https://www.elizabar.com/The-Vinegar-Factory.aspx (accessed 2.17.20).

Thorsson, S., Lindberg, F., Björklund, J., Holmer, B., Rayner, D., 2011. Potential changes in outdoor thermal comfort conditions in Gothenburg, Sweden due to climate change: The influence of urban geometry. Int. J. Climatol. 31, 324–335. https://doi.org/10.1002/joc.2231

Tian, W., Choudhary, R., 2012. A probabilistic energy model for non-domestic building sectors applied to analysis of school buildings in greater London. Energy Build. 54, 1–11. https://doi.org/10.1016/j.enbuild.2012.06.031

Tian, W., Heo, Y., de Wilde, P., Li, Z., Yan, D., Park, C.S., Feng, X., Augenbroe, G., 2018. A review of uncertainty analysis in building energy assessment. Renew. Sustain. Energy Rev. 93, 285–301. https://doi.org/10.1016/j.rser.2018.05.029

Toksar\i, M.D., 2009. Estimating the net electricity energy generation and demand using the ant colony optimization approach: Case of Turkey. Energy Policy 37, 1181–1187. https://doi.org/10.1016/j.enpol.2008.11.017

Toksar\i, M.D., 2007. Ant colony optimization approach to estimate energy demand of Turkey. Energy Policy 35, 3984–3990. https://doi.org/10.1016/j.enpol.2007.01.028

Tonn, B.E., White TN (USA)), D.L. (Oak R.N.L., 1988. Residential electricity use, wood use, and indoor temperature; An econometric model.

Tripathy, S.C., 1997. Demand forecasting in a power system. Energy Convers. Manag. 38, 1475–1481. https://doi.org/10.1016/s0196-8904(96)00101-x

Tunç, M., Çamdali, Ü., Parmaksizo\uglu, C., 2006. Comparison of Turkey{\textquotesingle}s electrical energy consumption and production with some European countries and optimization of future electrical power supply investments in Turkey. Energy Policy 34, 50–59. https://doi.org/10.1016/j.enpol.2004.04.027

U.S. Department of Energy, 2020. EnergyPlus | EnergyPlus. U.S. Dep. Energy.

Ünler, A., 2008. Improvement of energy demand forecasts using swarm intelligence: The case of Turkey with projections to 2025. Energy Policy 36, 1937–1944. https://doi.org/10.1016/j.enpol.2008.02.018

Vaillancourt, K., Alcocer, Y., Bahn, O., Fertel, C., Frenette, E., Garbouj, H., Kanudia, A., Labriet, M., Loulou, R., Marcy, M., Neji, Y., Waaub, J.-P., 2014. A Canadian 2050 energy outlook: Analysis with the multi-regional model {TIMES}-Canada. Appl. Energy 132, 56–65. https://doi.org/10.1016/j.apenergy.2014.06.072

Vogt, Y., 2003. Top{\textendash}down Energy Modeling. Strateg. Plan. Energy Environ. 22, 64–79. https://doi.org/10.1080/10485230309509626

Wan, K.S.Y., Yik, F.H.W., 2004. Representative building design and internal load patterns for modelling energy use in residential buildings in Hong Kong. Appl. Energy 77, 69–85.

https://doi.org/10.1016/s0306-2619(03)00104-1

Wang, C.K., Tindemans, S., Miller, C., Agugiaro, G., Stoter, J., 2020. Bayesian calibration at the urban scale: a case study on a large residential heating demand application in Amsterdam. J. Build. Perform. Simul. 13, 347–361. https://doi.org/10.1080/19401493.2020.1729862

Wang, J., Li, L., 2016. Sustainable energy development scenario forecasting and energy saving policy analysis of China. Renew. Sustain. Energy Rev. 58, 718–724. https://doi.org/10.1016/j.rser.2015.12.340

Wang, J., Zhu, S., Zhang, W., Lu, H., 2010. Combined modeling for electric load forecasting with adaptive particle swarm optimization. Energy 35, 1671–1678. https://doi.org/10.1016/j.energy.2009.12.015

Wang, J., Zhu, W., Zhang, W., Sun, D., 2009. A trend fixed on firstly and seasonal adjustment model combined with the $\upepsilon$-{SVR} for short-term forecasting of electricity demand. Energy Policy 37, 4901–4909. https://doi.org/10.1016/j.enpol.2009.06.046

Wang, S., Fang, C., Guan, X., Pang, B., Ma, H., 2014. Urbanisation, energy consumption, and carbon dioxide emissions in China: A panel data analysis of China's provinces. Appl. Energy 136, 738–749. https://doi.org/10.1016/j.apenergy.2014.09.059

Wei, Y.-M., Liang, Q.-M., Fan, Y., Okada, N., Tsai, H.-T., 2006. A scenario analysis of energy requirements and energy intensity for China{\textquotesingle}s rapidly developing society in the year 2020. Technol. Forecast. Soc. Change 73, 405–421. https://doi.org/10.1016/j.techfore.2004.12.003

Wetter, M., 2001. GenOpt®-A Generic Optimization Program GenOpt Ö-A Generic Optimization Program.

World Energy Outlook – Topics - IEA [WWW Document], n.d. URL https://www.iea.org/topics/world-energy-outlook (accessed 2.17.20).

Wright, L., Davidson, S., 2020. How to tell the difference between a model and a digital twin. Adv. Model. Simul. Eng. Sci. 7. https://doi.org/10.1186/S40323-020-00147-4

Wu, Z., Wang, B., Xia, X., 2016. Large-scale building energy efficiency retrofit: Concept, model and control. Energy 109, 456–465. https://doi.org/10.1016/j.energy.2016.04.124

Wu, Z., Xu, J., 2013. Predicting and optimization of energy consumption using system dynamics-fuzzy multiple objective programming in world heritage areas. Energy 49, 19–31. https://doi.org/10.1016/j.energy.2012.10.030

Xia, C., Wang, J., McMenemy, K., 2010. Short, medium and long term load forecasting model and virtual load forecaster based on radial basis function neural networks. Int. J. Electr. Power Energy Syst. 32, 743–750. https://doi.org/10.1016/j.ijepes.2010.01.009

Yalcinoz, T., Eminoglu, U., 2005. Short term and medium term power distribution load forecasting by neural networks. Energy Convers. Manag. 46, 1393–1405. https://doi.org/10.1016/j.enconman.2004.07.005

Yang, G., Li, Z., Augenbroe, G., 2017. Development of prototypical buildings for urban scale building energy modeling: A reduced order energy model approach. Sci. Technol. Built Environ. 24, 33–42. https://doi.org/10.1080/23744731.2017.1328943

Yang, T., Pan, Y., Mao, J., Wang, Y., Huang, Z., 2016. An automated optimization method for calibrating building energy simulation models with measured data: Orientation and a case study. Appl. Energy 179, 1220–1231. https://doi.org/10.1016/j.apenergy.2016.07.084

Yao, A.W.L., Chi, S.C., 2004. Analysis and design of a Taguchi{\textendash}Grey based electricity demand predictor for energy management systems. Energy Convers. Manag. 45, 1205–1217. https://doi.org/10.1016/j.enconman.2003.08.008

Yokoyama, R., Wakui, T., Satake, R., 2009. Prediction of energy demands using neural network with model identification by global optimization. Energy Convers. Manag. 50, 319–327. https://doi.org/10.1016/j.enconman.2008.09.017

Yuan, J.-H., Kang, J.-G., Zhao, C.-H., Hu, Z.-G., 2008. Energy consumption and economic growth: Evidence from China at both aggregated and disaggregated levels. Energy Econ. 30, 3077–3094. https://doi.org/10.1016/j.eneco.2008.03.007

YUMURTACI, Z., ASMAZ, E., 2004. Electric Energy Demand of Turkey for the Year 2050. Energy Sources 26, 1157–1164. https://doi.org/10.1080/00908310490441520

Zeng, C., Bai, X., Sun, L., Zhang, Y., Yuan, Y., 2017. Optimal parameters of green roofs in representative cities of four climate zones in China: A simulation study. Energy Build. 150, 118–131. https://doi.org/10.1016/j.enbuild.2017.05.079

Zhang, Q., 2004. Residential energy consumption in China and its comparison with Japan, Canada, and {USA}. Energy Build. 36, 1217–1225. https://doi.org/10.1016/j.enbuild.2003.08.002

Zhang, X., Wang, F., 2016. Hybrid input-output analysis for life-cycle energy consumption and carbon emissions of China's building sector. Build. Environ. 104, 188–197. https://doi.org/10.1016/j.buildenv.2016.05.018

Zhao, F., Lee, S.H., Augenbroe, G., 2016. Reconstructing building stock to replicate energy consumption data. Energy Build. 117, 301–312. https://doi.org/10.1016/j.enbuild.2015.10.001

Zhao, X., Wu, Y., 2007. Determinants of China{\textquotesingle}s energy imports: An empirical analysis. Energy Policy 35, 4235–4246. https://doi.org/10.1016/j.enpol.2007.02.034

Zheng, D., Yu, L., Wang, L., Tao, J., 2019. Integrating willingness analysis into investment prediction model for large scale building energy saving retrofit: Using fuzzy multiple attribute decision making method with Monte Carlo simulation. Sustain. Cities Soc. 44, 291–309. https://doi.org/10.1016/j.scs.2018.10.008

Zhou, M., Yan, J., Feng, D., 2019. Digital Twin Framework and Its Application to Power Grid Online Analysis. CSEE J. POWER ENERGY Syst. 5.

ZHOU, P., ANG, B., POH, K., 2006. A trigonometric grey prediction approach to forecasting electricity demand. Energy 31, 2839–2847. https://doi.org/10.1016/j.energy.2005.12.002